Universidade de Brasília
Instituto de Ciências Biológicas
Departamento de Biologia Celular

Detecção e caracterização de complexos multi-enzimáticos em secretoma de fungos filamentosos

Adelson Joel da Silva

Tese apresentada ao Departamento de Biologia Celular do Instituto de Ciências Biológicas da Universidade de Brasília como requisito parcial à obtenção do Grau de Doutor em Ciências Biológicas.

Brasília – DF (2012)

Banca Examinadora

Prof. Dr. Carlos André Ornelas Ricart (presidente, orientador)

Laboratório de Bioquímica e Química de Proteinas
Departamento de Biologia Celular
Universidade de Brasília

Profª. Drª. Angela Mehta dos Reis

EMBRAPA – CERNAGEM

Prof. Dr. Sébastien Olivier Charneau

Faculdade de Ceilândia
Universidade de Brasília

Prof. Dr. Cirano Ulhoa

Universidade Federal de Góias

Prof. Dr. Wagner Fontes

Laboratório de Bioquímica e Química de Proteinas
Departamento de Biologia Celular
Universidade de Brasília

Profª. Drª. Mariana de Souza Castro (suplente)

Laboratório de Toxinologia
Departamento de Biologia Celular
Universidade de Brasília

Este trabalho foi realizado no Laboratório de Bioquímica e Química de Proteínas e Laboratório de Enzimologia, ambos do Departamento de Biologia Celular da Universidade de Brasília. E teve cooperação do Laboratório de Espectrometria de Massas da Universidade Federal do Rio de Janeiro.

Área de concentração: Biologia Molecular

Orientador: Profº. Drº. Carlos André Ornelas Ricart (Laboratório de Bioquímica e Química de Proteínas – UnB)

Co-orientador: Edivaldo Ximenes Ferreira Filho (Laboratório de Enzimologia – UnB)

Abreviaturas e Símbolos

1D-BN-PAGE: primeira dimensão BN-PAGE
ABF: arabinofuranosidase
AXE: acetilxilano esterase
BDA: meio sólido contendo batata, dextrose e ágar.
bgl1**:** gene β-glicosidase I
BN-PAGE: Eletroforese em gel de poliacrilamida "blue native"
bxl1**:** gene β-xilosidase I
CBB: "Coomasie Brillant Blue G-250"
CBH: celobiohidrolase
cbh1**:** gene celobioidrolase I
cbh2**:** gene celobioidrolase II
CBM: módulo de ligação a carboidrato
egl1**:** gene endoglucanase I
GPI-EglC: β-endoglucanase ancorado a GPI (glicosilfosfatidil inositol)
LC-MS/MS: cromatografia líquida acoplada a espectrometria de massas
SBD: domíno de ligação a amido
SDS: dodecil sulfato de sódio.
SWOI: swolenina
Termo/BN-PAGE: mensurações termodinâmicas acoplado a BN-PAGE
xyn1**:** gene endoxilanase I
xyn2**:** gene endoxilanase II
Zimo/BN-PAGE (2D-BN/BN-PAGE): zimografia acoplada à segunda dimensão do BN/PAGE

Aos meus tesouros eternos:

Ana Maria de Conceição Silva

Manoel Renato da Silva

Ao meu amor imortal:

Joseana Luisa de Freitas

Agradecimentos

À Universidade de Brasília e seu excelente Programa de Pós-Graduação em Biologia Molecular.

Aos Professores Carlos André Ornelas Ricart e Marcelo Valle de Sousa que, gentis e compreensivelmente, autorizaram a realização do curso de doutorado no Laboratório de Bioquímica e Química de Proteínas.

Gratidão ao Professor Dr. Carlos André Ornelas Ricart, cuja capacidade de orientação segura e precisa na condução da minha formação acadêmica permitiu-me superar desafios e finalizar o curso de doutorado com alegria, gosto pela ciência e dentro do tempo previsto pelo Programa de Pós-Graduação em Biologia Molecular.

Ao Professor Dr. Edivaldo Ximenes Ferreira Filho, na condição de co-orientador, cujo suporte dentro do Laboratório de Enzimologia foi uma constante concernentemente ao cultivo dos microorganismos.

Ao Professor Dr. Magno Junqueira pela cooperação junto ao Instituto de Química da Universidade Federal do Rio de Janeiro no tocante à espectrometria de massas.

Ao Professor Dr. Bergman Moraes Ribeiro pela atenção, instrução e utilização da ultracentrífuga no Laboratório de Microscopia Eletrônica e Virologia (UnB).

À equipe de pesquisa sob a supervisão do Professor Dr. Carlos A. O. Ricart: doutorandos Diana Paola Gómez-Mendoza e Rayner Myr Lauterjung Queiroz, e Mestres Ana Carolline Toledo e Pedro Martins.

Gratidão à doutoranda Diana Paola Gómez-Mendoza pela amizade, companheirismo e confiança.

Gratidão à Mestre Joseana Luisa de Freitas, esposa e companheira amorosa, profissional competente. Parte da diagramação deste trabalho recebeu as suas sugestões oportunas.

À equipe técnica do Laboratório de Bioquímica e Química de Proteínas, Senhores Antonio Rufino e Nuno Manoel. Atenção e disponibilidade são marcas registradas desta equipe.

À equipe técnica do Laboratório de Enzimologia, Senhoras Marilsia e Margarete.

Aos demais Professores, aos colegas e amigos que compõem o grupo de trabalho do laboratório. A troca de ideias, sugestões e explicações foram sempre valiosas.

À banca examinadora pela gentileza em aceitar o convite de avaliar este trabalho e contribuir com a minha aprendizagem.

Ao Senhor José Valdo e sua digna esposa Senhora Aldenice Cousseiro.

À CAPES pelo suporte da bolsa de doutorado.

A todos que se sentirem contribuidores de alguma forma, meus agradecimentos.

Resumo

As enzimas que degradam parede celular vegetal produzidas por micro-organismos possuem aplicações biotecnológicas importantes, incluindo a produção de bioetanol. Algumas batérias anaeróbicas são capazes de produzir complexos multi-enzimáticos chamados de celulosomos, enquanto os fungos filamentosos normalmente secretam enzimas hidrolíticas individuais que atuam sinergisticamente no processo de degradação de polissacarídeo. Neste trabalho, nós mostramos que os fungos filamentosos *Trichoderma harzianum* e *Trichoderma reesei*, secretam complexos multi-enzimáticos ativos quando cultivados em meio contendo o resíduo agrícula bagaço de cana-de-açucar e lactose (ou galactose), respectivamente. O secretoma de ambos os fungos foram analisadas primeiramente por 1D-BN (blue native)-PAGE. Bandas eletroforéticas correspondendo a possíveis complexos foram submetidas à separação eletroforética usando sistema Tricina-SDS-PAGE para demonstrar que são constituídas de componentes menores. Ensaios zimográficos foram realizados usando 1D-BN-PAGE e 2D-BN/BN-PAGE para verificar atividades celulolítica e xilanolítica em um mesmo complexo. Finalmente, os complexos foram digeridas por tripsina e analisadas separadamente por LC-MS/MS e os programas MASCOT e MS-BLAST para identificação das proteínas constituintes. Os resultados mostraram que ambos os fungos produzem complexos constituídos por enzimas celulolítica e xilanolítica e outras proteínas, as quais apresentam uma complementariedade funcional no processo de degração de substratos polissacaridícos. Em *T. harzianum* foram analisados três complexos, os quais apresentaram os seguintes componentes: celobiohidrolase I, celobiohidrolase I-II, alfa-L-arabinofuranosidase, xilana 1,4-β-xilosidase (complexo I); acetilxilan esterase, endoquitinase, arabinogalactana, endo-1,4-β-galactosidase, celobiohidrolase I, cutinase, α-N-arabinofuranosidase e endo-β-1,4-xilanase (complexo II); glucoamilase, endo-beta-1,4-glucanase, swollenina, beta-endoglucanase ancorado a GPI, alfa-L-arabinofuranosidase, α-1,3-glucanase (complexo III). *T. reesei* produziu mais complexos multi-enzimáticos quando cultivado em meio contendo lactose que galactose. A composição dos complexos I e II em lactose parece torná-los melhores equipados para biodegradação. Os componentes dos complexos do meio com lactose são: glicosil hidrolases 20, 36, beta-1,3-endoglucanase, alfa-galactosidase, exo-beta-1,4-glucanase, aril-alcool oxidase, “predicted protein” 43, “predicted protein” 20 (complexo I); beta-1,3-endoglucanase, “predicted protein” 20, 48, 44, 61, 52, 42, glicosil hidrolase 37, quitinase (complexo II). Os complexos do meio com galactose são: glicosil hidrolases 16, 36, 54, 55, beta-1,3-endoglucanase, catalase/peroxidase bifuncional, “predicted protein” 20 (complexo I); “predicted protein” 20, 44, 61, 52, beta-1,3-endoglucanase, glicosil hidrolase 3, 37, quitinase, amidase (complexo II). Além disso, o complexo I é mais expresso em meio contendo lactose que galactose, ocorrendo inversamente com o complexo II. Juntos, esses dados mostram que a fonte de carbono influi na composição dos complexos multi-enzimáticos em *T. reesei*. A cooperatividade funcional entre os elementos dos complexos dos fungos são discutidos.

Palavras chaves: fungos filamentosos, BN-PAGE, Zimo/BN-PAGE, espectrometria de massas.

Abstract

Plant cell degrading enzymes produced by microorganisms possess important biotechnological applications; including the production of bioethanol. Some anaerobic bacteria are able to produce multienzymatic complexes called cellulosomes whilst filamentous fungi normally secrete individual hydrolytic enzymes that act synergically in the process of polysaccharide degradation. In the present work we demonstrated that the filamentous fungi *Trichoderma harzianum* and *Trichoderma reesei* secrete active multienzymatic complexes when cultivated in culture media supplemented with the agricultural residue sugarcane bagasse and lactose (galactose), respectively. The secretome of both fungi were analysed by 1D-BN (blue native) PAGE. Protein bands corresponding to possible complexes were submitted to electrophoretic separation using a Tricine-SDS system in order to demonstrate that they were constituted by smaller components. Zymographic assays were performed using 1D-BN-PAGE and 2D-BN/BN-PAGE o verify cellulolytic and cellulolytic activities in the complexes. Finally, the complexes were trypsin digested, subjected to LC-MS/MS and the results analyzed using the software MASCOT and MS-BLAST to identify their components. The results demonstrated that both organisms produced complexes constituted by cellulolytic and xylanolytic enzymes as well as other proteins related to polysaccharide degradation. Three *T. harzianum* complexes that were analyzed presented the following components: cellobiohydrolase I, cellobiohydrolase I-II, alpha-L-arabinofuranosidase, xylan 1,4-β-xylosidase (complex I); acetilxylan esterase, endochitinase, arabinogalactan, endo-1,4-β-galactosidase, cellobiohydrolase I, cutinase, α-N-arabinofuranosidase e endo-β-1,4-xylanase (complex II); glucoamilase, endo-beta-1,4-glucanase, swollenin, GPI-anchored beta-endoglucanase, alpha-L-arabinofuranosidase and α-1,3-glucanase (complexo III). *T. reesei* produced more multienzymatic complexes when grown in lactose than in galactose containing medium. The composition of complexes I and II in lactose possibly make them more suitable for biodegradation. The components of the complexes produced in the lactose medium are: glycosyl hydrolases 20, 36, beta-1,3-endoglucanase, alpha-galactosidase, exo-beta-1,4-glucanase, aryl-alcohol oxidase, "predicted protein" 43, "predicted protein" 20 (complex I); beta-1,3-endoglucanase, "predicted protein" 20, 48, 44, 61, 52, 42, glycosyl hydrolase 37, chitinase (complex II). The complexes produced in the galactose medium are glycosil hydrolases 16, 36, 54, 55, beta-1,3-endoglucanase, bifunctional catalase/peroxidase, "predicted protein" 20 (complex I); "predicted protein" 20, 44, 61, 52, beta-1,3-endoglucanase, glycosyl hydrolase 3, 37, chitinase and amidase (complex II). In addition, complex I is more expressed in lactose than in galactose medium while complex II is more expressed in galactose. Overall, the data show that the carbon source influence the composition of *T. reesei* multienzimatic complexes. The functional cooperativity between the elements of the complexes are discussed.

Key words: filamentous fungi, BN-PAGE, Zymo/BN-PAGE, mass spectrometry.

Índice

Lista de Figuras...xi

Lista de Tabelas..xiii

1. Introdução..1

1.1. Degradação enzimática de biomassa..2

1.2. Reconhecimento molecular...5

1.3. Lactose como indutor de enzimas celulolíticas.......................................6

1.4. Eletroforese *Blue Native* em Gel de Poliacrilamida (BN-PAGE)................10

2. Objetivos..11

2.1. Objetivos gerais..12

3. Materiais e Métodos...13

3.1. Cultivo e tratamento de amostra..14

3.2. BN-PAGE..15

3.3. Zimograma acoplado a BN-PAGE...16

3.4. Fração enriquecida de membrana plasmática..17

3.4.1. Ensaios para detecção de membrana...17

3.5. Método verde malaquita (“Malachite-Green”)..18

3.5.1. Solução de vanadato..18

3.5.2. Solução de verde malaquita/HCl”..18

3.5.3. Determinação de fosfato livre...19

3.6. BN-PAGE de proteinas membranosas..19

3.7. Identificação de proteínas...19

3.7.1. LC-MS/MS...19

3.7.2. Análise de dados..21

4. Resultados..22

4.1. Análise do secretoma de *T. harzianum*..23

4.2. Análise do secretoma de *Trichoderma reesei*...30

5. Discussão...35

5.1. Do método...36

5.2. Análise de complexos proteicos do secretoma de *Trichoderma harzianum*..39

5.3. Análise de complexos proteicos do secretoma de *Trichoderma reesei*......42

6. Conclusões e perspectivas..47

7. Artigos publicados...49

8. Referências..52

Lista de Figuras

Figura 1. Sistema clássico de degradação de celulose e hemicelulose. As enzimas livres em solução atuam cooperativamente no processo de degradação de polímeros de açucar . (a) Visão esquemática do sistema celulolítico. Os sítios para as principais atividades das enzimas celulolíticos são mostrados. Adicionalmente, uma rota para a formação de soforose por transglicosilação realizada pela beta-glicosidase é apresentada. (b) Visão esquemática do sistema degradativo da hemicelulose arabinoxilana. As enzimas atuando sobre o substrato estão listadas na tabela. Modificado de Aro e colaboradores (Aro, Pakula *et al.*, 2005)....3

Figura 2. Via de Leloir (Holden, Rayment *et al.*, 2003)....7

Figura 3. Diagrama do metabolismo da lactose em *T. reesei*. Enzimas envolvidas em ambas as vias possíveis são dadas em caixas cinzas e intermediários respectivos em caixas brancas. Ação indutora de Xyr1 ou galactitol (+) é indicado por seta (Stricker, Steiger *et al.*, 2007)....9

Figura 4. (A) 1D-BN-PAGE do secretoma de *T. harzianum* produzido em bagaço de cana. Este BN-PAGE dispõe de um gel de poliacrilamida 5-18%. Em cada poço foi aplicado 200 μg de proteínas do secretoma. O Gel foi fixado e corado com "Coomasie Brilliant Blue G-250". As três bandas mais intensas foram nomeadas: complexos I, II e III. (B) 1D-BN-PAGE do secretoma de *T. harzianum* em diferentes concentrações de proteínas. Nenhuma correlação entre concentração proteica (0,2 $mg.mL^{-1}$, 5,0 $mg.mL^{-1}$ and 10 $mg.mL^{-1}$) e agregação foi observado. Diferentes volumes de cada uma das amostras foi usada para tornar as bandas visíveis mesmo em baixas concentrações: 0,2 $mg.mL^{-1}$ (400 μL), 5,0 $mg.mL^{-1}$ (60 μL) and 10 $mg.mL^{-1}$ (20 μL)....24

Figura 5. Curva de regressão linear simples para estimar massa molecular dos complexos separados por 1D-BN-PAGE. A equação da reta obtida foi $f(x) = 0{,}734896 (\pm 0{,}075)x + 2{,}100147 (\pm 0{,}180)$; $r^2 = 0{,}97$, $p < 0{,}05$). Log *MW*: logarítmo de base 10 da massa molecular. *Rf*: fator de retenção relativa....25

Figura 6. 2D-BN-PAGE do secretoma de *T. harzianum* produzido em meio contendo bagaço de cana como fonte de carbono. Um gel gradiente 1D-BN-PAGE (5-18%) foi usado na primeira dimensão (*esquerda*) para separar os complexos. Este gel foi corado Comassie Brilliant Blue G-250. O gel Tricine-SDS-PAGE foi corado com prata e usado para analisar as subunidades dos complexos I, II e III na segunda dimensão (*direita*)....25

Figura 7. Zimografia 1D-BN-PAGE do secretoma do *T. harzianum*. Para detecção das atividades celulolítico e xilanolítico, substrates de xilana e celulose foram incorporados dentro dos géis. O gel às esquerda foi corado com Coomasie Brilliant Blue G-250. Os zimogramas foram corados com Congo Red, conforme descrito em Materiais e Métodos....27

Figura 8. Zimograma 2D-BN/BN-PAGE do secretoma de *T. harzianum*. Para a detecção das atividades celulolítica e xilanolítica, cellulose e xilana foram incorporados dentro dos géis. Os zimogramas foram corados com Congo Red como descrito em Materiais e Métodos....29

Figura 9. **(A)** Perfil eletroforético do secretoma de *T. reesei* em gel de poliacrilamida "blue-native" (BN-PAGE) sob diferentes concentrações: 10 $mg.mL^{-1}$ (a), 2 $mg.mL^{-1}$ (b), 0,3 $mg.mL^{-1}$ (c) e 0,0875 $mg.mL^{-1}$ (c*). O gradiente de poliacrilamida variou de 5 a 18% T para ambas as fontes de carbono. Diferentes quantidades de proteína total foram usadas para tornar visíveis as bandas menos intensas: 10 µL (a), 50 µL (b) and 300 µL (c and c*). c* e c correspondem à concentração específica encontrada na cultura contendo galactose (0,3%) e lactose (1%), respectivamente. Marcador molecular: tiroglobulina (669 kDa), ferritina (440 kDa), catalase (232 kDa), aldolase (158 kDa) e albumina (67 kDa) (SIGMA). As bandas I e II são complexos multiproteicos. Os experimentos foram feitos em triplicatas. **(B)** "Zoom" mostrando três complexos de alta massa molecular mas de baixa intenside e presentes na amostra crescida em latose marcados por astericos brancos. 31

Figura 10. Regressão linear simples. A equação da reta obtida foi $f(x) = -0{,}514821\ (\pm\ 0{,}014)x + 1{,}54386\ (\pm\ 0{,}035)$. Log *MW*: logarítmo de base 10 da massa molecular. *Rf*: fator de retenção relativa. ($r^2 = 0{,}997$; $p < 0{,}05$). Os valores das massas moleculares relativas de cada complexo podem ser encontrados na Tabela II..31

Figura 11. Zimograma 2D-BN/BN-PAGE do secretoma (10 $mg.mL^{-1}$) de *T. reesei* cultivado em lactose e galactose. Os géis de ambas as dimensões foram feitos com gradiente de poliacrilamida, variando de 5 a 18%. A concentração dos substratos (celulose e xilana) em gel foi de 0,01 $g.mL^{-1}$ (1%). A zona esbranquiçada paralela à seta tracejada corresponde à atividade enzimática. Marcador molecular: tiroglobulina (669 kDa), ferritina (440 kDa), catalase (232 kDa), aldolase (158 kDa) e albumina (67 kDa) (SIGMA). 32

Figura 12. Subfracionamento de membranas em *Trichoderma reesei* por ultracentrifugação isopícnica em gradiente de sacarose (20 – 50%). Fonte de carbono: β-Lactose. Marcadores: membrana plasmática (ensaio da ATPase sensível a vanadato) e membrana de golgi (ensaio da UDPase). A linha tracejada permite visualizar a tendência gráfica..34

Lista de Tabelas

Tabela I. Lista de proteínas identificadas por espectrometria de massa nos três complexos encontrados no secretoma de *T. harzianum*..28

Tabela II. Concentração da atividade enzimática (UI.mL^{-1}) de celulases e xilanases presentes no secretoma de *T. reesei* cultivado em meio contendo lactose e galactose como fontes de carbono. A concentração proteica das amostras foi de 10 mg.mL^{-1} (onde n = 3)..32

Tabela III. Proteínas identificadas por MASCOT dos complexos I e II presentes no secretoma de *T. reesei* cultivado em meio contendo lactose e galactose como fontes de carbono...34

1. Introdução

1.1. Degradação enzimática de biomassa

O material da parede celular dos vegetais, principalmente celulose, hemicelulose e pectina, não é acumulado na Terra devido à ação eficiente de micro-organismos como fungos e bactérias (De Castro, Pedro *et al.*, 2010).

A decomposição integral de celulose e hemicelulose a moléculas simples (glicose) depende da ação combinada de diferentes enzimas livres na solução e suas especificidades quanto ao substrato. No caso da celulose, as celobiohidrolases clivam unidades de celobiose a partir das extremidades das cadeias celulolíticas. As endoglicanases cortam as cadeias de celulose internamente, principalmente a partir das regiões amorfas, fornecendo às celobiohidrolases mais extremidades alvo. Finalmente, as beta-glicosidases hidrolisam celobiose a glicose, o qual serve como uma fonte facilmente metabolizável para os fungos. Esta mesma enzima pode converter celobiose em soforose, fenômeno denominado de transglicosilação (Figura 1a). Quanto à hemicelulose, sua decomposição é bem conhecida. A hidrólise das hemiceluloses processa pela ação coordenada de endo-enzimas que clivam internamente a cadeia principal. As exo-enzimas liberam açucares monoméricas da extremidade da molécula, enquanto as enzimas auxiliares clivam as cadeias laterais dos polímeros ou oligossacarídeos. Por exemplo, a decomposição da xilana envolve pelo menos endoxilanases e beta-xilosidases que atuam sobre a cadeia principal do açucar, e dependendo do tipo de xilana as cadeias laterais são clivadas por enzimas tais como alfa-glicuronidase e acetilxilano esterase (Figura 1b) (Aro, Pakula *et al.*, 2005).

Perante isso, percebe-se que a eficiência da degradação de biomassa vegetal é resultado de dois fatores correlacionados: grande número de enzimas extracelulares (celulases, hemicelulases e pectinases) secretadas por micro-organismos e o sinergismo existentes entre elas. Essa característica torna aqueles micro-organismos imprescindíveis na reciclagem de carbono no ecossistema (Mayer e Staples, 2002).

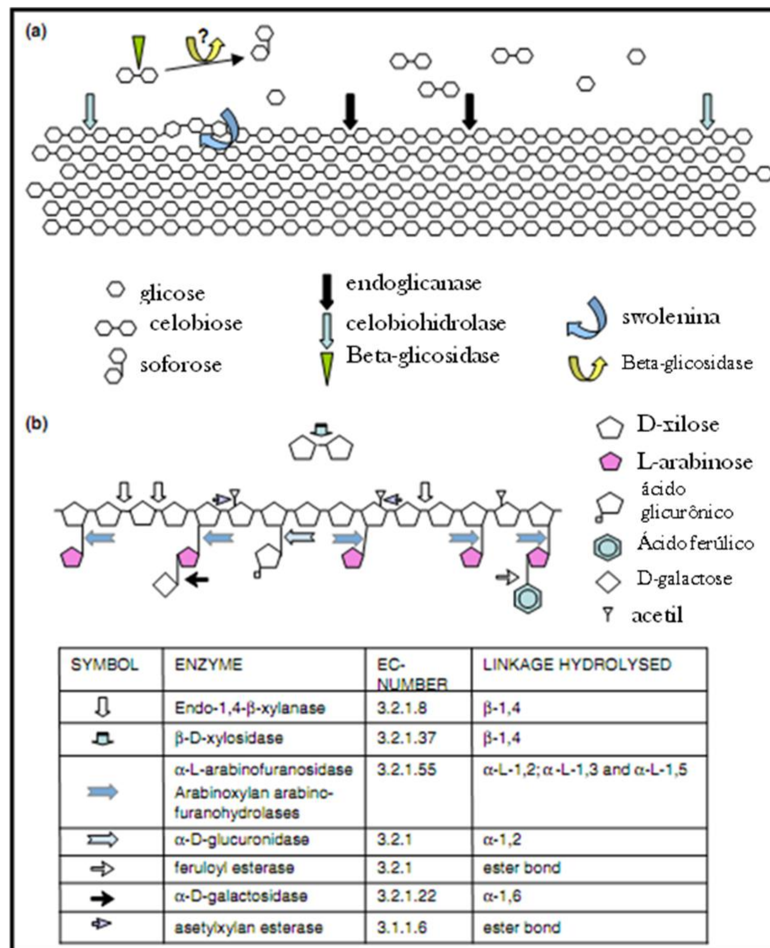

SYMBOL	ENZYME	EC-NUMBER	LINKAGE HYDROLYSED
⇩	Endo-1,4-β-xylanase	3.2.1.8	β-1,4
	β-D-xylosidase	3.2.1.37	β-1,4
➡	α-L-arabinofuranosidase Arabinoxylan arabino-furanohydrolases	3.2.1.55	α-L-1,2; α-L-1,3 and α-L-1,5
⇨	α-D-glucuronidase	3.2.1	α-1,2
⇨	feruloyl esterase	3.2.1	ester bond
→	α-D-galactosidase	3.2.1.22	α-1,6
	asetylxylan esterase	3.1.1.6	ester bond

Figura 1. Sistema clássico de degradação de celulose e hemicelulose. As enzimas livres em solução atuam cooperativamente no processo de degradação de polímeros de açucar . **(a)** Visão esquemática do sistema celulolítico. Os sítios para as principais atividades das enzimas celulolíticos são mostrados. Adicionalmente, uma rota para a formação de soforose por transglicosilação realizada pela beta-glicosidase é apresentada. **(b)** Visão esquemática do sistema degradativo da hemicelulose arabinoxilana. As enzimas atuando sobre o substrato estão listadas na tabela. Modificado de Aro e colaboradores (Aro, Pakula *et al*., 2005).

As bactérias anaeróbicas *Clostridium thermocellum*, *Clostridium cellulovorans*, *Acetivibrio cellulolyticus* e *Bacteroides cellulosolvens*, produzem e secretam complexos multi-enzimáticos chamados celulosomos, estruturas com alta eficiência de degradação de celulose, comparativamente ao clássico sistema de enzima livre, promovendo uma grande competitividade local desses micro-organismos (Shoham, Lamed *et al*., 1999). Um celulosomo consiste de duas partes: a parte não catalítica (representada pela proteína escafoldina, “scaffoldin”) integra as diferentes glicosil hidrolases que compõem a segunda parte, chamada catalítica (Fontes e Gilbert, 2010).

Diferentemente, as bactérias anaeróbicas *Butyvibrio fibrisolvens* e *Clostridium papyrosolvens* produzem complexos multi-enzimáticos que são estruturalmente distintos dos celulosomos encontrados em *C. thermocellum*, porquanto não possuem escafoldina

na sua composição. Por exemplo, *B. fibrisolvens* tem um complexo contendo 11 enzimas com atividade xilanolítica e três com atividades endoglucanase. Esta estrutura tem sido conhecida como "xilanosomo". O caso do *C. papyrosolvens* ainda é mais notável, porquanto seu supercomplexo enzimático contém sete complexos menores, ou subcomplexos, cujas massas moleculares variam de 500 a 600 kDa (Pohlschröder, Leschine *et al.*, 1994; Beg, Kapoor *et al.*, 2001).

Assim como *B. fibrisolvens* e *C. papyrosolvens*, os fungos anaeróbicos do gênero *Neocalimastix*, *Piromyces* e *Orpinomyces* não possui escafoldina em seus complexos multi-enzimáticos (Fontes e Gilbert, 2010). Uma glicosidase foi encontrada e identificada como uma escafoldina potencial em *Piromyces equi*s (Nagy, Tunnicliffe *et al.*, 2007). Trabalhos recentes relataram a presença de complexos multi-enzimáticos também em fungos filamentosos aeróbicos, como *Chaetomium* sp. e *Penicillium purpurogenum*. Como nos fungos e bactérias anaeróbicas mencionadas, estes fungos não possuem escafoldina, diferindo da estrutura típica de *Clostridium thermocellum*.(Ohtsuki, Suyanto *et al.*, 2005; Gonzalez-Vogel, Eyzaguirre *et al.*, 2011).

Os fungos filamentosos, como importantes produtores de enzimas degradadoras de biomassa vegetal, possuem grande potencial biotecnológico. Os fungos dos gêneros *Aspergillus* e *Trichoderma* são os mais utilizados para este fim devido ao amplo espectro de enzimas hidrolíticas de polissacarídeos que secretam (Stricker, Mach *et al.*, 2008).

Enzimas produzidas por fungos do gênero *Trichoderma*, por exemplo, possuem aplicações nas indústrias têxtil (Bhat, 2000), farmacêutica (Roseli Garcia Medeiros e Filho, 2007), de papel (Selvaraj, 2000) e de biocombustíveis (Polizeli, Rizzatti *et al.*, 2005). Além de produtores de enzimas de interesse industrial, espécies desse gênero, como o *Trichoderma harzianum*, são usadas comercialmente para controle biológico eficiente contra fungos fitopatogênicos, tais como *Rhizoctonia solani*, *Botrytis cinerea*, *Sclerotium rolfsii*, *Sclerotinia sclerotiorum* e *Pythium* spp. (Gary, 1998). Sua atividade micoparasítica consiste, particularmente, na produção de quitinases, proteases e beta-1,3-glicanases capazes de hidrolizar a parede celular dos fungos fitopatogênicos (Ulhoa e Peberdy, 1991; Grondona, Hermosa *et al.*, 1997; Viterbo, Ramot *et al.*, 2002; Monteiro, Do Nascimento Silva *et al.*, 2010). Além disso, *T. harzianum* vem se tornando também um organismo promissor na produção de celulases e xilanases sob condições apropriadas (Franco, Dias *et al.*, 2004). Uma cepa de *T. harzianum* (IOC-4038) produziu um conjunto bem

balanceado de enzimas celulolíticas, além de uma cinética rápida na produção de endoglicanases e β-glicosidases, quando comparado com *T. reesei* (De Castro, Pedro *et al.*, 2010).

A espécie *T. reesei* é considerado o principal produtor de celulases de interesse industrial. Este ascomiceto é um dos muitos fungos sapróbicos capazes de degradar eficientemente os polissacarídeos das paredes celulares vegetais.(Percival Zhang, Himmel *et al.*, 2006; Kumar, Singh *et al.*, 2008; Martinez, Berka *et al.*, 2008; Portnoy, Margeot *et al.*, 2011). A maquinaria celulolítica desse potente produtor de celulases é constituída por duas celobiohidrolases, cinco endoglicanases e duas β-glicosidases. Várias hemicelulases, incluindo xilanases, mananases e galactosidases são adicionalmente secretadas por esse fungo (Nidetzky, Steiner *et al.*, 1994).

Até o momento, não existem relatos da presença de complexos multi-enzimáticos em secretoma de *T. reesei* e *T. harzianum*. Considerando a importância industrial, biotecnológico e acadêmica desses fungos, verificar se possuem complexos de enzimas no secretoma é uma oportuna linha de investigação. A presença de tais complexos permitiria realizar pesquisas futuras que determinassem a sequência de associação dos componentes, a estequeometria de cada um deles, suas constantes de associação e se alteram seus componentes sob condições diferentes de fontes de carbono. Estes dados permitiram, consequentemente, a elaboração de protocolos para produção de diferentes complexos de degradação de substratos específicos.

1.2. Reconhecimento molecular

O mecanismo de reconhecimento molecular de polissacarídeos vegetais, sustentado atualmente, consiste na hipótese da secreção constitutiva basal. Segundo este modelo, o micro-organismo secretaria constantemente enzimas hidrolíticas em baixas concentrações. Tais enzimas degradariam os polissacarídeos, produzindo monossacarídeos, os quais entrariam na célula provocando a indução transcricional de determinados genes para enzimas celulolíticas e hemicelulolíticas. Esta hipótese exclui a possibilidade de existência de um receptor para o reconhecimento dos substratos na membrana plasmática. No entanto, dados recentes têm acrescentado novas ideias ao modelo vigente.

Surpreendentemente, o nível dos transcritos dos genes que codificam as celobiohidrolases I (*cbh1*) e II (*cbh2*) em *T. reesei* cultivado em lactose é maior que em D-galactose. No entanto, a indução de celulases por D-galactose ocorre somente em taxas baixas de crescimento (0,015 h^{-1}), sugerindo outra via de sinalização hipotética para o aumento da indução de celulases em meio lactose. A existência de uma permease para lactose e de uma β-galactosidase (enzima que hidrolisa lactose em galactose e glicose) intracelular seria pré-requisito para viabilizar tal mecanismo, porém, até agora, essas proteínas não foram encontradas nesse fungo (Karaffa, Fekete *et al.*, 2006).

Resultados semelhantes foram encontrados para celulose e soforose. Os dados mostraram que *T. reesei* apresenta maior atividade celulolítica em meio de cultura contendo celulose que soforose, indutor de celulases para esse fungo. O perfil eletroforético do meio de cultura contendo celulose mostrou bandas fortes de endo e exo-glicanases, inexistentes na cultura contendo soforose. Além disso, duas bandas de endoglicanases que são compartilhadas por ambos os meios diferiram em intensidade: a do meio contendo celulose é mais intensa (Sternberg e Mandels, 1979).

Estes dados supramencionados sugerem a existência de uma proteína receptora (sensora) situada na membrana plasmática de *T. reesei*, possivelmente acoplada a uma via de sinalização celular específica que intensificaria a produção de algumas enzimas e induziria outras.

1.3. Lactose como indutor de enzimas celulolíticas

A lactose (1,4-O-β-D-galactopiranosil-D-glicose) é um subproduto do leite. Cerca de 300.000 toneladas desse açucar são acumuladas anualmente, das quais 15% é fermentado por diversos micro-organismos. A lactose é a única fonte de carbono hidrosolúvel usada para a produção de celulases e exclusivamente requerida na produção de proteínas heterólogas sob controle de promotores de celulases em *T. reesei* (Seiboth, Hofmann *et al.*, 2002). O metabolismo da lactose é lento, mesmo assim esse dissacarídeo é uma fonte atrativa de carbono para a produção de enzimas em nível indústrial (Karaffa, Fekete *et al.*, 2006).

O metabolismo da lactose segue a via de Leloir, e envolve as seguintes enzimas: galactose mutarotase, galactoquinase, galactose-1-fosfato uridiltransferase e UDP-

galactose-4-epimerase. Resumidamente, a lactose é clivada extracelularmente a β-D-galactose e D-glicose pela β-galactosidase. A β-D-galactose é convertida a α-D-galactose (1ª etapa da via de Leloir), processo denominado epimerização e catalisado pela galactose mutarotase. Alfa-D-galactose é fosforilada a galactose-1-fosfato (2ª etapa) pela galactoquinase. A galactose-1-fosfato uridiltransferase catalisa a transferência de um grupo UMP a partir de UDP-glicose para a galactose-1-fosfato, formando a glicose-1-fosfato e UDP-galactose (3ª etapa). Esta, finalmente, é convertida a UDP-glicose pela UDP-galactose-4-epimerase (4ª etapa) (Figura 2) (Holden, Rayment *et al.*, 2003).

Dados anteriores relataram que as etapas metabólicas posteriores à produção de galactose-1-fosfato, catalizada pela enzima galactoquinase, não são essenciais para a indução de celulases (Seiboth, Hofmann *et al.*, 2002). Assim, experimentos visando a dectecção da molécula indutora de celulases focaram as enzimas galactosidase, galactoquinase e galactose mutarotase.

Experimentos de deleção do gene codificador da galactoquinase (*gal1*) reduziram consideravelmente a transcrição das celobiohidrolases *cbh1* e *cbh2*, sugerindo que o indutor de celulases em *T. reesei* é D-galactose ou galactose-1-fosfato. A baixa transcrição desses genes foi atribuída à outra via de produção de celulases, cujo intermediário metabólico é o aminoálcool galactitol (Seiboth, Hartl *et al.*, 2004).

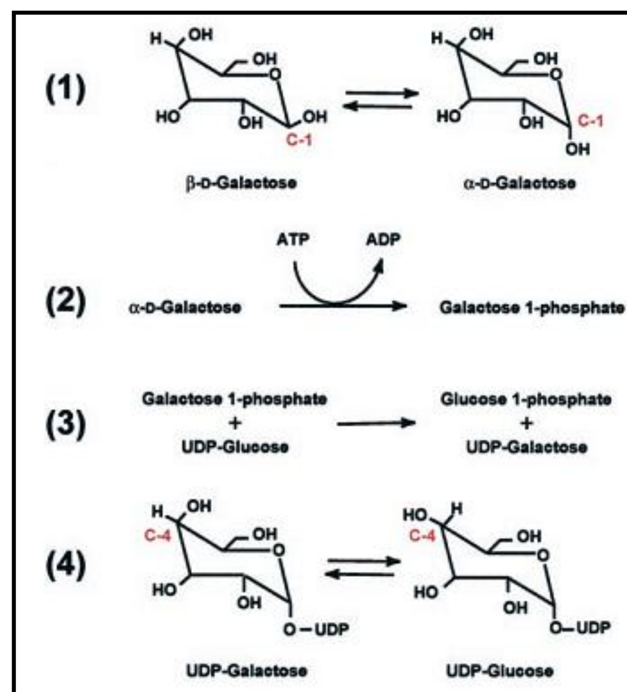

Figura 2. Via de Leloir (Holden, Rayment *et al.*, 2003).

Diferentemente das bactérias, *T. reesei* hidroliza a lactose extracelularmente pela β-galactosidase 1. Uma possível permease para o dissacarídeo não foi encontrada. A deleção do gene para β-galactosidase 1 aumentou a expressão de *cbh1* e *cbh2*, sugerindo a existência de uma atividade galactosidásica secundária, provavelmente mimetizada por alguma glicosidase. Por outro lado, sua superexpressão reduziu drasticamente a expressão das celobiohidrolases. Portanto, D-galactose ou galactose-1-fosfato seriam os indutores somente em faixa estreita de concentração intracelular. A superexpressão de *bga1* influi nos níveis estacionários dos indutores, promovendo o desligamento da transcrição enzimática (Seiboth, Hartl *et al.*, 2005).

A enzima galactose mutarotase está presente na maioria dos organismos (bactérias, fungos, plantas e mamíferos) (Keston, 1954; Bentley e Bhate, 1960; Wallenfels, Hucho *et al.*, 1965; Bailey, Fishman *et al.*, 1966). Essa enzima converte β-D-galactose em α-D-galactose, forma anomérica necessária para a via de Leloir, onde a galactoquinase tem papel imprescindível (Holden, Rayment *et al.*, 2003). O catabolismo da β-D-galactose por *T. reesei* ocorre mais fortemente por uma via alternativa que pela de Leloir, uma vez que esse fungo não apresenta atividade mutarotase, mesmo portando três genes para aldose-1-epimerase (*aep1*, *aep2* e *aep3*) (galactose mutarrotase) em seu genoma (Fekete, Seiboth *et al.*, 2008).

Embora a interconverção dos anômeros de D-galactose ocorra espontaneamente em água pura, a conversão eficiente *in vivo* depende da presença de mutarotases, indicando que a atividade intracelular da água não é alta o suficiente para permitir uma mutarrotação espontânea (Bouffard, Rudd *et al.*, 1994).

Em *T. reesei*, a presença de α-D-galactose intracelular é devida, provavelmente, à mutarrotação espontânea em ambiente extracelular, antes da sua absorção pelo fungo. Fekete e colaboradores mostraram que o indutor é indubitavelmente D-galactose (não galactose-1-fosfato), exigindo sua forma anomérica β. A ausência de atividade mutarrotase neste fungo é necessária para a indução das enzimas celulolíticas (Fekete, Seiboth *et al.*, 2008).

A proteína Xyr1 (“Xylanase regulator 1”) regula os genes que codificam as principais enzimas hidrolíticas no gênero *Trichoderma*: *cbh1* e *cbh2* (celobiohidrolases I e II), *egl1* (endoglucanase I), *xyn1* e *xyn2* (endoxilanases I e II) e *bxl1* (β-xilosidase I), e *bgl1* (β-glicosidase I). Xyr1 não é afetada pelas moléculas mediadoras da indução (xilose, xilobiose, soforose, galactose), além de ser indispensável a todas as formas de expressão gênica (basal, repressiva e indutiva) (Stricker, Grosstessner-Hain *et al.*, 2006).

Striker e colaboradores mostraram que a proteína Xyr1 recebe o sinal da lactose e intermedia a regulação transcricional dos genes de xilanases e celobiohidrolases (Figura 3). A D-xilose redutase – primeira enzima da via alternativa – é a responsável pela conversão de D-galactose em galactitol, o qual induz a transcrição de *bga1* e também a produção de celulases: Xyr1 age indiretamente sobre *bga1*. A análise *in silico* da região promotora de *xyl1* resultou na identificação de dois domínos de ligação para Xyr1, confirmando os resultados acima (Stricker, Steiger *et al.*, 2007).

Xyr1 possui dois sítios de ligação ao promotor do gene *xyn1*. A base da indução para esse gene consiste na dimerização de Xyr1, onde cada fator de transcrição ligará em um único sítio de ligação. A repressão da transcrição é mantida por um complexo formado por Xyr1, Ace1 (proteína repressora) e Aip (proteína associada a Ace1), dependente de glicose. Portanto, Ace1 compete com Xyr1 por um dos sítios de ligação na região promotora do *xyn1* (Stricker, Mach *et al.*, 2008). Esse mecanismo também foi encontrado para o gene *cbh1* (Ling, Qin *et al.*, 2009).

Dados mais recentes mostram que a indução de *xyr1* por lactose é completamente independente do metabolismo da galactose. O mecanismo pelo qual *xyr1* responde a lactose e a galactose ainda permanece desconhecido. Como lactose não é absorvido por *T. reesei*, então seu efeito, mesmo na ausência do metabolismo de D-galactose, deve ser devido a um processo de sinalização (Portnoy, Margeot *et al.*, 2011).

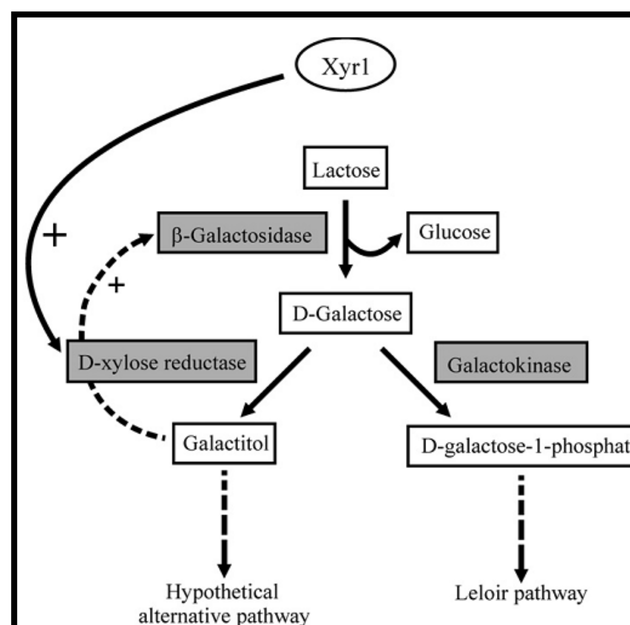

Figura 3. Diagrama do metabolismo da lactose em *T. reesei*. Enzimas envolvidas em ambas as vias possíveis são dadas em caixas cinzas e intermediários respectivos em caixas brancas. Ação indutora de Xyr1 ou galactitol (+) é indicado por seta (Stricker, Steiger *et al.*, 2007).

1.4. Eletroforese *Blue Native* em Gel de Poliacrilamida (BN-PAGE)

O método eletroforético "Blue Native" é uma técnica eletroforética nativa que consiste no uso de CBB para conversar estruturas oligoméricas proteicas em solução, dando carga negativa para o deslocamento das moléculas. A presença de CBB associado às proteínas evita a formação de agregados proteicos e conversa o estado nativo da amostra. BN-PAGE foi desenvolvido para separar complexos proteicos nativos a partir de membranas biológicas e de proteínas (ácida e básica) hidrossolúveis. Em combinação com uma segunda dimensão de SDS-PAGE, torna-se possível determinar a massa molecular, estados oligoméricos, detectar subcomplexos e o nível de pureza da amostra (Schägger, H., Cramer, W. *et al.*, 1994). O sucesso do BN-PAGE para proteínas de membrana depende da solubilização da amostra para que se possa estabelecer a concentração ótima do detergente não iônico (η-dodecil-β-maltosídeo, triton X-100 e digitonina) (Reisinger e Eichacker, 2008).

O método BN-PAGE tem contribuído na busca de respostas para diferentes questões: a existência de complexos multicristalinos nas frações de proteinas hidrossolúveis de alto peso molecular, presentes nas lentes oculares humanas normais e com cataratas (Srivastava, Chaves *et al.*, 2008), a verificação do envolvimento da maquinaria HSP (chaperona) na produção do vírus hepatite B (Liu, Qian *et al.*, 2009), a definição dos proteomas mitocondriais de alguns órgãos de rato submetidos a condições fisiologicamente significativas (Reifschneider, Goto *et al.*, 2006), estudo oligomérico ativo da ATP-Sintetase em mitocôndria de mamíferos (Krause, Reifschneider *et al.*, 2005), a análise do estado oligomérico da F1F0-ATP sintetase de mitocôndria de levedura (Arnold, Pfeiffer *et al.*, 1998), dentre outras.

Nesse contexto, e devido à versatilidade do método, BN-PAGE está sendo aplicada em diferentes áreas de pesquisa: importação celular de proteínas, dinâmica de biogênese, associação de complexos protéicos em membranas, alterações de mitocôndrias em apoptose, encefalopatias mitocondriais, carcinogênese e doenças neurodegenerativas (Wittig e Schägger, 2009).

2. Objetivos

2.1. Objetivos gerais

O presente trabalho objetivou verificar a presença e caracterizar complexos multi-enzimáticos em secretomas dos fungos filamentosos *T. harzianum* e *T. reesei*.

Para atingir os objetivos as etapas apresentadas abaixo foram realizadas.

1. Submeter amostras de secretoma de *T. harzianum* e *T. reesei*, cultivados em fontes de carbono de interesse industrial e biotecnológico (bagaço de cana de açucar, lactose e galactose, respectivamente), à eletroforese tipo BN-PAGE;

2. Caracterizar a composição dos complexos dos secretomas usando espectrometria de massas;

3. Verificar a atividade enzimática nos complexos dos secretomas usando métodos zimográficos;

4. Obter frações enriquecidas de membrana plasmática de *T. reesei* sob duas fontes diferentes de carbono (lactose e galactose) para análise por BN-PAGE;

3. Materiais e Métodos

3.1. Cultivo dos fungos e preparação dos secretomas

O fluxograma abaixo mostra as etapas de trabalho realizado nesta pesquisa.

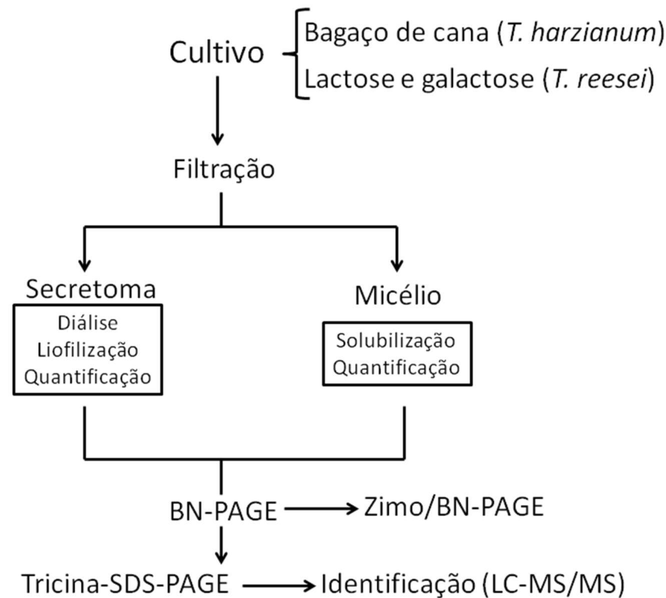

O *T. harzianum* (cepa T4) foi fornecido por I. S. Melo (Embrapa/CNPMA, Brasil), constituindo uma parte da coleção de cultura do Laboratorio de Enzimologia (Universidade of Brasília, UnB). O fungo foi cultivado em meio sólido SM (KH_2PO_4 680 mg, K_2HPO_4 870 mg, $(NH_4)_2SO_4$ 1,7 g, KCl 200 mg, $CaCl_2$ 200 mg, $MgSO_4.7\ H_2O$ 200 mg, $FeSO_4$ 2 mg, $MnSO_4$ 2 mg e $ZnSO_4$ 2 mg em 1 L de água destilada, pH 6,0) suplementado com 1% (m/v) de bagaço de cana como fonte de carbono (Suárez, Sanz *et al.*, 2005). O bagaço de cana foi lavado abundantemente com água destilada e esterilizada por autoclave 121^oC durante 1 h. O material vegetal foi seco "overnight" a 60^oC e moído. Após 6 dias de crescimento do fungo, uma suspensão de esporos (10^8 spores.mL^{-1}) foi inoculado em 300 mL de meio líquido SM (frasco de Erlenmeyer de 1 L) contendo 1% (m/v) de bagaço de cana e incubado a 28ºC sob agitação (150 rpm, durante 10 dias). Finalmente, o secretoma foi separado do micélio por filtração usando um papel Watmann nº 1.

O *T. reesei* foi cultivado em meio BDA (batata, dextrose e ágar). Os esporos obtidos foram transferidos para o seguinte meio (g.L^{-1}): NH_4H_2PO4 (8), Na_2HPO_4 (7), KH_2PO_4 (4), $CaCl_2$ (1), $MgSO_4$ (1), glicerol (10), peptona (0,1), FeSO4.7H2O (0,25), MnSO4.H2O

(0,08), $ZnSO_4.7H2O$ (0,07) e $CoCl_2$ (0,085) (Karaffa, Fekete *et al.*, 2006). Após 10 dias de cultivo em agitação (28ºC, 120 rpm), o micélio foi separado do secretoma por filtração usando papel Watmann nº 1. A biomassa micelar foi transferida para o mesmo meio, porém glicerol e peptona foram substituídos por lactose (1%, m/v) e galactose (0,3%, m/v) como única fonte de carbono e mantidos por mais 10 dias. Após cultivo, a massa micelar foi separado do secretoma como feito para *T. harzianum*.

Ambos os secretomas, *T. harzianum* e *T. reesei*, foram concentrados utilizando uma membrana discoidal (SIGMA. NMWL: 10.000 Da; diâmetro: 76 mm), dialisado e liofilizado. A amostra foi ressuspendida em água milli-Q, quantificada e armazenada a – 20ºC.

A concentração protéica nos secretomas e na membrana foi determinada pelo método do ácido bicinconínico, usando um "BCA Protein Assay kit" (Pierce Biotechnology, Rockford, IL). O BSA foi usado como molécula padrão para produção da curva de regressão linear simples.

3.2. BN-PAGE

O método BN-PAGE foi aplicado a proteínas hidrossolúveis, conforme descrito anteriormente (Schägger, H., Cramer, W. A. *et al.*, 1994). As proteínas do secretoma (*T. harzianum* e *T. reesei*) foi ressuspendida em tampão Bis/Tris-HCl 50 mM pH 7,0 contendo ácido aminocapróico 0,5 M e glicerol 15% (v/v).

Na primeira dimensão de BN-PAGE (1D-BN-PAGE), as amostras em diferentes concentrações foram aplicadas em géis gradientes 5-18% (m/v), sob corrente elétrica constante de 15 mA, a 4°C por 4h no sistema eletroforético 600 SE (Hoefer, Inc, San Francisco, CA). O tampão anódico continha Bis/Tris-HCl 50mM pH 7,0, enquanto o tampão catódico continha Tricina 50 mM, Bis/Tris-HCl 15mM pH 7,0 e CBB G-250 (Bio-Rad, Hercules, CA) 0,02 % (m/v). Os géis foram fixados e corados usando CBB G-250 (Schägger, 2006; Wittig, Braun *et al.*, 2006). Um kit de calibração (Pharmacia LKB, Piscataway, NJ) constituído de tiroglobulina (669 kDa), ferritina (440 kDa), catalase (232 kDa), lactato desidrogenase (158 kDa) e albumina do soro bovino (67 kDa) foi usado para estimativa da massa molecular relativa.

Na segunda dimensão BN-PAGE foi produzido um gel usando Tricina-SDS-PAGE, conforme descrito anteriormente (Schägger, H., Cramer, W. A. *et al.*, 1994). Primeiramente, pedaços de gel 1D-BN-PAGE, correspondendo a possíveis complexos proteicos, foram incubadas em solução SDS 1% (m/v), β-mercaptoethanol 1% (v/v) por 2 h

a temperatura ambiente. Os pedaços do gel foram lavados com água milli-Q para remover completamente o β-mercaptoethanol e, conseguintemente, posicionado entre as placas de vidro. Uma mistura de tricina, SDS e poliacrilamida 16% (m/v) (16% T e 3%C) foi colocado a 2 cm dos pedaços do gel da 1D-BN-PAGE. Após polimerização foi adicionado uma camada (1,5 cm) de gel Tricina-SDS-PAGE 10% (m/v) (10% T e 3%). Finalmente, os pedaços do gel foram embebidos em um gel nativo de poliacrilamidade 10% (m/v) contendo glicerol 10% (v/v) e SDS 0,2% (m/v). O sistema eletroforético foi submetido a uma corrente elétrica constante (50 mA), a 18ºC por aproximadamente 10 h. Os géis Tricina-SDS-PAGE foram fixados e corados com prata (Blum, Beier *et al.*, 1987).

3.3. Zimograma acoplado a BN-PAGE

Para zimografia usando 1D-BN-PAGE, os secretomas de ambos os fungos (*T. harzianum* e *T. reesei*) foram submetidos a 1D-BN-PAGE usando géis copolimerizados com xilana (*oat spelts*) ou carboximetilcelulose (CMC), a 0,1% (m/v) cada (Sigma-Aldrich Co, St Louis, MO). Este procedimento visou detectar as atividades xilanolítica e celulolítica dos complexos.

Alternativamente foram produzidos zimogramas bidimensionais do tipo 2D-BN-BN-PAGE. Para tanto, o primeiro passo foi obter géis de 1D-BN-PAGE não copolimerizado com os polissacarídeos. O segundo passo foi submeter as fitas desses géis a uma segunda dimensão de BN-PAGE com géis contendo celulose ou xilana (2-D-BN/BN-PAGE). Após corrida eletroforética, o gel 2-D-BN/BN-PAGE foi lavado 3 vezes com acetato de sódio 50 mM pH 5,5 e incubado por 10 min a 85°C – 90°C para ensaio de atividade xilanolítico (Sunna, Puls *et al.*, 1997) ou por 1 h a 55°C para ensaio de atividade celulolítico (Bischoff, Rooney *et al.*, 2006; Matsui e Ban-Tokuda, 2008). A reação foi finalizada incubando o gel a 4°C (“overnight”). Os géis foram corados com Congo Red 0,1% (m/v) por 30 min. A atividade enzimática foi observada como uma região esbranquiçada contrastando com o vermelho-escuro do “background”. A visualização desse contraste foi melhorada aditando ponderadamente ácido acético 0,5% (v/v) no gel.

Paralelamente, a quantificação da concentração da atividade enzimática (UI.mL^{-1}) para xilanase e celulase em solução foi realizada pelo método Miller (1959). Os seguintes ensaios foram realizados: enzima total (25 μL da amostra mais 50 μL de substrato, xilana ou CMC); branco substrato (50 μL de substrato mais 25 μL água milli-Q); branco enzima

(25 μL de amostra mais 50 μL de água milli-Q); branco-água (75 μL de água milli-Q). Todos foram incubados por 30 min a 50ºC, após o qual foi adicionado 150 μL de DNS e ferver por 10 min. Finalmente foi adicionado 750 μL de água milli-Q. A leitura foi realizado usando um espectrofotômetro SpectraMax.

3.4. Fração enriquecida de membrana plasmática

O micélio de *T. reesei* foi lavado com solução NaCl 0,9% e submetido a um tampão de moagem (HEPES-KOH 20 mM pH 7,5, KCl 10 mM, $MgCl_2$ 5 mM, EGTA 1 mM, DTT 1 mM e PMSF 200 μM, 3 mL por grama de micélio). A solução foi incubada em gelo por 30 minutos.

A solução foi macerada com almofariz e pistilo (em gelo) juntamente com bilhas de vidro (diâmetro: 0,45 – 50 mm). As bilhas e resíduos celulares foram removidos por centrifugação (4000 g, 10 minutos, 4ºC). O sobrenadante foi centrifugado 15.000 g por 10 minutos a 4ºC. O sobrenadante resultante foi submetido a uma nova centrifugação (100.000 g, 1 hora, 4ºC). O “pellet” foi ressuspendido em água e aplicado em tubo com gradiente de sacarose (25 a 50%), o qual foi submetido a uma centrifugação isopícnica (80.000 g, 10 horas, 4ºC).

Todas as centrifugações foram realizadas usando ultracentrífuga Beckamn (Laboratório de Microscopia e Virologia – UnB). O gradiente foi fracionado manualmente em volume de 1 mL. A amostra foi congelada em nitrogênio líquido e estocada em Freezer – 80ºC.

3.4.1. Ensaios para detecção de membrana

A pureza da membrana plasmática foi realisada indiretamente pelo ensaio da ATPase sensível ao vanadato. Vinte e cinco microlitros da amostra foram adicionados a 250 μL do tampão de ensaio da ATPase (Tris-Mes 40 mM pH 4,75, $MgSO_4$ 3 mM, Na_2MoO_4 1 mM, EGTA 10 mM, Triton X-100). O volume final da reação foi ajustado para 450 μL com água milli-Q e incubado por 3 min a 30ºC. Posteriormente foi adicionado ATP (concentração final: 3 mM, em Tris sal) e a amostra foi incubada por mais 30 minutos a 30ºC. A reação foi parada adicionando 50 μL de H_2SO_4 5 M. Os fosfatos liberados foram determinados pelo método “Malachite-Green”. As atividades ATPase sensível ao anadato foram calculados

pela diferença entre as atividades sem e com o inibidor (vanadato) (Day, Mcalvin *et al.*, 2000).

A detecção da membrana de Golgi consistiu em submeter 50 µL da amostra foram adicionado a 50 µL de tampão de ensaio (UDP 3 mM, $MnSO_4$ 3 mM, Mes-Tris pH 6,5) e incubado por 20 minutos a 37ºC (Day, Mcalvin *et al.*, 2000). O fosfato liberado foi quantificado pelo método verde malaquita (“Malachite-Green”.

A fração de membrana do retículo endoplasmático foi detectada utilizando um anitocorpo monoclonal específico para calnexina e observado por Western blot (Li, Su *et al.*, 1998; Day, Okada *et al.*, 2001).

3.5. Método verde malaquita (“Malachite-Green”) para detecção de fosfato livro

3.5.1. Preparação da solução de vanadato

Ortovanadato de sódio 5 mM foi dissolvido em água e mantido em “banho-maria” 38ºC por 3 horas. A solução foi resfriada a temperatura ambiente e o seu volume ajustado. A concentração da solução foi verificada (ε = 2925 $M^{-1}.cm^{-1}$) por absorbância (λ = 265 nm) após ajustar o pH para 9,5 usando pó de Mes. Finalmente, a solução foi ajustado para pH 7,2 com Mes e armazenada em frasco protegido da luz e à temperatura ambiente.

3.5.2. Preparação da solução de verde malaquita/HCl”

Três partes de malachite-gree/HCl 0,045% (w/v, em água) foram misturadas com uma parte de molibdato de amônio 4,2% (w/v, em HCl 4 M). A mistura foi mantida em agitação por 30 minutos e então filtrada por dois filtros Whatman Nº 1 (SIGMA). A cada 10 mL desta mistura doi adicionada 200 µL de Tergitol NP 2% (w/v) (esta solução sempre foi preparada e utilizada no mesmo dia).

3.5.3. Determinação de fosfato livre

Duzentos microlitros da solução "verde malaquita/HCl" foram adicionadas a 12,5 µL do tampão de ensaio ATPase. A mistura foi incubada por 1 minutos a temperatura ambiente. Após incubação, 25 µL de citrato de sódio dihidratada 34% (w/v) foi adicionada à reação e incubada por 1 hora a temperatura ambiente. A absorbância foi mensurada a 630 nm. Um curva de correlação linear simples foi feita usando fosfato monobásico de potássio variando de 0 a 30 nmol (Baykov, Evtushenko *et al.*, 1988).

3.6. BN-PAGE de proteinas membranosas

A fração enriquecida de membrana plasmática (200 µg de proteína) foi solubilizada em ácido aminocapróico 750 mM, Bis-Tris 50 mM pH 7,0 e Triton X-100 (concentrações variávies), e incubadas em gelo por 20 minutos. Posteriormente a amostra foi centrifugada a 100.000 g por 15 minutos. O pellet foi ressuspendido em ácido aminocapróico 1,5 M e Bis-Tris 0,1 M pH 7,0. O detergente neutro Triton X-100 foi adicionado em concentrações crescentes na amostra (volume final: 1,0 mL) para obter uma razão Triton X-100/proteína (g/g) variando de 0,25 a 2,00. A amostra foi incubada em gelo e levemente agitada. Após 1 hora, foi adicionado CBB (w/v) em ácido aminocapróico 500 mM para a obtenção de uma razão detergente/CBB de 4/1(Schägger, H., Cramer, W. *et al.*, 1994). A concentração total da proteína foi de 4,44 $mg.mL^{-1}$.

3.7. Identificação de proteínas

3.7.1. LC-MS/MS

As bandas da primeira dimensão (1D-PAGE) foram extraídas manualmente e reduzidas com DTT 10 mM em tampão NH_4HCO_3 10 mM a 56ºC por 1h, na ausência de luz. A carbamidometilação de cisteína foi realizada usando uma solução de iodoacetamida 50 mM por 1h a temperatura ambiente. As bandas foram desidratadas com ACN 100% e digeridas por tripsina 1µg/µL. Os peptídeos trípticos resultantes foram extraídos a partir da matriz do gel empregando ACN:H_2O:TFA (66:33:0,1; v/v/v) por 10 min, 3 vezes, sempre

após sonicação. Finalmente, os sobrenadantes foram recuperados e reunidos, secos em centrífuga a vácuo e reconstituído em 10 µL de solução de TFA 0,05%. Quatro microlitros da amostra foram injetados para cromatografia líquida (EASY-nLC II) acoplado a um espectrômetro de massa LTQ Orbitrap Velos (Thermo Scientific).

Primeiro os peptídeos foram carregados em uma coluna "trap" (30 x 0.1 mm) empacotada com partículas de 5 µm (Reprosil-Pur 120 C18-AQ) (Dr. Maish). Após 4 min lavando com solvente A, os peptídeos foram eluídos durante o gradiente em um coluna 120 x 0,05 mm (empacotada com partículas de 3 µm Reprosil-Pur 120 C18-AQ) (Dr. Maish) a um fluxo de 200 $nL.min^{-1}$ usando a seguinte fase móvel: solvente A foi H_2O/acetonitrila (95:5, v/v) com ácido fórmico 1% (v/v); sovente B foi H_2O/acetonitrila com ácido fórmico 0,1% (20:80, v/v).

O gradiente usado foi 5 a 20% do solvente B em 30 min, 20-50% B em 15 min, 50-100% em 5 min e 100% B durante 10 min. Os peptídeos foram dinamicamente eluídos para dentro do espectrômetro de massa via uma sonda de nanospray (Thermo Scientific, GmbH) usando um emissor de nanospray (20 µm i.d., 10 µm tip i.d.) (New Objective), a uma voltagem de 1,8 kV e temperatura capilar de transferência fixada a 180ºC. O DDA ("Automated Data Dependent Acquisition") foi controlado pelo programa Xcalibur 2.1 (Thermo Scientific, GmbH). A aquisição de ciclo consistiu de um scan de 300-1800 m/z a uma resolução de 60.000 (largura total) e m/z 400 no Orbitrap, seguido pela fragmentação dos precursores múltiplos carregados mais intensos no "linear ion trap" sob energia de colisão normalizada de 35%. O AGC ("Automatic Gain Control") foi fixado a 5×10^5 cargas para scan no Orbitrap e 5×10^4 para MS/MS no "ion trap", ambos portando um microscans. O limiar da seleção de íon para MS/MS foi fixado a 500 contagens usando uma janela de isolamento de precursor de 4 amu. O parâmetro de ativação "q" e o tempo de ativação foram fixados a 0,25 e 30 ms, respectivamente. Os *m/z* dos precursores já fragmentados foram dinamicamente excluídos durante o ciclo para 90 s.

3.7.2. Análise de dados

A identificação de proteínas foi realizada pelo MASCOT combinado com buscas de identificação por similaridade de sequência (apropriado para organismos com genoma não disponível), conforme descrito anteriormente (Junqueira, Spirin, Balbuena *et al.*, 2008).

Sinteticamente, os arquivos em formato .mgf foram filtrados usando o programa EagleEye v1.66 (Junqueira, Spirin, Santana Balbuena *et al.*, 2008), antes do sequenciamento *de-novo* pelo programa PepNovo (Frank e Pevzner, 2005) e MS BLAST (Shevchenko, Valcu *et al.*, 2009). Os espectros filtrados (retirar o efeito de contaminantes como querativa a tripsina) foram exportados e submetidos à base de dados NCBInr usando o programa MASCOT v.2.1 (Matrix Science, Ltda). Os parâmetros de busca estabelecidos foram: (1) *fungi* como taxonomia, (2) tripsina como enzima, (3) até duas clivagens perdidas permitidas, (4) 10 ppm de tolerância para a massa peptídica, (5) 0,6 Da de tolerância da massa do fragmento, (6) carbamidometilação de cisteína como modificação fixada (7) oxidação de metionina como modificação variável. As identificações confiáveis foram consideradas se a soma de pelo menos três peptídeos apresentarem um score maior que 60, para score íon individual o score maior que 20.

4. Resultados

4.1. Análise do secretoma de *T. harzianum*

O fungo *T. harzianum* produziu um secretoma cuja concentração proteica foi 0,2 mg.mL^{-1}. O secretoma submetido a 1D-BN-PAGE apresentou várias bandas, sugerindo a presença de complexos proteicos (Figura 4A). As bandas visualmente mais intensas foram nomeadas de complexos I, II e III.

Sabe-se que o CBB evita a agregação de proteínas durante o BN-PAGE por meio de repulsão eletrostática (Schägger, H., Cramer, W. et al., 1994; Neff e Dencher, 1999; Krause, 2006). Ainda assim, foi verificado se existiria qualquer correlação entre a concentração proteica do secretoma e a formação de bandas devido à associação inespecífica (agregação) nos experimentos de 1D-BN-PAGE. A separação eletroforética foi reproduzida usando três concentrações do secretoma: 0,2 mg.mL^{-1}, 5 mg.mL^{-1} and 10 mg.mL^{-1}. A Figura 4B mostra que as massas moleculares das bandas nos perfis 1D-BN-PAGE foram idênticos para todas as amostras, indicando ausência de agregação proteica. O mesmo perfil foi conservado em baixas concentrações (0,2 a 0.002 mg.mL^{-1}, dados não mostrados), demonstrando uma alta afinidade entre os componentes dos complexos.

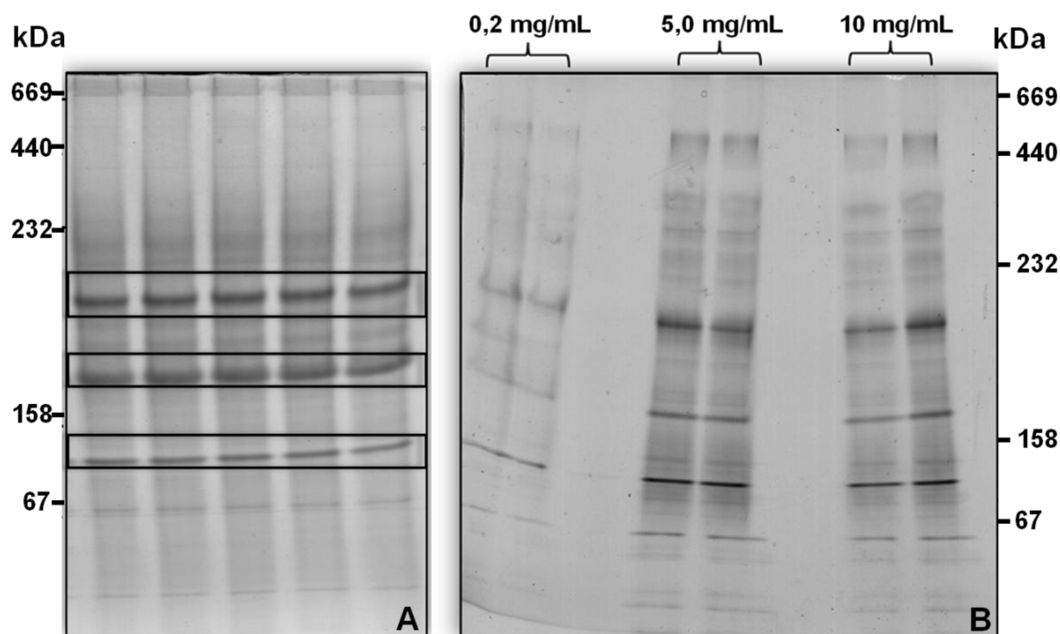

Figura 4. **(A)** 1D-BN-PAGE do secretoma de *T. harzianum* produzido em meio contendo bagaço de cana. O gel continha gradiente de concentração de poliacrilamida entre 5-18% T e em cada poço foram aplicados 200 μg de proteínas do secretoma. O Gel foi fixado e corado com "Coomasie Brilliant Blue G-250". As três bandas mais intensas foram nomeadas: complexos I, II e III. **(B)** 1D-BN-PAGE do secretoma de *T. harzianum* em diferentes concentrações de proteínas. Nenhuma correlação entre concentração proteica (0,2 $mg.mL^{-1}$, 5,0 $mg.mL^{-1}$ and 10 $mg.mL^{-1}$) e agregação foi observado. Diferentes volumes de cada uma das amostras foi usada para tornar as bandas visíveis mesmo em baixas concentrações: 0,2 $mg.mL^{-1}$ (400 μL), 5,0 $mg.mL^{-1}$ (60 μL) and 10 $mg.mL^{-1}$ (20 μL).

As massas moleculares estimadas correspondentes às bandas I, II e III foram obtidas plotando *Rf* (fração de retenção) em função do *Log MW* (Log *massa molecular*) (Figura 5). As massas moleculares relativas obtidas em gel BN-PAGE, correspondentes às bandas I, II e III foram 185,390 (*Rf* = 0,443), 115,013 (*Rf* = 0,586) e 78,032 (*Rf* = 0,710) kDa, respectivamente (regressão linear simples: Y = -0,734896 (± 0,075)X + 2,100147 (± 0,180); r^2 = 0,97, p < 0,005), sugerindo a presença de complexos multiprotéicos. A segunda dimensão (Tricina-SDS-PAGE) e espectrometria de massa (LC-MS/MS) dessas bandas confirmaram nossa espectativa, porquanto cada banda foi decomposta em componentes com diferentes massas moleculares.

As bandas correspondentes aos complexos I, II e III foram extraídas do gel 1D-BN-PAGE e submetidas a condições de dissociação em uma segunda dimensão eletroforética (Tricina-SDS-PAGE). O gel resultante (2D-BN-PAGE) (Figura 6) mostra que os complexos dissociaram-se em pequenos componentes, excluindo a possibilidade dos complexos serem proteínas de alta massa molecular que co-migraram juntas. No entanto, o complexo I foi decomposto em componentes de massa molecular alta comparando com os outros complexos, sugerindo uma dissociação incompleta mesmo

sob condições desnaturantes. Perante isso, as bandas visualizadas no 2D-BN-PAGE não foram analizadas. Alternativamente, os complexos I, II e III foram extraídos diretamente do gel 1D-BN-PAGE, digerido com tripsina e submetido ao LC-MS/MS para posterior identificação das proteínas.

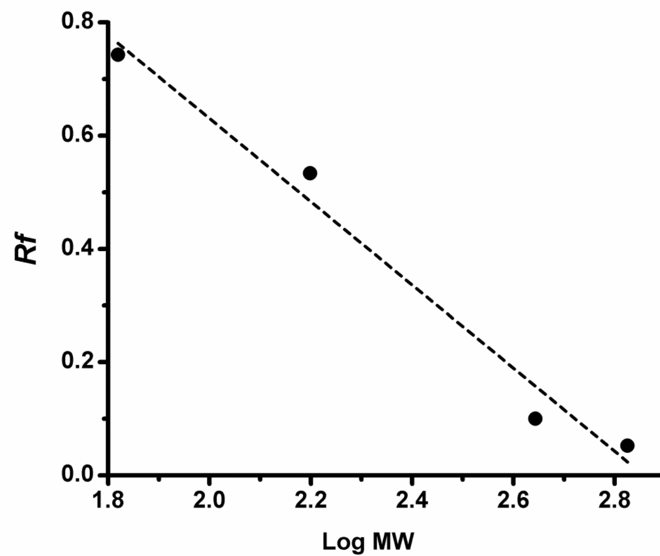

Figura 5. Regressão linear simples para estimar massa molecular dos complexos separados por 1D-BN-PAGE. A equação da reta obtida foi $f(x) = 0,734896\ (\pm\ 0,075)x + 2,100147\ (\pm\ 0,180)$; $r^2 = 0,97$, $p < 0,05$). Log *MW*: logarítmo de base 10 da massa molecular. *Rf*: fator de retenção relativa.

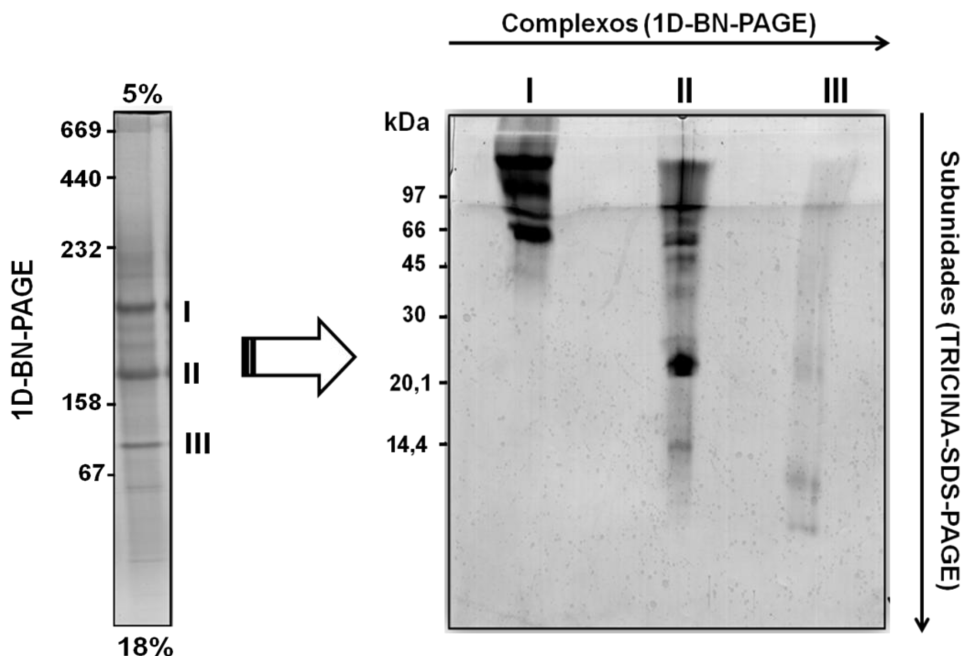

Figura 6. 2D-BN-PAGE do secretoma de *T. harzianum* produzido em meio contendo bagaço de cana como fonte de carbono. Um gel gradiente 1D-BN-PAGE (5-18% T) foi usado na primeira dimensão (*esquerda*) para separar os complexos. Este gel foi corado Comassie Brilliant Blue G-250. O gel Tricine-SDS-PAGE foi corado com prata e usado para analisar as subunidades dos complexos I, II e III na segunda dimensão (*direita*).

A identificação das proteínas foi realizada usando duas abordagens: abordagem por correspondência estrita (identidade) de espectros peptídicos usando o programa MASCOT e a abordagem de identificação de proteínas tolerante à erros orientada por homologia entre espécies usando o programas PepNovo e MS BLAST (Shevchenko, Valcu *et al.*, 2009). Os resultados são mostrados na Tabela I.

Como já era esperado devido ao fato da sequencia do genoma do *T. harzianum* não estar publicamente disponível, a abordagem por homologia entre espécies forneceu maior número de identificações proteicas que a abordagem convencional (MASCOT) (Junqueira, Spirin, Balbuena *et al.*, 2008). Por exemplo, ambas as abordagens identificaram uma celobiohidrolase I no complex I, no entanto, somente a abordagem por homologia permitiu a identificação de enzimas envolvidas na degradação de xilana, ou seja, alfa-L-arabinofuranosidase e endo-beta-1,4-xilanase. Concernentemente ao complexo II, celobiohidrolases, enzimas degradadoras de xilana e endoquitinases foram identificadas por ambos os métodos. No entanto, a cutinase e a galactosidase foram identificadas apenas por homologia usando o MS BLAST. A busca pelo MASCOT foi incapaz de fornecer a identificação dos componentes do complexo III, enquanto várias proteínas, tais como alfa e beta-glucanases, uma glicoamilase, uma alfa-L-arabinofuranosidase e uma swolenina, foram identificadas pela abordagem alternativa (MS BLAST).

Conforme mencionado anteriormente, a degradação da parede celular da cana-de-açucar depende principalmente da ação coordenada de celulases e hemicelulases (especialmente xilanases). Assim, análises zimográficas usando géis 1D-BN-PAGE contendo celulose e xilana foram realizados para investigar as atividades de degradação de biomassa dos complexos.

A Figura 7 mostra a detecção das atividades celulolítica e xilanolítica no secretoma. No entanto, no gel contendo xilana a atividade foi observada como um longo rastro esbranquiçado, indicando a presença de várias xilanases com diferentes tamanhos, ou uma ou poucas xilanases que hidrolizaram o substrato durante a mobilidade eletroforética.

Para excluir a segunda possibilidade, foi desenvolvido um zimograma 2D-BN/BN-PAGE, onde a amostra foi submetida a um 1D-BN-PAGE padrão na primeira dimensão e outro 1D-BN-PAGE (desta vez usando um gel de poliacrilamida com celulose ou xilana)

na segunda dimensão (Figura 8). A zimografia 2D-BN/BN-PAGE confirmou a detecção das atividades celulolítica e xilanolítica, correspondendo a proteinas de diferentes massas moleculares e, consequentemente, indicando que os resultados encontrados usando a zimografia 1D-BN-PAGE não foram devidos à hidrólise do substrato durante a mobilidade eletroforética da primeira dimensão. Como BN-PAGE preserva a integridade estrutural e funcional de complexos multi-enzimáticos (Wittig e Schägger, 2008), outras proteínas dentro dos complexos I, II e III que não estão diretamente relacionados a atividades celulolítica e xilanolítica detectadas nos zimogramas (isto é, glicoamilase, andoquitinase, swolenina) possivelmente também estão ativas.

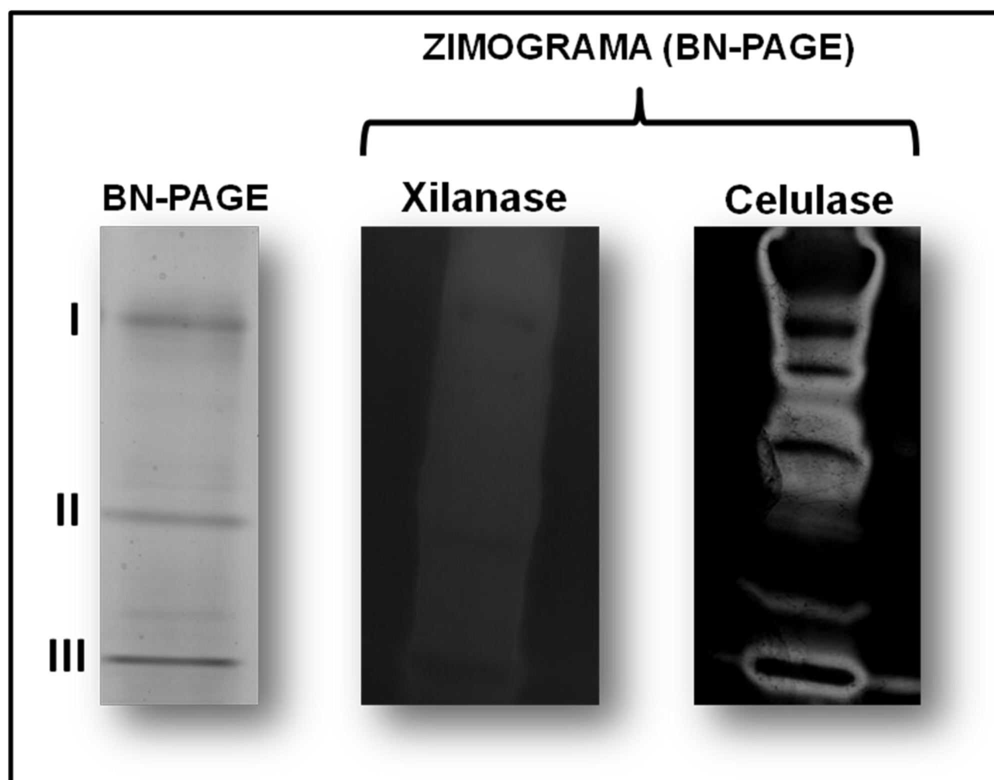

Figura 7. Zimografia 1D-BN-PAGE do secretoma do *T. harzianum*. Para detecção das atividades celulolítico e xilanolítico, substratos de xilana e celulose foram incorporados dentro dos géis. O gel à esquerda foi corado com Coomasie Brilliant Blue G-250. Os zimogramas foram corados com Congo Red, conforme descrito em Materiais e Métodos.

Tabela I. Lista de proteínas identificadas por espectrometria de massa nos três complexos encontrados no secretoma de *T. harzianum*.

MASCOT					MS BLAST				
Proteína	Organismo	Gi (a)	Matches (b)	Total Score (c)	Proteína	Organismo	Gi	HSPs (d)	Total Score
Complexo I									
Celobiohidrolase I	*T. asperellum*	42741023	21	87	Celobiohidrolase I	*H. virens*	194719525	39	2355
"Predicted protein"	*T. reesei* QM6a	340516597	1	58	Celobiohidrolase I-II	*V. volvacea*	49333365	4	234
					α-L-arabinofuranosidase	*Penicilium* sp.LYG 0704	315259518	4	308
					Xylan 1,4-β-xylosidase	*S. sviceus* ATCC 29083	297197679	3	207
Complexo II									
Acetil xilana esterase "Chain A, Cat Core Dom"	*T. reesei*	1151345	21	130	Acetil xilana esterase	*H. jecorina*	41016921	43	2665
Endoquitinase	*H. lixii*	487419	6	117	Endoquitinase	*H. lixii*	88191687	1	84
Endoquitinase 42	*T. stromaticum*	310892959	5	63	Celobiohidrolase I	*H. virens*	194719525	9	
Celobiohidrolase II	*A. cellulolyticus* Y-94	4200031	4	98	Arabinogalactana endo-1,4-β-galactosidase GalA	*T. stipitatus* ATCC 10500	242822204	1	84
Celobiohidrolase I	*P. occitanis*	5124302	8	100	Celobiohidrolase I	*H. virens*	194719525	9	537
GH 18	*T. reesei*	340514044	4	88	Cutinase	*G. graminicola* M1.001	310799541	8	485
Endo-1,4-xilanase D	*P. funiculosum*	53747929	1	56	α-N-arabinofuranosidase	*A. terreus* NIH2624	115401944	8	453
					Endo-β-1,4-xilanase	*Bispora* sp. MEY-1	225420804	12	955
Complexo III									
					Glicoamilase	*H. lixii*	61657886	10	748
					Endo-β-1,4-glucanase	*H. jecorina*	60593233	2	189
					Swolenina	*H. jecorina*	8052455	2	163
					β-endoglucanase ancorado a GPI (associado a parede celular)	*G. clavigera* kw 1407	320590163	2	153
					α -L-arabinofuranosidase fúngico putativo	*P. mmefei* ATCC 18224	212528630	1	84
					α-1,3-glucanase	*H. lixii*	18076080	1	79

[a] "GenInfo Identifier", Banco de dados do NCBI. [b] Número de "matching" dos peptídeos. [c] "Score" significante, $p < 0.05$. [d] Sequências de peptídeos *de novo* que produziram "High Scoring Pairs" (HSP) pelo MS BLAST. [e] "Score" estatisticamente significante do HSP.

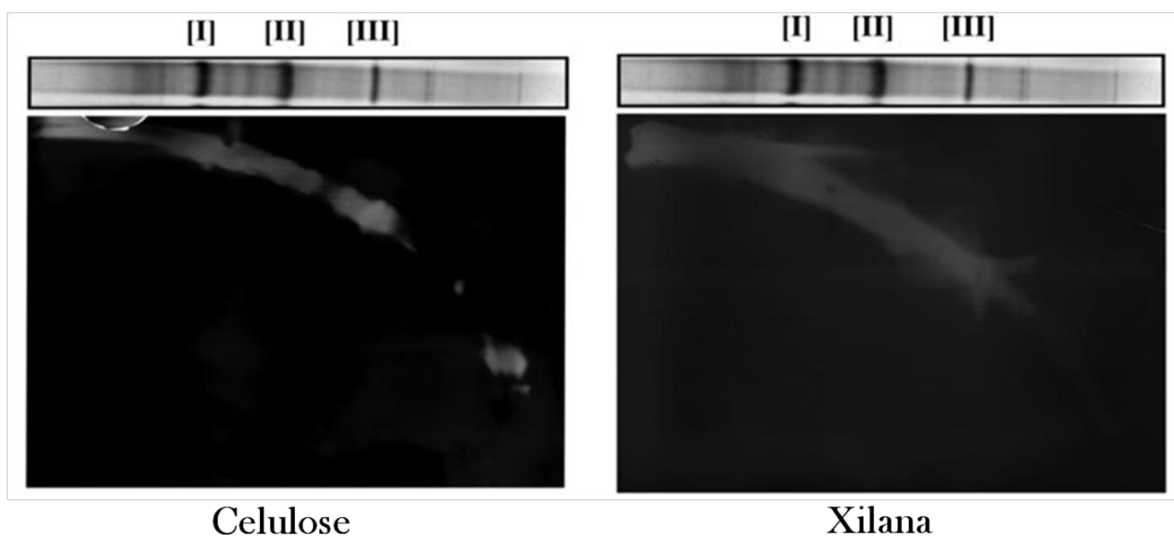

Figura 8. Zimograma 2D-BN/BN-PAGE do secretoma de *T. harzianum*. Para a detecção das atividades celulolítica e xilanolítica, cellulose e xilana foram incorporados dentro dos géis. Os zimogramas foram corados com Congo Red como descrito em Materiais e Métodos.

Os resultados apresentados aqui indicaram que *T. harzianum* é capaz de secretar complexos multi-enzimáticos ativos. A composição heterogênea dos complexos sugere uma reação sinergística possível entre as diferentes proteínas que atuariam de modo cooperativo para degradar eficientemente o bagaço de cana-de-açúcar usado como substrato.

O esquema abaixo mostra um modelo que sintetiza uma nova proposta da mecânica de degradação de bagaço de cana por *T. harzianum*.

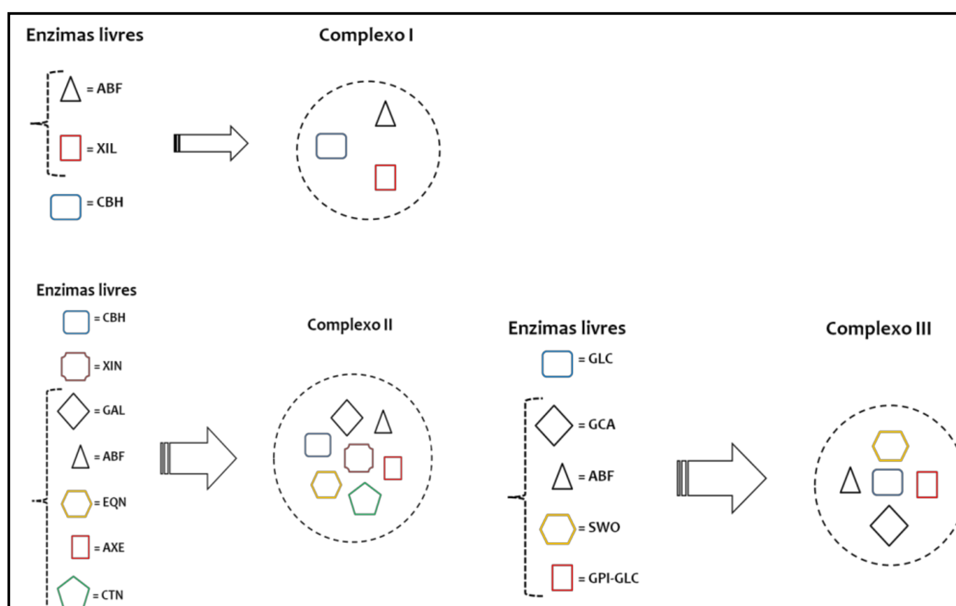

4.2. Análise do secretoma de *Trichoderma reesei*

Após 10 dias de cultivo em meio contendo lactose e galactose, o secretoma de *T. reesei* apresentou respectivamente 0,3 e 0,1 mg.mL^{-1} de proteína total. A aplicação do método BN-PAGE ao secretoma mostrou a existência de complexos multiproteicos em ambas as fontes de carbono. Está bem estabelecido que o CBB reduz a formação de agregados proteicos por repulsão eletrostática (Schägger, H., Cramer, W. *et al.*, 1994; Neff e Dencher, 1999; Krause, 2006), porém, como em *T. harzianum*, a relação de dependência entre agregação e altas concentrações proteicas em BN-PAGE foi verificado para o *T. reesei*. Os resultados mostraram o mesmo perfil eletroforético em todas as concentrações estudadas, excluindo definitivamente qualquer possibilidade de agregação (Figura 9A). As bandas I e II correspondem aos complexos multiproteicos e foram selecionados para análise devido à diferença característica na intensidade de sua coloração por CBB. Mesmo apresentando massas moleculares praticamente identicas, o complexo I obtido em meio galactose apresentou intensa coloração comparativamente ao complexo I obtido em meio lactose. Inversamente, o complexo II oriundo do meio lactose é fortemente corado relativamente ao encontrado em meio galactose. Além disso, algumas bandas com massas moleculares superiores à do complexo I e fracamente visualizadas, parecem exclusivas de meio lactose (Figura 9B).

As massas moleculares estimadas correspondentes aos complexos I e II foram obtidas plotando *Rf* (fator de retenção) em função do *Log MW* (Log *massa molecular*) (Figura 10). As massas moleculares estimadas do complexo I, encontradas em meio contendo lactose e galactose, foram 368,186 kDa e 354,716, respectivamente. As do complexo II foram 174,715 para ambas as fontes de carbono.

A funcionalidade enzimática dos complexos foi verificada (zimografia 2D-BN/BN-PAGE), porquanto a atividade sinergística deles é um fator crítico para aplicações industriais e biotecnológicas (Stricker, Mach *et al.*, 2008). A Figura 11 mostra que os complexos (i) são ativos, (ii) apresentam ambas as atividades, celulolítica e xilanolítica, e (iii) tais atividades são aparentemente maiores quando o fungo é cultivado em lactose do que em galactose.

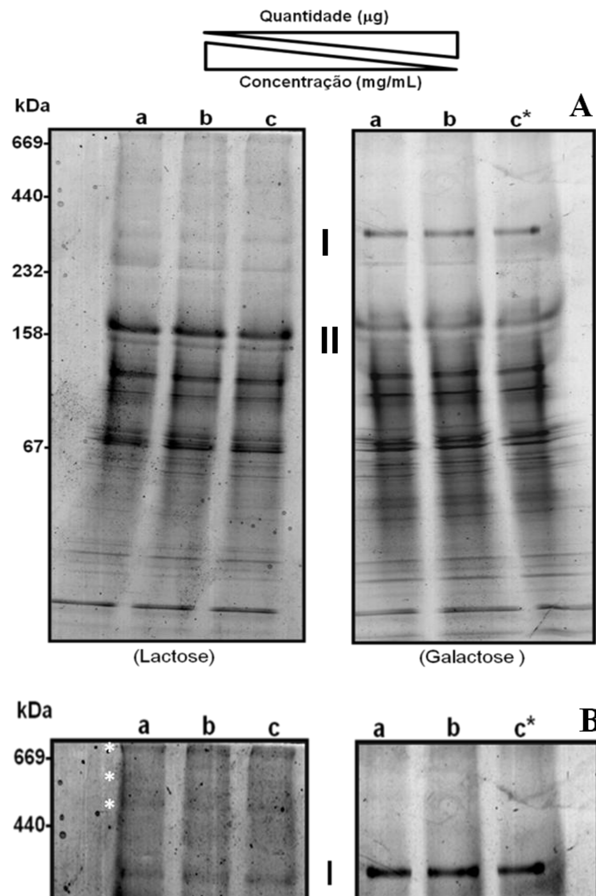

Figura 9. **(A)** Perfil eletroforético do secretoma de *T. reesei* em gel de poliacrilamida "blue-native" (BN-PAGE) sob diferentes concentrações: 10 mg.mL^{-1} (a), 2 mg.mL^{-1} (b), 0,3 mg.mL^{-1} (c) e 0,0875 mg.mL^{-1} (c*). O gradiente de poliacrilamida variou de 5 a 18% T para ambas as fontes de carbono. Diferentes quantidades de proteína total foram usadas para tornar visíveis as bandas menos intensas: 10 µL (a), 50 µL (b) and 300 µL (c and c*). c* e c correspondem à concentração específica encontrada na cultura contendo galactose (0,3%) e lactose (1%), respectivamente. Marcador molecular: tiroglobulina (669 kDa), ferritina (440 kDa), catalase (232 kDa), aldolase (158 kDa) e albumina (67 kDa) (SIGMA). As bandas I e II são complexos multiproteicos. Os experimentos foram feitos em triplicatas. **(B)** "Zoom" mostrando três complexos de alta massa molecular mas de baixa intenside e presentes na amostra crescida em latose marcados por astericos brancos.

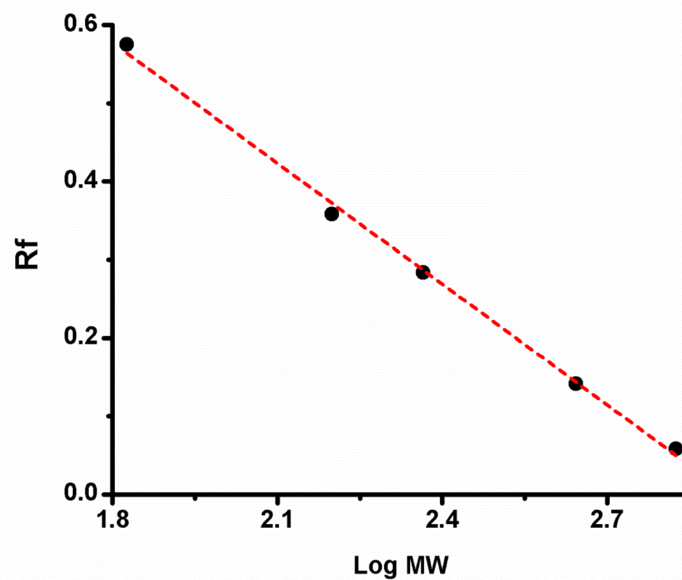

Figura 10. Regressão linear simples. A equação da reta obtida foi $f(x) = -0{,}514821\ (\pm\ 0{,}014)x + 1{,}54386\ (\pm\ 0{,}035)$. Log *MW*: logarítmo de base 10 da massa molecular. *Rf*: fator de retenção relativa. ($r^2 = 0{,}99$; $p < 0{,}05$).

Dados quantitativos da atividade enzimática foram obtidos das amostras em solução. A medida da concentração de atividade enzimática, dada em UI.mL^{-1}, mostrou que *T. reesei* apresenta: (i) atividades celulolítica e xilanolítica em ambas as fontes de carbono; (ii) a atividade xilanolítica é maior que celulolítica nas duas condições estudadas; (iii) a atividade celulolítica é 5 vezes maior em meio lactose que galactose, já a xilanolítica é apenas 1,5 vezes maior (Tabela II).

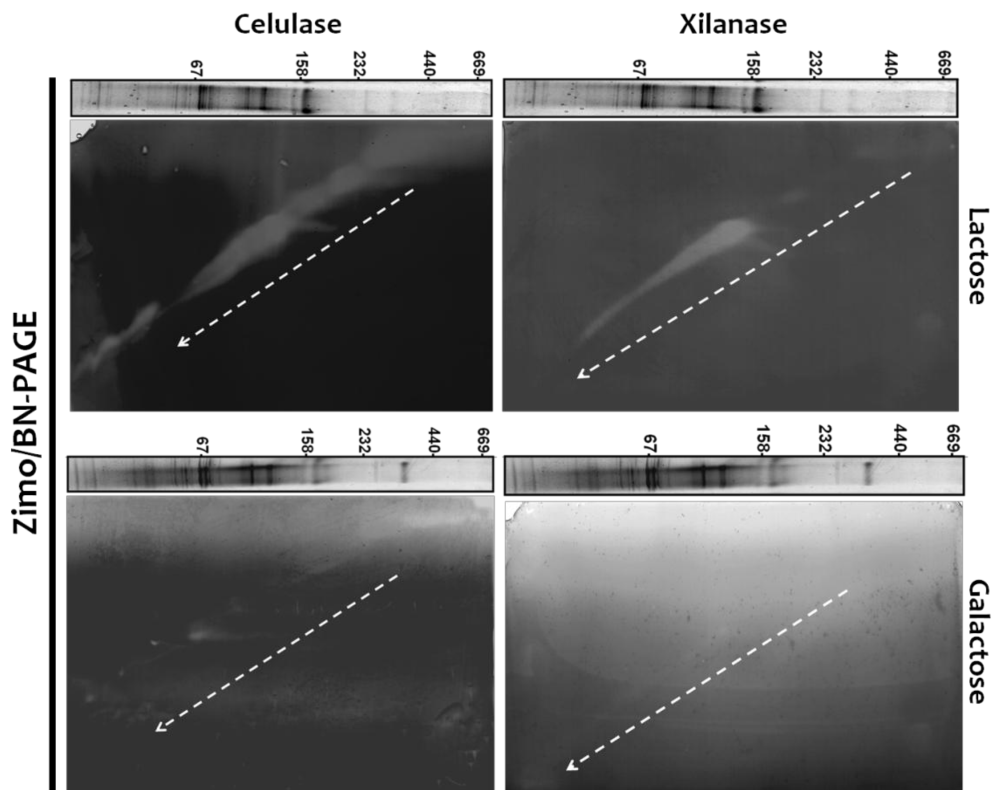

Figura 11. Zimograma 2D-BN/BN-PAGE do secretoma (10 mg.mL^{-1}) de *T. reesei* cultivado em lactose e galactose. Os géis de ambas as dimensões foram feitos com gradiente de poliacrilamida, variando de 5 a 18%. A concentração dos substratos (celulose e xilana) em gel foi de 0,01 g.mL^{-1} (1%). A zona esbranquiçada paralela à seta tracejada corresponde à atividade enzimática. Marcador molecular: tiroglobulina (669 kDa), ferritina (440 kDa), catalase (232 kDa), aldolase (158 kDa) e albumina (67 ka) (SIGMA).

Tabela II. Concentração da atividade enzimática (UI.mL^{-1}) de celulases e xilanases presentes no secretoma de *T. reesei* cultivado em meio contendo lactose e galactose como fontes de carbono. A concentração proteica das amostras foi de 10 mg.mL^{-1} (onde n = 3).

Atividade (UI.mL^{-1})	**Fonte de carbono usada no crescimento**	
	Lactose	**Galactose**
Celulolítica	0,781 (± 0,32)	0,155 (± 0,02)
Xilanolítica	1,315 (± 0,35)	0,840 (± 0,15)

Dados de regressão linear simples: $f(x) = 4{,}075596\ (\pm\ 0{,}045)x - 0{,}011743\ (\pm\ 0{,}005)$. ($r^2 = 0{,}999$; $p < 0{,}05$).

O procedimento adotado para *T. harzianum* também foi utilizado aqui para os complexos I e II do *T. reesei*: extração das bandas diretamente do gel 1D-BN-PAGE, digestão e submissão ao LC-MS/MS. Considerando que *T. reesei* tem seu genoma disponível publicamente, utilizamos apenas o método estringente de análise de dados utilizando o *software* MASCOT para identificação das proteínas.

A Tabela III mostra os componentes proteicos presentes em cada complexo estudado. A fonte de carbono lactose parece induzir maior heterogeneidade proteica na composição dos complexos analisados comparativamente à galactose.

Conforme já mencionado na introdução deste trabalho, a galactose é o indutor das celulases presente na constituição da lactose. No entanto, resultados vêm mostrando que a lactose, antes de catalizada em galactose e glicose pela galactosidase, intensifica a produção de algumas enzimas (além de induzir outras) através de vias diferentes, possivelmente por proteínas de membrana (Karaffa, Fekete *et al.*, 2006). Por isso, decidimos obter frações enriquecidas de membrana plasmática para verificar, por BN-PAGE, se existem alguma diferença na organização das proteínas membranosas para as fontes de carbano estudadas.

Nós conseguimos obter frações enriquecidas de membrana plasmática de *T. reesei* a partir de cultura contendo lactose, as quais podem ser observadas na Figura 12. As frações de membrana plasmática foram monitoradas por meio da atividade ATPásica específica, enquanto a membrana de Golgi corresponde à atividade de hidrólise de UDP (UDPase). As frações de membrana celular começam a partir da fração 15. A quantidade de proteína presente nestas frações e nas obtidas em cultura contendo galactose foram insuficientes para a realização do BN-PAGE e dos ensaios de detecção de membranas, respectivamente. Novas culturas deverão ser feitas em quantidades maiores de micélio para atender ao redimento proteico suficiente para a realização do BN-PAGE. Esta meta ficará reservada como uma perspectiva deste trabalho.

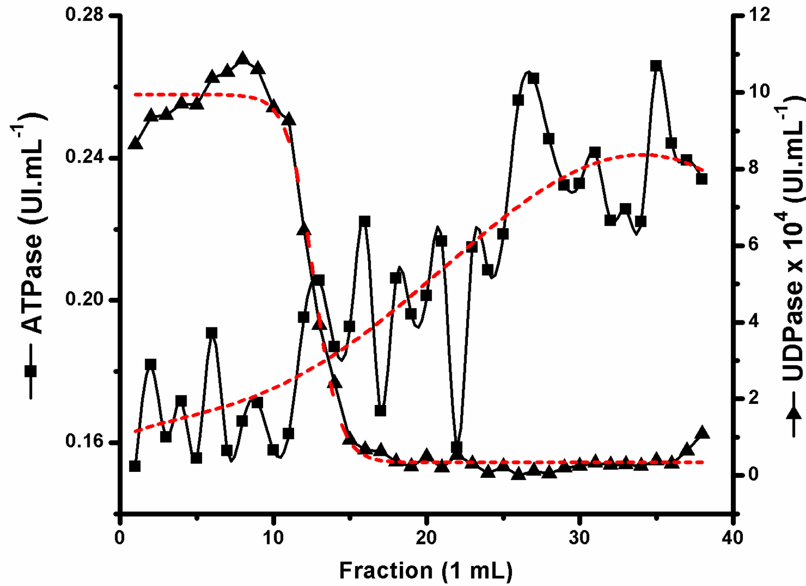

Figura 12. Subfracionamento de membranas em *Trichoderma reesei* por ultracentrifugação isopícnica em gradiente de sacarose (20 – 50%). Fonte de carbono: β-Lactose. Marcadores: membrana plasmática (ensaio da ATPase sensível a vanadato) e membrana de golgi (ensaio da UDPase). A linha tracejada permite visualizar a tendência gráfica.

Tabela III. Proteínas identificadas por MASCOT dos complexos I e II presentes no secretoma de *T. reesei* cultivado em meio contendo lactose e galactose como fontes de carbono.

<table>
<tr><th colspan="4">Galactose</th><th colspan="4">Lactose</th></tr>
<tr><th>Proteína</th><th>Massa (Da)</th><th>Match</th><th>Score</th><th>Proteína</th><th>Massa (Da)</th><th>Match</th><th>Score</th></tr>
<tr><td colspan="8">COMPLEXO I</td></tr>
<tr><td>GH 36 (gi|340514461)</td><td>82.098</td><td>37 (27)</td><td>568</td><td>GH 36 (gi|340514461)</td><td>82.098</td><td>21 (11)</td><td>243</td></tr>
<tr><td>Beta-1,3-endoglucanase (gi|340517806)</td><td>42.420</td><td>3 (3)</td><td>133</td><td>Beta-1,3-endoglucanase (gi|340517806)</td><td>42.420</td><td>3 (3)</td><td>118</td></tr>
<tr><td>GH 55 (gi|340513925)</td><td>79.726</td><td>7 (6)</td><td>139</td><td></td><td></td><td></td><td></td></tr>
<tr><td>GH 54 (gi|340521563)</td><td>53.664</td><td>6 (4)</td><td>137</td><td></td><td></td><td></td><td></td></tr>
<tr><td>GH 16 (gi|340515048)</td><td>31.095</td><td>4 (3)</td><td>104</td><td></td><td></td><td></td><td></td></tr>
<tr><td>Catalase/peroxidase (gi|340513959)</td><td>85.915</td><td>2 (2)</td><td>64</td><td></td><td></td><td></td><td></td></tr>
<tr><td></td><td></td><td></td><td></td><td>Alfa-galactosidase 2 (gi|74630548)</td><td>82.085</td><td>14 (9)</td><td>219</td></tr>
<tr><td></td><td></td><td></td><td></td><td>GH 20 (gi|340520576)</td><td>64.562</td><td>7 (4)</td><td>128</td></tr>
<tr><td></td><td></td><td></td><td></td><td>Exo-beta-1,4-glucanase específico para xiloglucano (gi|74619305)</td><td>87.307</td><td>4 (2)</td><td>98</td></tr>
<tr><td></td><td></td><td></td><td></td><td>Aril-alcool oxidase (gi|340515821)</td><td>65.028</td><td>7 (4)</td><td>87</td></tr>
<tr><td></td><td></td><td></td><td></td><td>“Predicted protein” (gi|340518010)</td><td>43.819</td><td>6 (5)</td><td>173</td></tr>
<tr><td>“Predicted protein” (gi|340518236)</td><td>20.272</td><td>3 (2)</td><td>119</td><td>“Predicted protein” (gi|340518236)</td><td>20.272</td><td>4 (3)</td><td>94</td></tr>
<tr><td colspan="8">COMPLEXO II</td></tr>
<tr><td>Beta-1,3-endoglucanase(gi|340517806)</td><td>42.420</td><td>3 (3)</td><td>151</td><td>Beta-1,3-endoglucanase (gi|340517806)</td><td>42.420</td><td>3 (2)</td><td>120</td></tr>
<tr><td>GH 37 (gi|340515893)</td><td>77.196</td><td>3 (2)</td><td>107</td><td>GH 37 (gi|340515893)</td><td>77.196</td><td>9 (3)</td><td>77</td></tr>
<tr><td>Quitinase (gi|340514611)</td><td>67.713</td><td>11 (5)</td><td>83</td><td>Quitinase (gi|340514611)</td><td>67.713</td><td>7 (3)</td><td>63</td></tr>
<tr><td>Amidase (gi|340514363)</td><td>60.120</td><td>11 (4)</td><td>86</td><td></td><td></td><td></td><td></td></tr>
<tr><td>GH 3 (gi|340519849)</td><td>85.058</td><td>3 (2)</td><td>97</td><td></td><td></td><td></td><td></td></tr>
<tr><td>“Predicted protein” (gi|340514386)</td><td>25.474</td><td>4 (2)</td><td>106</td><td></td><td></td><td></td><td></td></tr>
<tr><td></td><td></td><td></td><td></td><td>GH 95 (gi|340519793)</td><td>47004</td><td>2 (1)*</td><td>73</td></tr>
<tr><td></td><td></td><td></td><td></td><td>“Predicted protein” (gi|340516521)</td><td>20.259</td><td>2 (2)</td><td>82</td></tr>
<tr><td></td><td></td><td></td><td></td><td>“Predicted protein” (gi|340518010)</td><td>43.819</td><td>3 (2)</td><td>84</td></tr>
<tr><td>“Predicted protein” (gi|340519476)</td><td>44.510</td><td>17 (14)</td><td>452</td><td>“Predicted protein” (gi|340519476)</td><td>44.510</td><td>15 (11)</td><td>334</td></tr>
<tr><td>“Predicted protein” (gi|340522459)</td><td>61.385</td><td>6 (4)</td><td>155</td><td>“Predicted protein” (gi|340522459)</td><td>61.385</td><td>11 (7)</td><td>186</td></tr>
<tr><td>“Predicted protein” (gi|340518236)</td><td>20.272</td><td>7 (4)</td><td>130</td><td>“Predicted protein” (gi|340518236)</td><td>20.272</td><td>6 (4)</td><td>152</td></tr>
<tr><td>“Predicted protein” (gi|340513779)</td><td>52.069</td><td>3 (2)</td><td>99</td><td>“Predicted protein” (gi|340513779)</td><td>52.069</td><td>4 (2)</td><td>82</td></tr>
</table>

GH: Glicosil Hidrolase.

5. Discussão

5.1. Do método

A escolha do método BN-PAGE para o estudo de complexos multiprotéicos foi baseada na atribuição dos *valores lógicos* (VERDADEIRO ou FALSO) às seguintes proposições:

1. BN-PAGE é método mais adequado para verificar a presença de complexos multiprotéicos.

2. BN-PAGE é utilizado para ensaios de atividades de complexos multiprotéicos em gel.

Evidências científicas (artigos) referenciadas abaixo permitiram atribuir o valor lógico VERDADEIRO a ambas as proposições, indicando BN-PAGE como um método adequado no estudo de complexos multiprotéicos secretados (secretoma) ou presentes em membranas biológicas de micro-organismos.

A análise das propriedades hidrodinâmicas de proteinas, particularmente de proteinas de membrana, é difícil de ser realizada pelos métodos de ultracentrifugação analítica (Von Jagow, Schägger *et al.*, 1977). Outros métodos de menor resolução, como centrifugação em gradiente de densidade e cromatografia de exclusão molecular (gel filtração), têm sido empregados (Schägger, H., Cramer, W. *et al.*, 1994).

Os métodos espectroscópicos por espalhamento de luz dinâmica (DLS, “Dynamic Light Scattering”) e estática (SLS, “Static Light Scattering”) também são inapropriados, porquanto oligômeros com diferentes tamanhos em solução provocam uma ampla variedade na intensidade de espalhamento da luz, resultando numa razão sinal/ruído muito baixa (Berne e Pecora, 2000; Borgstahl, 2007).

O método BN-PAGE tem substituído os métodos supramencionados, porquanto apresenta alta resolução no isolamento de complexos multiprotéicos ativos a partir de membranas biológicas, além de atribuir massas moleculares relativas aos complexos encontrados (Schägger e Von Jagow, 1991; Schägger, H., Cramer, W. *et al.*, 1994).

Além de separar complexos multiprotéicos nativos de membranas biológicas, BN-PAGE também isola proteinas hidrossolúveis, ácidas e básicas. Assim, BN-PAGE se tornou um método analítico na determinação de estados oligoméricos, subcomplexos, interação proteína-proteína e pureza da amostra (Schägger, H., Cramer, W. *et al.*, 1994; Krause, 2006).

Ensaios de atividade catalítica usando géis de BN-PAGE têm sido aplicados para identificar e quantificar complexos de fosforilação oxidativa mitocondrial (OXPHOS) e

outras enzimas tais como dihidrolipoamida desidrogenase, NAD quinase e enzimas produtoras de NADPH (Wittig e Schägger, 2008). Recentemente, BN-PAGE foi aplicado para estudar complexos multiprotéicos do fungo filamentoso *Penicillium purpurogenum* (Gonzalez-Vogel, Eyzaguirre *et al.*, 2011) e *Trypanosoma brucei* (Geiger, Hirtz *et al.*, 2010).

A atividade de cada componente dos complexos é uma consequência do seu estado nativo. Considerando que a técnica BN-PAGE conserva o estado nativo e funcional dos componentes dos complexos multiprotéicos, ensaios de atividade seriam desnecessários. Mesmo assim, neste trabalho os ensaios de atividades enzimáticas por zimograma em gel BN-PAGE foram realizados para celulase e xilanase. A zona esbranquiçada, contornada pela coloração avermelhada ("background"), característica do corante "Congo Red" (as Figuras foram apresentadas em preto e branco), é resultante da atividade enzimática (Sunna e Antranikian, 1997; Matsui e Ban-Tokuda, 2008). As Figuras 5, 6 e 9 evidenciam essa característica, e como ambas as atividades (celulolítica e xilanolítica) estão presentes no mesmo complexo, isto indica que celulases e xilanases fazem parte desse complexo, o qual foi encontrado e identificado por espectrometria de massas.

O método BN-PAGE tem contribuído na busca de respostas para diferentes questões: (i) a existência de complexos multicristalinos nas frações de proteinas hidrosolúveis de alto peso molecular, presentes nas lentes oculares humanas normais e com cataratas (Srivastava, Chaves *et al.*, 2008); (ii) a verificação do envolvimento da maquinaria hsp (chaperona) na produção do vírus hepatite B (Liu, Qian *et al.*, 2009); (iii) a definição dos proteomas mitocondriais de alguns órgãos de rato submetidos a condições fisiologicamente significativos (Reifschneider, Goto *et al.*, 2006); (iv) estudo oligomérico ativo da ATP-Sintetase em mitocôndria de mamíferos (Krause, Reifschneider *et al.*, 2005); (v) a análise do estado oligomérico da F1F0-ATP sintetase de mitocôndria de levedura (Arnold, Pfeiffer *et al.*, 1998); (vi) importe celular de proteínas, dinâmica de biogênese, associação de complexos protéicos em membranas, alterações mitocondriais em apoptose, encefalopatias mitocondriais, carcinogênese e doenças neurodegenerativas (Wittig e Schägger, 2009).

As vantagens atribuídas ao BN-PAGE são devidas às propriedades da molécula "Coomassie Brilliant Blue G-250" (CBB). Ao ligar nos domínios hidrofóbicos existentes na superfície das proteinas, o CBB exerce os seguintes efeitos:

(1) Carrega negativamente as proteinas, conserva a estrutura nativa e promove a mobilidade eletroforética das proteinas básicas para a região anódica do sistema;

(2) Reduz a agregação das proteinas devido à repulsão eletrostática de sua superfície carregada negativamente;

(3) As bandas protéicas são visíveis durante a eletroforese, e uma coloração subsequente do gel é opcional;

(4) As proteinas hidrofóbicas são convertidas em proteinas solúveis em água. A eletroforese é processada sem qualquer detergente na matriz do gel (Schägger, H., Cramer, W. *et al.*, 1994; Neff e Dencher, 1999; Krause, 2006).

No entanto, a estimativa acurada do tamanho dos complexos multiprotéicos por BN-PAGE ainda é um desafio**.** Diferentemente do gel nativo tradicional, os tamanhos aparentes dos complexos de proteínas no gel BN-PAGE são sensivelmente influenciados pelas moléculas de CBB, porque esse corante liga-se inespecificamente à superfície hidrofóbica das proteínas. O CBB tem uma massa molecular de 854,04 Da, uma massa que não deve ser ignorada, especialmente quando as proteinas apresentam tamanhos variando de 50 a 150 kDa. A ligação diferencial do CBB – a qual é devido às diferenças nas superfícies hidrofóbicas expostas entre as proteínas marcadoras e aquelas das proteinas da amostra –, provocará uma falsa estimativa da massa molecular (Heuberger, Veenhoff *et al.*, 2002; Wang, Xu *et al.*, 2007).

Nesse contexto, resultados obtidos por Wang e colaboradores mostraram que o tamanho calculado dos homotetrâmeros de gliceraldeído-3-fosfato desidrogenase e fosfoglicerato mutase são 144 e 113 kDa, respectivamente. No entanto, a massa obtida por BN-PAGE dessas enzimas foram respectivamente 110 e 90 kDa (Heuberger, Veenhoff *et al.*, 2002; Wang, Xu *et al.*, 2007).

Por isso, é procedimento padrão acoplar BN-PAGE (primeira dimensão) à SDS-PAGE (Tricina-SDS-PAGE) (segunda dimensão) para dirimir quaisquer dúvidas relativamente às bandas. Caso as bandas apresentem componentes, trata-se de um complexo, caso não, é interferência do CBB associado às regiões hidrofóficas das proteinas marcadoras e das proteinas das amostras (Wittig, Braun *et al.*, 2006; Geiger, Hirtz *et al.*, 2010). No entanto, alguns complexos apresentam resistência à dissociação completa por tratamento destanurante (Wang, Xu *et al.*, 2007). Perante isso, a verificação de possíveis componentes têm sido realizada pela extração da banda diretamente da primeira dimensão, digerida e aplicada ao sistema LC-MS/MS para posterior identificação (MASCOT e/ou MS BLAST).

A técnica BN-PAGE é promissora no estudo de complexos, conforme referências supracitadas, porém ainda aguarda a resolução da problemática das medidas das massas moleculares, a qual não é uma proposição de nosso trabalho.

Definitivamente, a fundamentação teórica do BN-PAGE e os resultados obtidos neste trabalho mostraram-se concordes, corroborando os trabalhos anteriores que demonstraram BN-PAGE como a técnica mais apropriada no estudo de complexos multiprotéicos.

5.2. Análise de complexos proteicos do secretoma de *Trichoderma harzianum*

Os resultados obtidos neste trblho evidenciaram que o *T. harzianum* secreta complexos multienzimáticos heterogêneos e ativos quando cultivados em meio contendo bagaço de cana como fonte de carbono. A análise constitucional de cada complexo reportado na Tabela I sugere uma reação sinergística possível entre as diferentes enzimas, uma consequência da interação cooperativa para degradação eficiente do bagaço de cana.

Nesse contexto, a enzima ABF encontrada nos três complexos desfaria o impedimento estérico pela clivagem das ligações alfa-L-arabinofuranosil dos ramos de arabinose presente em xilanas para melhor desempenho das celulases (Murashima, Kosugi *et al.*, 2003; Seiboth e Metz, 2011). Assim, no complexo I os ABFs cooperam possivelmente com a 1,4-beta-xilosidase para remover sucessivamente os monômeros de D-xilose a partir do esqueleto de xilana, permitindo as CBHs penetrar profundamente na parede celular vegetal.

Similarmente à ABF, AXE e cutinase, encontradas no complexo II facilitariam, respectivamente, às endoxilanases acessarem o esqueleto de xilana pela remoção das cadeias laterais acetiladas (Beg, Kapoor *et al.*, 2001) e acessorar outras enzimas hidrolíticas a atingir os polímeros da parede celular durante o processo de degradação vegetal no crescimento saprofítico (Rubio, Cardoza *et al.*, 2008). Adicionalmente, as xilanases e celulases atuam como elicitores de proteínas relacionadas a patógenos em plantas, as quais poderiam justificar a presença da enzima de controle biológico endoquitinase no mesmo complexo (Yang, Yang *et al.*, 2009). Recentemente, a endoquitinase mostrou-se um excelente agente biológico contra *Rhizoctonia solani* e *Fusarium solani* (Mishra, Kshirsagar *et al.*, 2012). Neste contexto, *T. harzianum* enrola-

se à hifa do hospedeiro e usa a alfa-1,3-glucanase (mutanase) (complexo III) para penetrar na parede celular (Wiater, Janczarek *et al.*, 2011).

Assim como em *T. harzianum*, uma relação sinergística similar entre celulases e hemicelulases foi anteriormente reportado na conversão de substratos complexos como palhas de trigo (Tabka e Sigoillot, 2006) e milho (Selig, Knoshaug *et al.*, 2008) em açúcares simples por enzimas isoladas por outros fungos filamentosos. O sinergismo entre xilanases e celulases também foi observado no micro-organismo anaeróbico *C. cellulovorans* durante a degradação do bagaço de cana de açucar. Neste caso, a relação sinergística ocorre em celulosomas (Tabka e Sigoillot, 2008). A estrutura de um celulosoma possui uma proteína não catalítica denominada de escafoldina ("Scaffoldin"), o qual integra o complexo glicosil hidrolases, liga-o à superfície celular e ancora o complexo inteiro na celulose cristalina (Fontes e Gilbert, 2010).

Neste trabalho não foi encontrada uma escafoldina em qualquer dos complexos estudados, sugerindo que tais complexos apresentam uma organização estrutural diferente do celulosoma bacteriano típico. No entanto, os dados de dissociação incompleta e dos perfis BN-PAGE preservados em diferentes concentrações proteicas sugere uma interação tipo coesina-dockerina. A literatura relata que os domínios coesina e dockerina medeiam uma interação de alta afinidade entre as subunidades em celulosomas (bactérica anaeróbica) e complexos enzimáticos (fungos anaeróbicos e bactérias aeróbicas), cuja constante de associação é maior que 10^9 M^{-1} (Shoham, Lamed *et al.*, 1999; Kosugi, Murashima *et al.*, 2002; Miras, Schaeffer *et al.*, 2002; Schaeffer, Matuschek *et al.*, 2002; Fontes e Gilbert, 2010).

Uma enzima chamada glicosidase foi encontrada e identificada como uma escafoldina potencial no fungo anaeróbico *Piromyces equi*. Resultados mostraram que o domínio duplo de dockerina presente na Cel45A (celobiohidrolase) of *P. equi* conecta-se à aquela glucosidase (~ 100 kDa) (Fanutti, Ponyi *et al.*, 1995; Nagy, Tunnicliffe *et al.*, 2007). No entanto, nenhum dos complexos analisados neste trabalho tiveram essa enzima, a qual pode ser provavelmente devido às diferentes fontes de carbono. Por exemplo, dados anteriores mostraram que as diferenças no tipo de enzima hidrolítica secretado pelos fungos filamentosos são uma consequência da fonte de carbono presente nos meios de cultura (Jørgensen, Goosen *et al.*, 2009; Fernández-Acero, Colby *et al.*, 2010; Lu, Sun *et al.*, 2010; Mahajan e Master, 2010; Jun, Kieselbach *et al.*, 2011), sugerindo que a estrutura e a função de cada complexo multimérico no secretoma de *T.*

harzianum pode ser também especificamente induzido pela fonte de carbono, conforme descrito alhures (Gonzalez-Vogel, Eyzaguirre *et al.*, 2011).

Pela primeira vez foi encontrado SWOI e GPI-EglC na forma complexada em secretoma de *T. harzianum* (complexo III). A proteína semelhante a SWOI, descrita primeiramente por (Saloheimo, Paloheimo *et al.*, 2002), atua no afrouxamento da biomassa lignocelulósica sem produzir quantidades detectáveis de açúcares redutores (Saloheimo, Paloheimo *et al.*, 2002; Arantes, V. e Saddler, J., 2010). Esta proteína promove a amorfogênese das microfibrilas de celulose e aumenta a eficiência da atividade celulolítica (Arantes, V. e Saddler, J. N., 2010).

Semelhante à SWOI, o SBD ("Starch Binding Domain") encontrado em glicoamilase também conhecido como amiloglicosidase ou γ-amilase (EC 3.2.1.3), tem sido proposto aumentar a hidrólise de amido ou oligossacarídeos relacionados ao afrouxamento de sua estrutura e posicionar os domínios catalíticos ou outras glicosídeos hidrolases sobre a superfície do substrato vegetal. Esse domínio pode ser funcionalmente independente do seu domínio catalítico; o SBD pertence à família CBMs ("carbohydrate-binding modules") (Bolam, Ciruela *et al.*, 1998; Southall, Simpson *et al.*, 1999; Giardina, Gunning *et al.*, 2001; Tung, Chang *et al.*, 2008).

Finalmente, GPI-EglC ligaria o complexo III à célula fúngica, aumentando a eficiência de degradação devido ao íntimo contato entre as diferentes enzimas e a biomassa vegetal. Essa molécula também foi encontrada em *Aspergillus fumigates*, mas não associada a complexos multienzimáticos (Mouyna, Sarfati *et al.*, 2002; Mouyna, Morelle *et al.*, 2005; Gastebois, Mouyna *et al.*, 2010; Hartl, Gastebois *et al.*, 2011). As proteínas ancoradas a GPI têm mostradas, repetidamente, um papel na remodelagem dos polissacarídeos da parede celular. No entanto, GPI-EglC tem uma função que não foi diretamente relacionada à sua atividade enzimática, e sua função no crescimento morfogenético dos fungos filamentosos ainda permanece uma questão aberta (Mouyna, Sarfati *et al.*, 2002; Mouyna, Morelle *et al.*, 2005; Gastebois, Mouyna *et al.*, 2010; Hartl, Gastebois *et al.*, 2011).

5.3. Análise de complexos proteicos do secretoma de *Trichoderma reesei*

A espécie *T. reesei* é alvo de interesse acadêmico, biotecnológico e industrial, sendo o principal produtor de celulases até o momento. O sistema de degradação vigente para este fungo é o sistema de enzimas livres presentes no seu secretoma (Shoham 1999). Em contraste a este sistema atribuído a *T. reesei*, este trabalho mostrou a presença de complexos multi-enzimáticos ativos no seu secretoma. Além disso, a análise de dois complexos mostraram que os seus componentes diferem-se, dependendo da fonte de carbono utilizada (lactose e galactose).

A técnica BN-PAGE mostrou que o complexo I é aparentemente mais expresso em lactose que galactose, ocorrendo inversamente com o complexo II, o qual é aparentemente mais expresso em galactose que lactose. Esta diferença de expressão, como um efeito da diferença na intensidade da coloração por CBB entre as bandas foi possível ser estabelecido devido à normalização entre as amostras obtidas de culturas com fontes de carbonos em concentrações diferentes (lactose 1% (m/v) e galactose 0,3% (m/v)), antes da aplicação no gel. Esta diferença na concentração das fontes de carbono se justifica, porquanto concentrações acima de 0,3% para galactose não induziu a produção de celulases em *T. reesei*. Acredita-se que a indução desse monossacarídeo processa-se apenas em baixas concentrações dentro do fungo. Experimentos de superexpressão do gene *bga1* (o qual aumenta a disponibilidade intracelular de galactose), realizado por Seiboth e colaboradores, promoveu o desligamento da transcrição enzimática (celobiohidrolases I e II) quando a atividade galactosidásica variou de 3 $U.g^{-1}$ até 12 $U.g^{-1}$ (Seiboth, Hartl *et al.*, 2005). Quanto à biomassa úmida micelar cultivada, uma quantidade fixa (aproximadamente 60 g) foi estabelecida para ambas as fontes de carbono.

Os três complexos marcados com asterisco, bem como as enzimas exclusivas na constituição dos complexos I e II presentes em meio lactose parecem explicar a maior concentração da atividade enzimática (celulolítica e xilanolítica) em lactose comparativamente a galactose. Interessantemente, *T. reesei* produziu mais complexos multi-enzimáticos e uma composição específica nos complexos I e II parece torná-los melhores equipados para biodegradação (discutiremos abaixo) quando cultivado em meio contendo lactose que cultivado em meio contendo o seu indutor galactose.

Muitos trabalhos mostraram que a galactose é realmente o indutor de celulases para *T. reesei*, quando este é cultivado em meio contendo lactose. Paralelamente, o indutor

mais potente para indução de celulases em *T. reesei* é soforose, um dissacarídeo resultante da despolimerização da celulose e posterior transglicosilação da celobiose. Interessantemente, os resultados obtidos por Sternberg e Mandels mostraram que *T. reesei* cultivado em meio contendo celulose apresenta maior atividade enzimática que cultivado sob meio contendo o seu indutor soforose. Os autores explicam esta diferença devido a maior expressão enzimática e celulases exclusivas encontradas no secretoma produzido em meio contendo celulose que soforese (Sternberg e Mandels, 1979).

A comparação acima mostra uma resposta similar do fungo a essas fontes de carbono, sugerindo lactose e celulose devam possuir uma via de sinalização alternativa (não exatamente a mesma para ambas) que, uma vez disparada a nível de membrana plasmática pela presença dos sacarídeos, intensifique a expressão gênica e induza a transcrição de genes distintos para a formação de complexos, possivelmente para atender a complexidade do polissacarídeo a ser degradado. Nós hipotetizamos que uma proteína sensora registra a presença das moléculas de lactose antes de serem totalmente catalizadas pela beta-galactosidase. Esse tempo necessário poderia estar correlacionado à baixa eficiência catalítica da enzima sobre o substrato lactose (kcat/Km = 0,23 ± 0,02) comparativamente aos substratos O-Nitrophenil-β-D-galactopiranosídeo (kcat/Km = 159,41 ± 5,41), lactulose (kcat/Km = 7,98 ± 0,78) e galactobiose (kcat/Km = 1,83 ± 0,51) (Gamauf, Marchetti *et al.*, 2007). Um receptor para o polissacarídio quitina foi encontrado em vertebrados (Day, Okada *et al.*, 2001).

Neste contexto, BN-PAGE das frações enriquecidas de membrana plasmática de *T. reesei* é uma sugestão experimental apropriada para verificar a organização das proteínas de membrana em meio contendo lactose e galactose. Neste trabalho nós obtivemos as frações enriquecidas de membrana celular de *T. reesei*, no entanto em baixo redimento, o que exige maior quantidade de massa micelar inicial ou melhoramento do protocolo utilizado. Por uma questão de tempo disponível para a finalização do doutorado, a continuação deste objetivo específico ficou reservado como perspectivas.

Assim como em *T. harzianum*, a atividade celulolítica e xilanolítica presente nos complexos estudados em *T. reesei* sugere uma cooperatividade funcional no processo de degradação de subtratos. A enzima beta-1,3-endoglucanase é encontrada em ambos os complexos estudados. Esta enzima está ligada à parede celular de fungos. Dados reportados não relacionam-na diretamente com a sua atividade enzimática específica, que é sua participar da remodelação da parede celular do fungo para o seu crescimento.

Esta função nos fungos filamentosos ainda permanece uma questão aberta (Mouyna, Sarfati *et al.*, 2002; Mouyna, Morelle *et al.*, 2005; Gastebois, Mouyna *et al.*, 2010; Hartl, Gastebois *et al.*, 2011).

Neste trabalho, a atividade beta-1,3-endoglucanase, representada pelas GHs 16 e 17, poderia estar ancorada a GPI, conectando os complexos à membrana celular fúngica. Esta hipótese é corroborada pelo fato de beta-1,3-endoglucanase, atribuída à GH 16, ter sido encontrada ancorada a GPI em *Aspergillus fumigatus* (Hartl, Gastebois *et al.*, 2011). Recentemente, a mesma enzima foi encontrada como componente de um complexo multi-enzimático presente no secretoma de *T. harzianum*, além de associada a GPI, indicando um papel de ligação do complexo à célula do fungo (Silva, Gómez-Mendoza *et al.*, 2012a). Adicionalmente, uma “predicted protein” (gi|340518236), também encontrada nos complexos estudados, teve sua descrição sequencial por “Blast2go” sendo identificada como uma proteína de parede celular.

Portanto, a associação dos complexos I e II ao fungo pela beta-1,3-endoglucanase e pela proteína de parede celular fúngico (“Blast2go” da “predicted protein”**,** gi|340518236) poderia aumentar a eficiência de degradação devido o contato entre as diferentes enzimas do complexo e o substrato.

As proteínas constituintes dos complexos associaram-se com maior heterogeneidade quando a fonte de carbono foi a lactose. Por exemplo, a alfa-1,3-endoglucanase (“Blast2go” da “predicted protein”, gi|340518010), beta-N-acetilhexosaminidase (“Blast2go” da GH 20, gi|340520576) e alfa-fucosidase (GH 95) foi encontrada somente nos complexos oriundos do meio contendo lactose.

Juntas no mesmo complexo: beta-1,3-endoglucanase, proteína de parede celular (“predicted protein”**,** gi|340518236), alfa-1,3-endoglucanase e beta-N-acetilhexosaminidase apresentariam uma cooperatividade funcional no processo de degradação de paredes de fungos e exoesqueletos de crustáceos e insetos. A beta-1,3-endoglicanase e a proteína de parede fúngica ligariam os complexos I e II à hifa de *T. reesei*, havendo ainda a possibilidade de a endoglucanase manter os complexos aderidos ao substrato polissacarídico pelo CBM, típico domínio de ligação a carbohidratos das celulases e xilanases (Tung, Chang *et al.*, 2008).

A enzima alfa-1,3-endoglucanase, que pertence à família GH 71, catalisa a degradação de alfa-glucanas, um polissacarídeo insolúvel em água e presente na parede celular de muitos fungos, incluindo os filamentosos. Após sua ação inicial intracadeia, a hidrólise prossegue repetitiva para a extremidade não redutora do

polímero, liberando resíduos de beta-glicose como produto principal. O micoparasita *T. harzianum* utiliza esta mesma enzima para degradar a parede celular dos fungos fitopatogênicos como *Rhizoctonia solani* e *Fusarium solani*. (Grün, Dekker *et al.*, 2006; Mishra, Kshirsagar *et al.*, 2012).

Finalmente, a beta-N-acetilhexosaminidase atuaria sobre os oligossacarídeos de quitina produzidos por quitinases (presente somente no complexo II para ambas as fontes de carbono), cooperando com o processo degradativo do substrato. Como esta enzima prefere substratos curtos de β-N-acetilglicosamina, quitobiose e p-nitrophenil-N-acetil-β-D-glicosamina, também é chamada de quitobiase (Drouillard, Armand *et al.*, 1997). Recentemente foi relatada uma beta-N-acetilhexosaminidase que produz N-acetilglicosamina a partir de cadeias longas de quitina, isto é, atua diretamente no polímero da macromolécula (Konno, Takahashi *et al.*, 2012).

Diferentemente de *T. harzianum* (Silva, Gómez-Mendoza *et al.*, 2012b), uma beta-glucosidase (análise por “Blast2go” da proteína identificada como GH 55) foi encontrada no complexo I do secretoma produzido em cultura contendo galactose em *T. reesei*. Interessantemente, esta enzima aparece somente nos complexos onde a alfa-N-arabinofuranosidase (“Blast2go” da GH 54) está presente. Esta beta-glucosidase não poderá ser identificada como uma escafoldina potencial, como a encontrada por Nagy e colaboradores no fungo anaeróbico *P. Equi*, porquanto a beta-glucosidase por eles encontrada pertence à família GH 3 (Fanutti, Ponyi *et al.*, 1995; Nagy, Tunnicliffe *et al.*, 2007). No entanto, o complexo II do mesmo meio possui uma proteína pertencente à família GH 3. Uma análise “Blast2go” desta proteína mostrou portar atividade hidrolase, mas nenhum código de reação mais específico. A massa molecular da GH 3 e a encontrada por Nagy e colaboradores diferem-se por 6 kDa. No sistema de classificação de enzimas CAZy (“Classification System of Carbohydrate Active Enzymes”), elaborado por Coutinho e Henrissat, a família GH 3 apresenta as seguintes reações: β-glucosidase (EC 3.2.1.21), xilan 1,4-β-xilosidase (EC 3.2.1.37), β-N-acetilhexosaminidase (EC 3.2.1.52), glucan 1,3-β-glucosidase (EC 3.2.1.58), glucan 1,4-β-glucosidase (EC 3.2.1.74), exo-1,3-1,4-glucanase (EC 3.2.1.-) e α-L-arabinofuranosidase (EC 3.2.1.55). Experimentos adicionais serão necessários para afirmar categoricamente que a proteína GH 3 encontrada aqui é uma beta-glucosidase já reportada para *P. equi* (Nagy, Tunnicliffe *et al.*, 2007).

Algumas hemicelulases estão distribuídas pelos complexos. Notadamente, o complexo I obtido do meio com galactose apresenta atividades alfa-galactosidase (GH 36) e arabinofuranosidase (GH 54), enquanto o complexo I do meio lactose apresenta alfa-galactosidase e xiloglucanase. Não existe lactose no ambiente natural de *T. reesei* ou qualquer outro fungo filamentoso, porém as beta-galactosidases envolvidas na hidrólise inicial de lactose (produzido galactose e glicose) tenha outros papéis no metabolismo fúngico, tais como a clivagem de resíduos de proteínas glicosiladas ou estruturas poliméricas encontradas em diferentes paredes celulares vegetal ou fúngico (Gamauf, Marchetti *et al.*, 2007).

A cooperatividade funcional destas enzimas desfazem os impedimentos estéricos: (i) ligações alfa-D-galactosídeos em alfa-galactosídeos, como oligossacarídeos de galactose, galactomananas e galactolipídeos (alfa-galactosidase,), além de alfa-fucosídeos (alfa-fucosidase, GH 95); (ii) ligações alfa-L-arabinofuranosil dos ramos de arabinose (arabiofuranosidase), e (iii) ligações 1,4-beta-D-glicosídico em xiloglucana (exo-beta-1,4-glucanase xiloglucana específica), permitindo as endocelulases atingir as fibras de celulose (Murashima, Kosugi *et al.*, 2003; M.G. Tabka, 2006; Selig, Knoshaug *et al.*, 2008; Seiboth e Metz, 2011).

6. Conclusões e perspectivas

O método BN-PAGE mostrou-se uma técnica apropriada para a detecção de complexos multi-enzimáticos secretados por fungos filamentosos. Em todos os ensaios não houve agregações proteicas a altas concentrações da amostra, reforçando o importante papel do corante “Coomasie Brilhant Blue G-250”, o qual não interfere na funcionalidade das proteínas.

A identificação de proteínas oriunda de microorganismos sem genoma disponível em bancos de dados por espectrometria de massas tipo LC-MS/MS e método de tolerância a erros e homologia mostroram melhores resultados que o método estringente por identidade, utilizando o *software* MASCOT.

Este trabalho mostra pela primeira vez que ambos os fungos, *T. harzianum* e *T. reesei*, possuem complexos multi-enzimáticos ativos no secretoma. Consequentemente, o modelo atual de degradação de polissacarídeos de parede celular vegetal por sinergismo entre enzimas livres em solução parece não refletir completamente a realidade para estes fungos.

Os complexos multiproteicos em *T. reesei* alteram seus componentes dependendo da fonte de carbono utilizada.

Este trabalho suscitou ideias que complementam e aprofundam nossas conclusões, tais como verificar as alterações que as diferentes fontes de carbono provocam na composição dos complexos multiproteicos em secretomas. Outras ideias já estão encaminhadas, tais como o (i) desenvolvimento de métodos que associe BN-PAGE e Termodinâmica (Termo/BN-PAGE) para determinar as forças não covalentes que governam a interação entre cada componente na formação do complexo multi-enzimático, (ii) que resolva o problema da massa molecular, sempre discutido por autores como sendo um “gargalo” da técnica BN-PAGE, (iii) que quantifique a atividade de degradação dos componentes em complexos e livres de modo a compreender melhor o papel do sinergismo nestes sistemas.

7. Artigos publicados

Artigo publicado durante o doutorado e relativo à tese

RESEARCH ARTICLE

Blue native-PAGE analysis of *Trichoderma harzianum* secretome reveals cellulases and hemicellulases working as multienzymatic complexes

Adelson Joel da Silva[1], Diana Paola Gómez-Mendoza[1]*, Magno Junqueira[1], Gilberto Barbosa Domont[2], Edivaldo Ximenes Ferreira Filho[3], Marcelo Valle de Sousa[1] and Carlos André Ornelas Ricart[1]*

[1] Laboratório de Bioquímica e Química de Proteínas, Departamento de Biologia Celular, Universidade de Brasília, Brasília, DF, Brazil
[2] Instituto de Química, Universidade Federal do Rio de Janeiro, Rio de Janeiro, RJ, Brazil
[3] Laboratório de Enzimologia, Departamento de Biologia Celular, Universidade de Brasília, Brasília, DF, Brazil

Plant cell wall-degrading enzymes produced by microorganisms possess important biotechnological applications, including biofuel production. Some anaerobic bacteria are able to produce multienzymatic complexes called cellulosomes while filamentous fungi normally secrete individual hydrolytic enzymes that act synergistically for polysaccharide degradation. Here, we present evidence that the fungus *Trichoderma harzianum*, cultivated in medium containing the agricultural residue sugarcane bagasse, is able to secrete multienzymatic complexes. The *T. harzianum* secretome was firstly analyzed by 1D-BN (blue native)-PAGE that revealed several putative complexes. The three most intense 1D-BN-PAGE bands, named complexes [I], [II], and [III], were subsequently subjected to tricine SDS-PAGE that demonstrated that they were composed of smaller subunits. Zymographic assays were performed using 1D-BN-PAGE and 2D-BN/BN-PAGE demonstrating that the complexes bore cellulolytic and xylanolytic activities. The complexes [I], [II], and [III] were then trypsin digested and analyzed separately by LC-MS/MS that revealed their protein composition. Since *T. harzianum* has an unsequenced genome, a homology-driven proteomics approach provided a higher number of identified proteins than a conventional peptide-spectrum matching strategy. The results indicate that the complexes are formed by cellulolytic and hemicellulolytic enzymes and other proteins such as chitinase, cutinase, and swollenin, which may act synergistically to degrade plant cell wall components.

Received: February 6, 2012
Revised: June 8, 2012
Accepted: June 12, 2012

Keywords:
BN-PAGE / Microbiology / Multienzymatic complex / Secretome / Sugarcane bagasse / *Trichoderma harzianum*

Correspondence: Dr. Carlos André Ornelas Ricart. Laboratório de Bioquímica e Química de Proteínas, Departamento de Biologia Celular, Campus Universitário Darcy Ribeiro, Brasília, DF -70910-900, Brazil.
E-mail: ricart@unb.br
Fax: +55-61-32720003

Abbreviations: ABF, arabinofuranosidase; **BN-PAGE**, blue native-PAGE; **CBH**, cellobiohydrolase; **GPI-EglC**, Glycosylphosphatidylinositol-anchored cell wall beta-endoglucanase; **HSP**, high-scoring segment pairs; **SWOI**, swollenin

1 Introduction

Cellulose and hemicellulose, although abundant components of plant biomass, do not accumulate on earth due to the efficient activity of cellulolytic and hemicellulolytic enzymes produced by microorganisms. These enzymes have potential in biotechnological applications, including degradation of agricultural residues aiming at generating fermentable sugars that are suitable for the production of second-generation

*These authors contributed equally to this work.

© 2012 WILEY-VCH Verlag GmbH & Co. KGaA, Weinheim

bioethanol [1, 2]. In Brazil, the world's most competitive producer of bioethanol, the main agroindustrial residue is sugarcane bagasse, the fibrous matter that remains after sugarcane (*Saccharum officinarum* Linnaeus) stalks are crushed to extract their juice. Similarly to other agricultural residues, sugarcane bagasse is mainly composed of cellulose and a complex mixture of heteropolysaccharides known as hemicellulose (in which the main component is xylan), embedded in a lignin matrix [3].

The biodegradation of plant cell wall polysaccharides (cellulose and hemicelluloses) depends on the coordinate action of different enzymes over both the main chain and the ramification of hemicelluloses. The filamentous fungi of the *Trichoderma* genus are ubiquitous colonizers of cellulosic material and the plant cell wall-degrading enzymes produced by these organisms have been extensively characterized and used in industrial processes [4, 5]. The most studied species of *Trichoderma* is *T. reesei*, a potent cellulase producer, whose cellulolytic machinery is composed of two cellobiohydrolases (CBHs) (Cel7A, Cel 6A), five endoglucanases (Cel7B, Cel5A, Cel12A, Cel61A, and Cel45A), and two β-glucosidases (BGLI and BGLII). Several hemicellulases including xylanases, mannanases, and galactosidases are additionally secreted by *T. reesei* [6].

By contrast, the mycoparasitic species *T. harzianum* has been shown to be an efficient biocontrol agent against several phytopathogenic fungi. The mycoparasitic activity of *T. harzianum* relies particularly on the production of enzymes able to hydrolyze components of the fungal cell wall, such as chitinases, proteases, and beta-1,3-glucanases [7–10]. Nonetheless, in recent years, *T. harzianum* has also become a promising organism for cellulase and xylanase production under appropriate conditions [11]. In fact, a *T. harzianum* strain (IOC-4038) has been shown to produce a well-balanced set of cellulolytic enzymes and a fast kinetics for the production of endoglucanase and beta-glucosidases when compared with *T. reesei* [12].

Some anaerobic bacteria, such as *Clostridium thermocellum*, are also able to carry out plant cell wall degradation. These organisms produce and secrete multienzymatic complexes called cellulosomes that possess a higher cellulose degradation efficiency than free enzyme systems produced by fungi and aerobic bacteria. Cellulosomes can also attach to insoluble substrates, which promotes a greater competitiveness of individual microbial cells [13]. Interestingly, the anaerobic bacteria *Butyvibrio fibrisolvens* and *Clostridium papyrosolvens* produce multienzymatic complexes that are structurally distinct from *C. thermocellum* cellulosomes. For instance, *B. fibrisolvens* has an enzyme complex (called "xylanosome"), which contains 11 proteins with xylanolytic activity and three with endoglucanase activity. The case of *C. papyrosolvens* is even more remarkable because its enzyme supercomplex that can deconstruct cellulose and xylan contains seven smaller complexes with molecular weight ranging from 500 to 600 kDa [14, 15].

It is generally accepted that aerobic fungi do not produce cellulosome-like complexes. For these fungi, including *Trichoderma* sp., the classic mechanism of biomass depolymerization by synergism between free enzymes normally applies. However, two groups recently reported the production of multienzymatic complexes in the thermophilic fungus *Chaetomium* sp. [16] and in the soft-rot fungus *Penicillium purpurogenum* [17].

The blue native-polyacrylamide (BN-PAGE) technique has been extensively used to analyze native protein complexes from biological membranes as well as protein–protein interactions in water soluble proteins. This methodology in combination with a denaturing second dimension (SDS-PAGE) makes it possible to determine molecular mass, oligomeric states, subcomplexes, and sample purity. BN-PAGE is processed without any detergent in the gel matrix and its features depend on the CBB properties. CBB binds to hydrophobic domains on the protein complex surface, causing (1) introduction of negative charges that conserve the native structure and promote protein mobility to the anode, (2) reduction of protein aggregation due to electrostatic repulsion, and (3) conversion of hydrophobic into water soluble proteins [18].

Due to its versatility, BN-PAGE has been applied to the study of different biological processes. In-gel catalytic activity assays using BN-PAGE gels have been applied to identify and quantify mitochondrial oxidative phosphorylation complexes and other enzymes such as dihydrolipoamide dehydrogenase, NAD kinase, and NADPH producing enzymes [19]. Recently, BN-PAGE was applied to study multienzymatic complexes secreted by the filamentous fungus *P. purpurogenum* [17].

Given the biotechnological importance of *Trichoderma* sp. as producers of hydrolytic enzymes and the value of sugarcane bagasse as a major biomass source for biofuel production, the objectives of this work were to assess the presence of multienzymatic complexes in the secretome of *T. harzianum* grown in sugarcane-containing medium by means of BN-PAGE, zymography/BN-PAGE, and mass spectrometric methods.

2 Materials and methods

2.1 *Trichoderma harzianum* culture and secretome preparation

The *T. harzianum* strain T4 was provided by I. S. Melo (Embrapa/CNPMA, Brazil) and forms part of the culture collection of the Laboratory of Enzymology (University of Brasília, Brazil). *Trichoderma harzianum* conidiospores were produced in solid-state synthetic medium (SM; 680 mg·L^{-1} KH_2PO_4, 870 mg·L^{-1} K_2HPO_4, 1.7 g· L^{-1} $(NH_4)_2SO_4$, 200 mg· L^{-1} KCl, 200 mg· L^{-1} $CaCl_2$, 200 mg· L^{-1} $MgSO_4$· 7 H_2O, 2 mg· L^{-1} $FeSO_4$, 2 mg· L^{-1} $MnSO_4$ and 2 mg· L^{-1} $ZnSO_4$,

© 2012 WILEY-VCH Verlag GmbH & Co. KGaA, Weinheim

20 g· L^{-1} agar, pH 6.0) supplemented with 1% (w/v) sugarcane bagasse as carbon source [20]. Prior to use, sugarcane bagasse was washed with distilled water, sterilized by autoclaving at 121°C for 1 h, incubated overnight at 60°C, and finally pulverized. After 6 days of growth, spores were harvested and a suspension (10^8 spores·mL^{-1}) inoculated into 300 mL of liquid-state SM medium (1 L Erlenmeyer flask) containing 1% (w/v) sugarcane bagasse. The culture was incubated at 28°C on a rotatory shaker at 150 rpm, during 9 days and the secretome was then separated from mycelium by filtration using a Whatman No.1 paper followed by dialysis and lyophilization. Protein concentration was determined by the BCA Protein Assay kit (Pierce Biotechnology, Rockford, IL, USA) using BSA as standard.

2.2 BN-PAGE

BN-PAGE was carried out making use of a method for water-soluble proteins, as previously described [18, 21]. Lyophilized proteins from *T. harzianum* secretome were resuspended in a buffer containing 0.05 mol·L^{-1} Bis/Tris-HCl pH 7.0, and 15% (w/v) glycerol. For 1D-BN-PAGE, different protein concentrations (0.2 mg·mL^{-1}, 5.0 mg·mL^{-1}, and 10.0 mg·mL^{-1}) were applied onto 5–18% (w/v) polyacrylamide gradient gels and run at 15 mA constant current at 4°C for 4 h in a SE 600 electrophoresis system (Hoefer, Inc., San Francisco, CA, USA). The anode buffer consisted of 0.05 mol·L^{-1} Bis-Tris HCl pH 7.0 while the cathode buffer was composed of 0.05 mol·L^{-1} Tricine, 0.015 mol·L^{-1} Bis-Tris-HCl pH 7.0 and 0.02% (w/v) CBB G-250 (Bio-Rad, Hercules, CA, USA). Subsequently, gels were fixed and stained using CBB G-250. The proteins thyroglobulin (669 kDa), ferritin (440 kDa), catalase (232 kDa), lactate dehydrogenase (158 kDa), and BSA (67 kDa) were used as molecular weight markers.

BN-PAGE second dimension was carried out using Tricine-SDS-PAGE as previously described [22]. First, 1D-BN-PAGE gel pieces corresponding to the putative protein complexes were incubated in 1% (w/v) SDS and 1% (v/v) beta-mercaptoethanol solution for 2 h at room temperature. The gel pieces were then washed with ultrapure water to completely remove the beta-mercaptoethanol and subsequently placed between glass plates. A 16% (w/v) polyacrylamide Tricine SDS mixture was poured living a 2 cm gap to the gel pieces. Following polymerization, a layer (1.5 cm) of 10% (w/v) polyacrylamide Tricine SDS gel was added. Finally, gel pieces were embedded in a 10% (w/v) polyacrylamide native gel containing 10% (v/v) glycerol and 0.2% (w/v) SDS. Electrophoresis was run at 50 mA constant current and 18°C for approximately 10 h. Tricine-SDS-PAGE gels were fixed and silver stained [23].

2.3 1D-BN-PAGE and 2D-BN/BN-PAGE zymographic analysis

Trichoderma harzianum secretome proteins were subjected to 1D-BN-PAGE using gels copolymerized with 0.1% (w/v) oat spelts xylan or carboxy methyl cellulose (Sigma-Aldrich Co., St Louis, MO, USA) in order to detect xylanolytic and cellulolytic activities, respectively. Samples were also subjected to 2D-BN/BN-PAGE zymographic analysis. Therefore, samples were first subjected to 1D-BN-PAGE without copolymerized polysaccharides. 1D-BN-PAGE lanes were then submitted to a second BN-PAGE dimension on gels containing cellulose or xylan. After 1D-BN-PAGE or 2D-BN/BN-PAGE, gels were washed with 0.05 mol·L^{-1} sodium acetate, pH 5.5 and incubated for 10 min at 85–90°C for xylanolytic [24] or for 1 h at 55°C for cellulolytic activity assay [25]; the reaction was stopped by incubating gels at 4°C overnight. The gels were then stained with 0.1% (w/v) Congo red for 30 min. Enzyme activity was observed as a clear zone contrasting with a dark red background after addition of 0.5% (v/v) acetic acid to gels to improve visualization.

2.4 In-gel digestion and MS analysis

Gel slices from 1D-BN-PAGE were manually excised for identification by LC-MS/MS on a LTQ Orbitrap Velos mass spectrometer (Thermo Fisher Scientific, Germany). Gel bands were reduced with 0.01 mol·L^{-1} DTT in 0.01 mol·L^{-1} NH_4HCO_3 at 56°C for 1 h in the dark. Cystein carbamidomethylation of each sample was performed with 0.05 mol·L^{-1} iodoacetamide for 1 h at room temperature. Bands were dehydrated with 100% ACN, and further digested using sequencing grade modified porcine trypsin (Promega, Fitchburg, WI, USA). The resulting tryptic peptides were extracted from gel matrix by three cycles of 10 min incubation with ACN:H_2O:TFA (66:33:0.1, v/v/v) followed by 10 min sonication. The extracts were dried in a vacuum centrifuge, reconstituted in 10 μL of 0.05% TFA solution, and injected onto an EASY-nLC II nano-LC (Proxeon, Denmark) interfaced to a LTQ Orbitrap Velos. Peptide pools were first loaded onto a trap column (30 × 0.1 mm) packed with Reprosil-Pur 120 C18-AQ 5 μm particles (Dr. Maish, Germany). After 4 min washing with solvent A (H_2O:acetonitrile (95:5, v/v), 0.1% (v/v) formic acid) peptides were eluted during the gradient on a 120 × 0.05 mm column packed with C18 Reprosil-Pur 120 C18-AQ 3 μm particles (Dr. Maish) at a flow rate of 200 nL·min^{-1}. Gradient was 5–20% of solvent B (H_2O:acetonitrile [20:80, v/v], 0.1% [v/v] formic acid) for 30 min, 20–50% B for 15 min, 50–100% B for 5 min, and 100% B for 10 min. Peptides were dynamically eluted into the mass spectrometer via a nanospray probe (Thermo Scientific, Germany) using a nanospray emitter (20 μm id, 10 μm tip id) (New Objective, Inc, Woburn, MA, USA) with a spray voltage of 1.8 kV, and the transfer capillary temperature was set at 180°C. Automated Data Dependent Acquisition was controlled by Xcalibur 2.1 software (Thermo Scientific). The acquisition cycle consisted of a survey scan from 300–1800 m/z at 60 000 resolution (full width at half maximum) at m/z 400 on the Orbitrap followed by fragmentation of the ten most intense multiple charged precursors on the linear ion trap under the normalized

© 2012 WILEY-VCH Verlag GmbH & Co. KGaA, Weinheim

collision energy of 35%. The automatic gain control was set to 5×10^5 charges for the survey scan on the Orbitrap using one microscan and 5×10^4 charges for MS/MS on the ion trap using one microscan. The ion selection threshold for MS/MS was set to 500 counts using a precursor isolation window of 4 amu. Activation parameter "q" and activation time were set to 0.25 and 30 ms, respectively. Precursors already fragmented were dynamically excluded during the cycle for a further 90 s.

2.5 Data analysis

MASCOT stringent conventional database searches were applied in combination with sequence similarity searches for cross-species error tolerant protein identification, as previously described [26]. Briefly, the .mgf format files were filtered using EagleEye software v1.66 [27] prior to automatic de novo sequencing by PepNovo software [28] and MS-BLAST search reviewed in [29] searched against a curated version of NCBInr (nrdb95) protein database (http://genetics.bwh.harvard.edu/msblast/iblast_databases .html). The filtered spectra were exported and searched against the NCBInr protein database (release 20 110 729, containing 14 821 581 sequences, 5 074 018 658 residues; http://www.ncbi.nlm.nih.gov/) using MASCOT software v.2.1 (Matrix Science, Ltd., http://www.matrixscience.com/). Search parameters established were: (i) fungi as taxonomy, (ii) trypsin as enzyme, (iii) up to two missed cleavages allowed, (iv) peptide mass tolerance 10 ppm, (v) fragment mass tolerance 0.6 Da, (vi) cystein carboxyamidomethylation as fixed modification, and (vii) methionine oxidation as variable modification. MASCOT identifications were considered confident without further consideration if produced by matching of at least three MS/MS spectra with peptide ions scores above 20 or two spectra with ion score above 30. Identifications based on a single matched spectrum were considered borderline hits. The MS-BLAST statistical confidence of database searching hits was estimated according to MS-BLAST scoring scheme [30] considering only high-scoring segment pairs (HSP) with scores above 55. The results of MASCOT and MS-BLAST were combined and used to validate the statistical borderline hits as described in [31].

3 Results and discussion

Trichoderma harzianum was grown in synthetic medium supplemented with sugarcane bagasse and produced a secretome with a protein concentration of 0.2 mg·mL^{-1}. The secretome sample was submitted to 1D-BN-PAGE and displayed several bands corresponding to putative protein complexes (Fig. 1A). The three most intense bands were denominated complexes [I], [II], and [III]. The apparent molecular weight of complexes [I], [II], and [III], based on their relative mobilities, were not estimated since the accurate determination of the complex size by BN-PAGE can still be considered as a challenge. Wang et al. [32], working with cytoplasmic complexes verified that the molecular weight estimated by BN-PAGE were, in many cases, significantly smaller than the theoretical molecular masses. The authors proposed that these differences could be due to the differential binding of CBB to the hydrophobic surface of proteins. In fact, CBB binding was reported by a different group to cause a factor of 1.8-fold difference in molecular weight estimation [33].

It is well known that CBB prevents protein aggregation during BN-PAGE by means of electrostatic repulsion [18]. Nonetheless, it was verified if the formation of protein bands in 1D-BN-PAGE gels could be due to unspecific association (aggregation). Thus, the electrophoretic separation was repeated using three protein concentrations (0.2 mg·mL^{-1}, 5 mg·mL^{-1}, and 10 mg·mL^{-1}). Figure 1B shows that the molecular masses of protein bands observed in the 1D-BN-PAGE profiles were identical in all samples, indicating absence of protein aggregation. The profile was also preserved

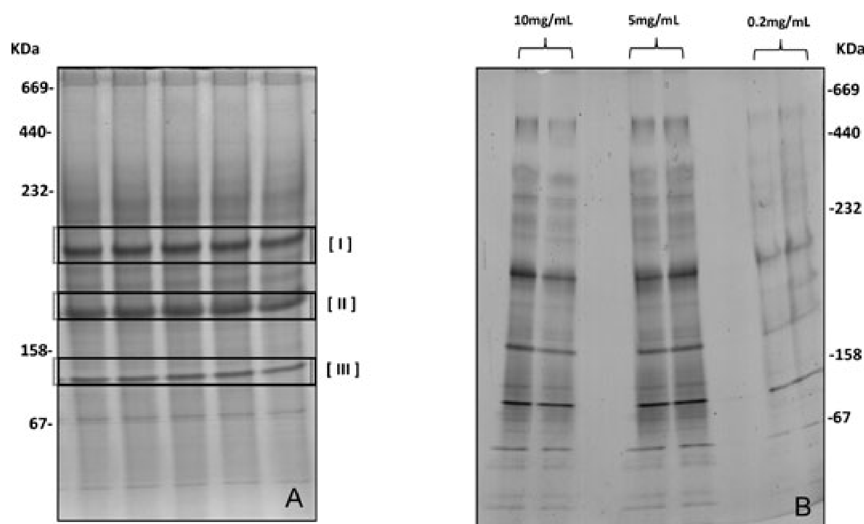

Figure 1. (A) 1D-BN-PAGE of *T. harzianum* secretome produced in sugarcane bagasse as sole carbon source. BN-PAGE was conducted using a 5–18% (w/v) polyacrylamide gradient gel. A total of 200 μg secretome protein per lane was applied. The gel was fixed and stained with CBB. The three most intense bands were denominated as complexes [I], [II], and [III]. (B) 1D-BN-PAGE of *T. harzianum* secretome in different protein concentrations. No correlation between protein concentration (0.2, 5, and 10 mg·mL^{-1}) and aggregation was observed. Different volumes of each sample were used to make the proteins visible even in low concentrations: 0.2 (400 μL), 5 (60 μL), and 10 mg·mL^{-1} (20 μL).

© 2012 WILEY-VCH Verlag GmbH & Co. KGaA, Weinheim

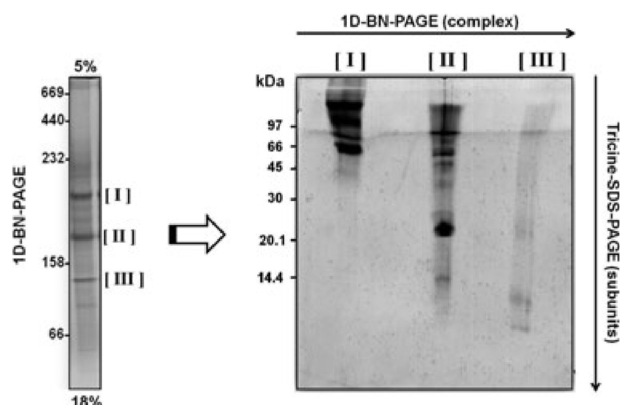

Figure 2. 2D-BN-PAGE of *T. harzianum* secretome produced in sugarcane bagasse as sole carbon source. A 1D-BN-PAGE gradient gel (5–18% [w/v]) was used in first dimension (left) to separate the protein complex and stained with CBB. Silver-stained Tricine-SDS-PAGE was used to analyze the protein subunit composition of complexes [I], [II], and [III] in the second dimension (right).

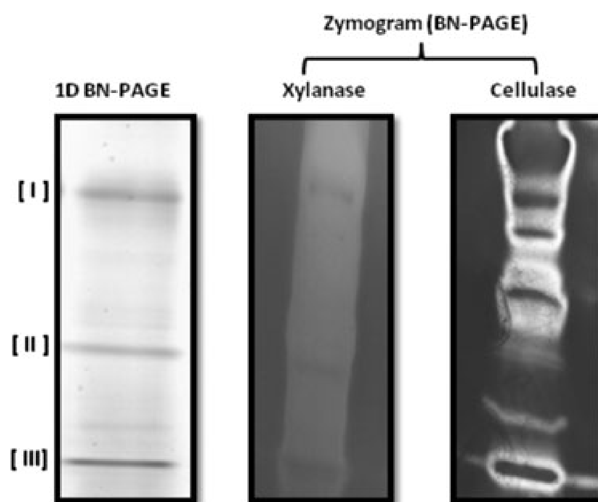

Figure 3. 1D-BN-PAGE zymography of *T. harzianum* secretome for the detection of xylanolytic and cellulolytic activities. The gel in the left was stained with CBB. Zymograms were stained with Congo red.

even in lower concentrations (from 0.2 to 0.002 mg·mL^{-1}, data not shown), demonstrating a high affinity between the components of the complexes. Protein bands corresponding to the putative complexes [I], [II], and [III] were excised from the 1D-BN-PAGE gel and submitted to a second dimension electrophoretic step (Tricine-SDS-PAGE) in dissociating conditions. The resulting 2D-BN-PAGE gel (Fig. 2) shows that the complexes disintegrated into smaller components and ruled out the possibility that the complexes were in fact high molecular mass proteins that comigrated in native gels. It was observed that complex [I] was decomposed into components with higher molecular masses compared to complexes [II] and [III], suggesting an incomplete dissociation even under denaturing conditions. Since there was a possibility of incomplete complex dissociation, the 2D-BN-PAGE bands were not subjected to MS analysis. Instead, the complexes [I], [II], and [III] were directly excised from the 1D-BN-PAGE gel, digested with trypsin, and then submitted to LC-MS/MS for protein identification.

Protein identification searches were performed using two different approaches, a stringent peptide-spectrum matching method using MASCOT software and a homology-driven approach that allows an error tolerant search based on the de novo sequence of acquired MS/MS spectra, and sequence similarity matches [29] using PepNovo software followed by MS-BLAST search. The results are shown in Table 1. As expected, the homology-driven approach provided a higher number of identifications than the stringent conventional database search [26]. For instance, both approaches identified a CBH I in complex [I] but only the homology-driven approach using MS-BLAST provided identification of enzymes involved in xylan degradation, i.e. alpha-L-arabinofuranosidase (alpha-L-ABF) and endo-beta-1,4-xylanase. Concerning complex [II], CBHs, xylan-degrading enzymes, as well as endochitinases were identified by both methods. However, a cutinase and a galactosidase were identified only when MS-BLAST search was used. MASCOT search was unable to provide identification of complex [III] components while several proteins such as alpha- and beta-glucanases, a glucoamylase, an ABF, and a swollenin (SWOI) were identified by the MS-BLAST approach.

As mentioned before, the degradation of sugarcane cell wall depends mainly on the coordinate action of cellulases and hemicellulases (especially xylanases). Therefore, zymographic analyses using 1D-BN-PAGE gels containing cellulose or xylan were performed in order to investigate biomass-degrading activities of the putative complexes. Figure 3 shows the detection of cellulolytic and xylanolytic activities in the secretome. However, in the xylan-containing gel, the activity was observed as a white trail along the gel, indicating either the presence of several xylanases with different sizes or that one or few xylanases hydrolyzed the substrate during the electrophoretic run. To rule out the latter possibility, we developed a 2D-BN/BN-PAGE zymography in which the sample was subjected to a standard 1D-BN-PAGE in the first dimension and to another 1D-BN-PAGE (this time using a polyacrylamide gel cross-reacted with cellulose or xylan) in the second dimension (Fig. 4). The 2D-BN/BN-PAGE zymography confirmed the detection of cellulolytic and xylanolytic activities corresponding to proteins of different molecular masses and consequently indicated that the results achieved using 1D-BN-PAGE zymography were not due to substrate hydrolysis during the first dimension run. Since BN-PAGE preserves structural and functional integrity of multienzymatic complexes [19], other proteins within the complexes [I], [II], and [III] that are not directly related to the cellulolytic and xylanolytic activities detected in the zymograms (e.g. glucoamylase, endochitinase, SWOI) might also be active.

© 2012 WILEY-VCH Verlag GmbH & Co. KGaA, Weinheim

Table 1. List of proteins identified by MS in the three complexes found in the *T. harzianum* secretome

MASCOT					MS-BLAST				
Protein name	Organism	gi number[a]	# Match[b]	Total score[c]	Protein name	Organism	gi number	# HSPs[d]	Total score[e]
Complex [I]									
Cellobiohydrolase I	*T. asperellum*	42741023	21	87	Cellobiohydrolase I	*H. virens*	194719525	39	2355
Predicted protein	*T. reesei* QM6a	340516597	1	58	Cellobiohydrolase I-II	*V. volvacea*	49333365	4	234
					Alpha-L-arabinofuranosidase	*Penicillium* sp. LYG 0704	315259518	4	308
					Xylan 1,4-β-xylosidase	*S. sviceus* ATCC 29083	297197679	3	207
Complex [II]									
Chain A, Catalytic Core Domain Acetyl xylan esterase	*T. reesei*	11 513 450	21	130	Acetylxylan esterase	*H. jecorina*	41016921	43	2665
Endochitinase	*H. lixii*	4 87 419	6	117	Endochitinase	*H. lixii*	88191687	1	84
Endochitinase 42	*T. stromaticum*	310 892 959	5	63	Arabinogalactan endo-1,4-β-galactosidase GalA	*T. stipitatus* ATCC 10 500	242822204	13	849
Cellobiohydrolase II	*A. cellulolyticus* Y-94	4 200 031	4	98	Cellobiohydrolase I	*H. virens*	194719525	9	537
Cellobiohydrolase I	*P. occitanis*	51 243 029	8	100	Cutinase	*G. graminicola* M1.001	310799541	8	485
GH fam 18	*T.reesei* QM6a	340 514 040	4	88	α-N-arabinofuranosidase precursor	*A. terreus* NIH2624	115401944	8	453
Endo-1,4-xylanase D	*P. funiculosum*	53 747 929	1	56	Endo-β-1,4-xylanase	*Bispora sp.* MEY-1	225420804	12	955
Complex [III]									
					Glucoamylase	*H. lixii*	61 657 886	10	748
					Endo-beta-1,4-glucanase	*H. jecorina*	60 593 233	2	189
					Swollenin	*H. jecorina*	8 052 455	2	163
					GPI-anchored cell wall beta-endoglucanase	*G. clavigera* kw1407	320 590 163	2	153
					Fungal alpha-L-arabinofuranosidase, putative	*P. marneffei* ATCC 18 224	212 528 630	1	84
					α-1,3-glucanase	*H. lixii*	18 076 080	1	79

a) GenInfo identifier from NCBI databank.
b) Number of matching peptides.
c) Significant score $p < 0.05$.
d) De novo peptides sequences that produced HSPs in MS-BLAST search.
e) Statistically significant score of the HSP.

© 2012 WILEY-VCH Verlag GmbH & Co. KGaA, Weinheim

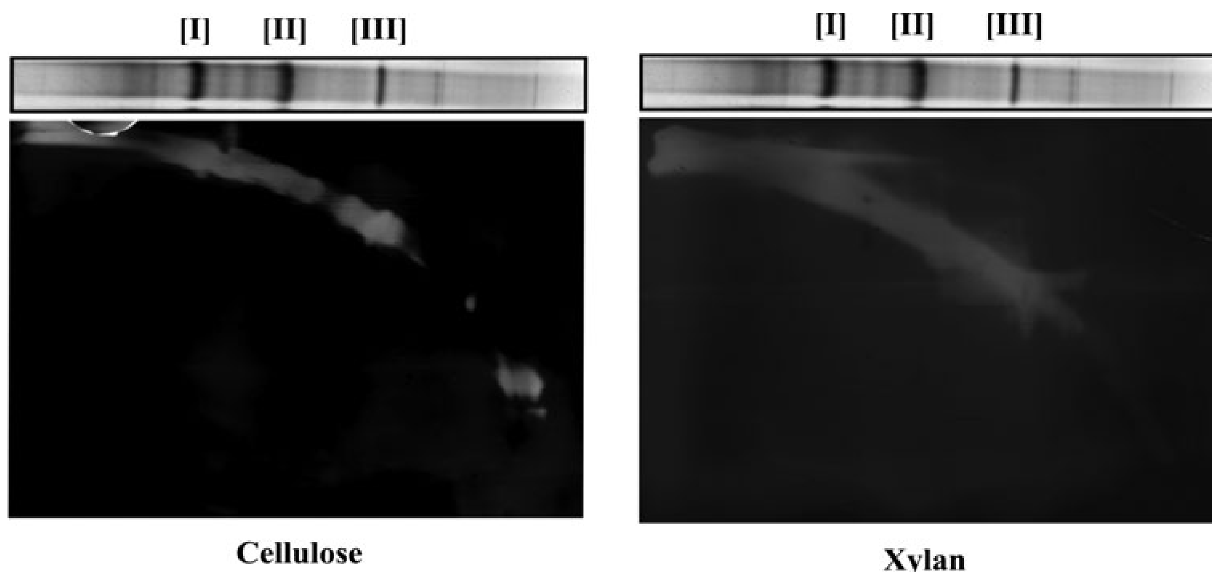

Figure 4. 2D-BN/BN-PAGE zymography of *T. harzianum* secretome for the detection of xylanolytic and cellulolytic activities. A 1D-BN-PAGE gradient gel (5–18% [w/v]) was used in first dimension to separate the protein complexes (*top*). 1D-BN-PAGE lanes were then submitted to a second BN-PAGE dimension on gels (*bottom*) containing cellulose or xylan. Zymograms were stained with Congo Red.

The results presented here indicate that *T. harzianum* is able to secrete active multienzimatic enzyme complexes. The heterogeneous composition of the complexes suggests a possible synergistic reaction among different proteins that would act in a cooperative manner to degrade efficiently the sugarcane bagasse used as substrate.

ABFs were found in all three complexes. This debranching enzyme cleaves alpha-L-arabinofuranosyl linkages from arabinose branches present in xylans that promote steric hindrance for action of xylanases [34]. Therefore, in complex [I], ABF possibly cooperates with 1,4-beta-xylosidase that removes successively D-xylose monomers from xylan backbone, facilitating the CBHs to penetrate deeply in the plant cell wall.

Similarly to ABF, in complex [II], acetylxylan esterase could increase xylan backbone accessibility to the endoxylanases by removing acetylated side chains [14]. In the same complex, a cutinase was found. Cutinases are serine esterases that catalyze the hydrolysis of cutin, the major component of the plant cuticle. These enzymes are known to help other hydrolytic enzymes to reach cell wall polymers during saprophytic plant degradation [35]. Additionally, xylanases and cellulases act as elicitors of pathogen-related proteins in plants, which could justify the presence of endochitinase in the same complex [36]. *Trichoderma harzianum* is a mycoparasite that secretes hydrolytic enzymes, including chitinases and glucanases in order to attack cell wall polymers of other fungi [37]. This ability has been exploited in the development of biocontrol strategies using *T. harzianum* against plant pathogenic fungi, particularly *Rhizoctonia solani* and *Fusarium solani* [38]. Synergistic relationship between cellulases and hemicellulases was previously reported in the conversion of complex carbon sources such as wheat straw [39] and corn stover [40] using enzymes isolated from filamentous fungi. The synergism was also observed in the anaerobic organism *C. cellulovorans* during sugarcane bagasse degradation. In this case, the synergistic relationship occurs in the cellulosomes. The modular structure of cellulosomes posses a noncatalytic protein called scaffoldin that integrates the glycosyl hydrolase complex, links it to the cell surface, and anchors the entire complex onto crystalline cellulose [41]. Here, scaffoldin was not found in any of the studied complexes, suggesting that they display a structural organization different from typical bacterial cellulosome. However, data showing incomplete dissociation (Fig. 2) and preserved BN-PAGE profile in different protein concentrations (Fig. 1B) suggest a cohesin–dockerin type interaction. It has been reported that cohesin and dockerin domains mediate a high-affinity interaction between subunits in cellulosomes (anaerobic bacteria) and other enzyme complexes (anaerobic fungi and aerobic bacteria) that have association constants higher than 10^9 M [41–44].

A glucosidase was found and identified as a potential scaffoldin in the anaerobic fungus *Piromyces equi*. The double dockerin domain of the *P. equi* CBH Cel45A was shown to bind to the glucosidase [45, 46]. However, none of the *T. harzianum* complexes analyzed here displayed glucosidases, which may be due to the different fungal species or even the carbon source used, since previous data showed that differences in the composition of enzyme complexes in *P. purpurogenum* are a consequence of carbon source present in the growth culture [17].

A SWOI, a glucoamylase, and a glycosylphosphatidylinositol-anchored cell wall beta-endoglucanase (GPI-EglC) were detected in complex [III]. The expansin-like protein SWOI first acts in the disruption of lignocellulosic biomass promoting the amorphogenesis of cellulose

© 2012 WILEY-VCH Verlag GmbH & Co. KGaA, Weinheim

microfibrils and enhancement in the efficiency of cellulolytic activity [47, 48]. Similarly, the starch-binding domain found in glucoamylase has been proposed to disrupt the raw starch and related oligosaccharide structure, concentrating its catalytic domain or other glycoside hydrolase on the polysaccharide substrate [49–52]. Concerning the GPI-EglC found in complex [III], GPI-anchored proteins have been repeatedly shown to play a role in the cell wall polysaccharide remodeling. This enzyme was also found in *Aspergillus fumigatus*, but not associated to multienzymatic complexes [53]. It is possible that the GPI-EglC described here could attach complex [III] to a fungal cell, which would increase the degradation efficiency due to close contact between the different enzymes and the plant biomass.

4 Concluding remarks

This work contributes to the understanding of plant biomass degradation processes by aerobic filamentous fungi, particularly *T. harzianum*. By means of BN-PAGE and MS methods, we have disclosed the presence of multienzymatic complexes as components of the *T. harzianum* secretion under growth in the heterogeneous carbon source sugarcane bagasse. The fungal response resulted in a singular composition of each protein complex apparently required for the efficient and specific conversion of the biomass polymers. The results support the existence of hydrolysis mechanisms based on multienzymatic complexes in *T. harzianum* and other aerobic filamentous fungi.

We expect that the present work may contribute to open a path for future experiments aiming at characterizing the multienzymatic complexes in terms of stoichiometry of components, interactions that maintain the oligomeric status, as well as the influence of the carbon source used in the culture medium.

This project was supported by FAPDF (Federal District Foundation for Science and Research Supporting – grant no. 193.000.584/2009). FINEP (Design and Project Financing Agency), Petrobras, (Brazilian Oil Corporation, CENPES 11007), CNPq (National Council for Scientific and Technological Development grant no. 478066/2010–4 MCT/CNPq – Universal), UnB (University of Brasilia), UFRJ (Universidade Federal do Rio de Janeiro). CNPq and CAPES (Foundation for the Development of Higher Education) provided scholarships for DPGM and AJS, respectively. The authors thankfully acknowledge Dr. Robert Miller for the critical reading of the manuscript.

The authors have declared no conflict of interest

5 References

[1] Kuhad, R. C., Gupta, R., Singh, A., Microbial cellulases and their industrial applications. *Enzyme Res.* 2011, *2011*, 280696.

[2] Polizeli, M. L., Rizzatti, A. C., Monti, R., Terenzi, H. F. et al., Xylanases from fungi: properties and industrial applications. *Appl. Microbiol. Biotechnol.* 2005, *67*, 577–591.

[3] Amorim, H. V., Lopes, M. L., de Castro Oliveira, J. V., Buckeridge, M. S. et al., Scientific challenges of bioethanol production in Brazil. *Appl. Microbiol. Biotechnol.* 2011, *91*, 1267–1275.

[4] Harman, G. E., Herrera-Estrella, A. H., Horwitz, B. A., Lorito, M., Special issue: *Trichoderma* – from basic biology to biotechnology. *Microbiology* 2012, *158*, 1–2.

[5] Schuster, A., Schmoll, M., Biology and biotechnology of *Trichoderma*. *Appl. Microbiol. Biotechnol.* 2010, *87*, 787–799.

[6] Nidetzky, B., Steiner, W., Hayn, M., Claeyssens, M., Cellulose hydrolysis by the cellulases from *Trichoderma reesei*: a new model for synergistic interaction. *Biochem. J.* 1994, *298*(Pt 3), 705–710.

[7] Grondona, I., Hermosa, R., Tejada, M., Gomis, M. et al., Physiological and biochemical characterization of *Trichoderma harzianum*, a biological control agent against soilborne fungal plant pathogens. *Appl. Environ. Microbiol.* 1997, *63*, 3189–3198.

[8] Viterbo, A., Ramot, O., Chemin, L., Chet, I., Significance of lytic enzymes from *Trichoderma* spp. in the biocontrol of fungal plant pathogens. *Antonie Van Leeuwenhoek* 2002, *81*, 549–556.

[9] Monteiro, V. N., do Nascimento Silva, R., Steindorff, A. S., Costa, F. T. et al., New insights in *Trichoderma harzianum* antagonism of fungal plant pathogens by secreted protein analysis. *Curr. Microbiol.* 2010, *61*, 298–305.

[10] Ulhoa, C. J., Peberdy, J. F., Regulation of chitinase synthesis in *Trichoderma harzianum*. *J. Gen. Microbiol.* 1991, *137*, 2163–2169.

[11] Franco, P., Ferreira, H., Ferreira, E., Production and characterization of hemicellulase activities from *Trichoderma harzianum* strain T4. *Biotechnol. Appl. Biochem.* 2004, *40*, 255–259.

[12] de Castro, A., Pedro, K., da Cruz, J., Ferreira, M. et al., Trichoderma harzianum IOC-4038: a promising strain for the production of a cellulolytic complex with significant beta-glucosidase activity from sugarcane bagasse cellulignin. *Appl. Biochem. Biotechnol.* 2010, *162*, 2111–2122.

[13] Shoham, Y., Lamed, R., Bayer, E., The cellulosome concept as an efficient microbial strategy for the degradation of insoluble polysaccharides. *Trends Microbiol.* 1999, *7*, 275–281.

[14] Beg, Q. K., Kapoor, M., Mahajan, L., Hoondal, G. S., Microbial xylanases and their industrial applications: a review. *Appl. Microbiol. Biotechnol.* 2001, *56*, 326–338.

[15] Pohlschröder, M., Leschine, S. B., Canale-Parola, E., Multicomplex cellulase-xylanase system of *Clostridium papyrosolvens* C7. *J. Bacteriol.* 1994, *176*, 70–76.

[16] Ohtsuki, T., Suyanto, Yazaki, S., Ui, S., Mimura, A., Production of large multienzyme complex by aerobic thermophilic fungus *Chaetomium* sp nov MS-017 grown on palm oil mill fibre. *Letters in Applied Microbiology* 2005, *40*, 111–116.

[17] Gonzalez-Vogel, A., Eyzaguirre, J., Oleas, G., Callegari, E. et al., Proteomic analysis in non-denaturing condition of the

© 2012 WILEY-VCH Verlag GmbH & Co. KGaA, Weinheim

secretome reveals the presence of multienzyme complexes in *Penicillium purpurogenum*. *Appl. Microbiol. Biotechnol.* 2011, *89*, 145–155.

[18] Schägger, H., Cramer, W., von Jagow, G., Analysis of molecular masses and oligomeric states of protein complexes by blue native electrophoresis and isolation of membrane protein complexes by two-dimensional native electrophoresis. *Anal. Biochem.* 1994, *217*, 220–230.

[19] Wittig, I., Schägger, H., Features and applications of blue-native and clear-native electrophoresis. *Proteomics* 2008, *8*, 3974–3990.

[20] Suárez, M. B., Sanz, L., Chamorro, M. I., Rey, M. et al., Proteomic analysis of secreted proteins from *Trichoderma harzianum.* Identification of a fungal cell wall-induced aspartic protease. *Fungal Genet. Biol.* 2005, *42*, 924–934.

[21] Wittig, I., Braun, H., Schägger, H., Blue native PAGE. *Nat. Protoc.* 2006, *1*, 418–428.

[22] Schägger, H., Cramer, W. A., von Jagow, G., Analysis of molecular masses and oligomeric states of protein complexes by blue native electrophoresis and isolation of membrane protein complexes by two-dimensional native electrophoresis. *Anal. Biochem.* 1994, *217*, 220–230.

[23] Blum, H., Beier, H., Gross, H. J., Improved silver staining of plant proteins, RNA and DNA in polyacrylamide gels. *Electrophoresis* 1987, *8*, 93–99.

[24] Sunna, A., Puls, J., Antranikian, G., Characterization of the xylanolytic enzyme system of the extreme thermophilic anaerobic bacteria *Thermotoga maritima*, *T. neapolitana*, and *T. thermarum*. *Comp. Biochem. Physiol. Part A* 1997, *118*, 453–461.

[25] Matsui, H., Ban-Tokuda, T., Studies on carboxymethyl cellulase and xylanase activities of anaerobic fungal isolate CR4 from the bovine rumen. *Curr. Microbiol.* 2008, *57*, 615–619.

[26] Junqueira, M., Spirin, V., Balbuena, T. S., Thomas, H. et al., Protein identification pipeline for the homology-driven proteomics. *J. Proteomics* 2008, *71*, 346–356.

[27] Junqueira, M., Spirin, V., Santana Balbuena, T., Waridel, P. et al., Separating the wheat from the chaff: unbiased filtering of background tandem mass spectra improves protein identification. *J. Proteome Res.* 2008, *7*, 3382–3395.

[28] Frank, A., Pevzner, P., PepNovo: de novo peptide sequencing via probabilistic network modeling. *Anal. Chem.* 2005, *77*, 964–973.

[29] Shevchenko, A., Valcu, C. M., Junqueira, M., Tools for exploring the proteomosphere. *J. Proteomics* 2009, *72*, 137–144.

[30] Habermann, B., Oegema, J., Sunyaev, S., Shevchenko, A., The power and the limitations of cross-species protein identification by mass spectrometry-driven sequence similarity searches. *Mol. Cell Proteomics* 2004, *3*, 238–249.

[31] Wielsch, N., Thomas, H., Surendranath, V., Waridel, P. et al., Rapid validation of protein identifications with the borderline statistical confidence via de novo sequencing and MS BLAST searches. *J. Proteome Res.* 2006, *5*, 2448–2456.

[32] Wang, Z. J., Xu, X. P., Fan, K. Q., Jia, C. J. et al., Sample preparation for two-dimensional blue native/SDS polyacrylamide gel electrophoresis in the identification of *Streptomyces coelicolor* cytoplasmic protein complexes. *J. Biochem. Biophys. Methods* 2007, *70*, 565–572.

[33] Heuberger, E. H., Veenhoff, L. M., Duurkens, R. H., Friesen, R. H. et al., Oligomeric state of membrane transport proteins analyzed with blue native electrophoresis and analytical ultracentrifugation. *J. Mol. Biol.* 2002, *317*, 591–600.

[34] Seiboth, B., Metz, B., Fungal arabinan and L-arabinose metabolism. *Appl. Microbiol. Biotechnol.* 2011, *89*, 1665–1673.

[35] Rubio, M. B., Cardoza, R. E., Hermosa, R., Gutiérrez, S. et al., Cloning and characterization of the Thcut1 gene encoding a cutinase of *Trichoderma harzianum* T34. *Curr. Genet.* 2008, *54*, 301–312.

[36] Yang, H. H., Yang, S. L., Peng, K. C., Lo, C. T. et al., Induced proteome of *Trichoderma harzianum* by *Botrytis cinerea*. *Mycol. Res.* 2009, *113*, 924–932.

[37] Chet, I., Inbar, J., Biological control of fungal pathogens. *Appl. Biochem. Biotechnol.* 1994, *48*, 37–43.

[38] Mishra, P., Kshirsagar, P. R., Nilegaonkar, S. S., Singh, S. K., Statistical optimization of medium components for production of extracellular chitinase by *Basidiobolus ranarum*: a novel biocontrol agent against plant pathogenic fungi. *J. Basic Microbiol.* 2012 [Epub ahead of print]. doi:10.1002/jobm.201100446.

[39] Tabka, M. G., Herpoel-Gimbert, I., Monod, F., Asther, M., Sigoillot, J. C., Enzymatic saccharification of wheat straw for bioethanol production by a combined cellulase xylanase and feruloyl esterase treatment. *Enzyme Microb. Tech*. 2006, *39*, 897–902.

[40] Selig, M. J., Knoshaug, E. P., Adney, W. S., Himmel, M. E. et al., Synergistic enhancement of cellobiohydrolase performance on pretreated corn stover by addition of xylanase and esterase activities. *Bioresour. Technol.* 2008, *99*, 4997–5005.

[41] Fontes, C. M., Gilbert, H. J., Cellulosomes: highly efficient nanomachines designed to deconstruct plant cell wall complex carbohydrates. *Annu. Rev. Biochem.* 2010, *79*, 655–681.

[42] Schaeffer, F., Matuschek, M., Guglielmi, G., Miras, I. et al., Duplicated dockerin subdomains of *Clostridium thermocellum* endoglucanase CelD bind to a cohesin domain of the scaffolding protein CipA with distinct thermodynamic parameters and a negative cooperativity. *Biochemistry* 2002, *41*, 2106–2114.

[43] Miras, I., Schaeffer, F., Béguin, P., Alzari, P. M., Mapping by site-directed mutagenesis of the region responsible for cohesin-dockerin interaction on the surface of the seventh cohesin domain of *Clostridium thermocellum* CipA. *Biochemistry* 2002, *41*, 2115–2119.

[44] Kosugi, A., Murashima, K., Tamaru, Y., Doi, R. H., Cell-surface-anchoring role of N-terminal surface layer homology domains of *Clostridium cellulovorans* EngE. *J. Bacteriol.* 2002, *184*, 884–888.

[45] Nagy, T., Tunnicliffe, R. B., Higgins, L. D., Walters, C. et al., Characterization of a double dockerin from the cellulosome of the anaerobic fungus *Piromyces equi*. *J. Mol. Biol.* 2007, *373*, 612–622.

© 2012 WILEY-VCH Verlag GmbH & Co. KGaA, Weinheim

[46] Fanutti, C., Ponyi, T., Black, G. W., Hazlewood, G. P. et al., The conserved noncatalytic 40-residue sequence in cellulases and hemicellulases from anaerobic fungi functions as a protein docking domain. *J. Biol. Chem.* 1995, *270*, 29314–29322.

[47] Saloheimo, M., Paloheimo, M., Hakola, S., Pere, J. et al., Swollenin, a *Trichoderma reesei* protein with sequence similarity to the plant expansins, exhibits disruption activity on cellulosic materials. *Eur. J. Biochem.* 2002, *269*, 4202–4211.

[48] Arantes, V., Saddler, J., Access to cellulose limits the efficiency of enzymatic hydrolysis: the role of amorphogenesis. *Biotechnol. Biofuels* 2010, *3*.

[49] Tung, J. Y., Chang, M. D., Chou, W. I., Liu, Y. Y. et al., Crystal structures of the starch-binding domain from *Rhizopus oryzae* glucoamylase reveal a polysaccharide-binding path. *Biochem. J.* 2008, *416*, 27–36.

[50] Southall, S. M., Simpson, P. J., Gilbert, H. J., Williamson, G. et al., The starch-binding domain from glucoamylase disrupts the structure of starch. *FEBS Lett.* 1999, *447*, 58–60.

[51] Bolam, D. N., Ciruela, A., McQueen-Mason, S., Simpson, P. et al., Pseudomonas cellulose-binding domains mediate their effects by increasing enzyme substrate proximity. *Biochem. J.* 1998, *331*(Pt 3), 775–781.

[52] Giardina, T., Gunning, A. P., Juge, N., Faulds, C. B. et al., Both binding sites of the starch-binding domain of *Aspergillus niger* glucoamylase are essential for inducing a conformational change in amylose. *J. Mol. Biol.* 2001, *313*, 1149–1159.

[53] Hartl, L., Gastebois, A., Aimanianda, V., Latgé, J. P., Characterization of the GPI-anchored endo β-1,3-glucanase Eng2 of *Aspergillus fumigatus*. *Fungal. Genet. Biol.* 2011, *48*, 185–191.

© 2012 WILEY-VCH Verlag GmbH & Co. KGaA, Weinheim

Artigos publicados durante o doutorado, mas não relativos à tese

Acta Crystallographica Section F
Structural Biology and Crystallization Communications
ISSN 1744-3091

Purification, crystallization and preliminary crystallographic studies of SPCI–chymotrypsin complex at 2.8 Å resolution

Adelson Joel da Silva,[a] Rozeni Chagas Lima Teles,[a] Gisele Ferreira Esteves,[a] Camila Ramos dos Santos,[b] João Alexandre Ribeiro Gonçalves Barbosa[b]* and Sonia Maria de Freitas[a]*

[a]Biophysics Laboratory, Biological Sciences Institute, University of Brasília, Brasília-DF, 70910-900, Brazil, and [b]Center for Structural Molecular Biology (CeBiME), Brazilian Synchrotron Light Laboratory (LNLS), CP 6192, Campinas-SP, 13083-970, Brazil

Correspondence e-mail: joao@lnls.br, nina@unb.br

Received 6 August 2008
Accepted 20 August 2008

A binary complex of the *Schizolobium parahyba* chymotrypsin inhibitor (SPCI) with chymotrypsin was purified by size-exclusion chromatography and crystallized by the sitting-drop vapour-diffusion method with 100 m*M* MES–NaOH pH 5.5, 20%(*w*/*v*) PEG 6000, 200 m*M* LiCl as precipitant and 200 m*M* nondetergent sulfobetaine molecular weight 201 Da (NDSB-201) as an additive. SPCI is a small protein with 180 amino-acid residues isolated from *S. parahyba* seeds and is able to inhibit chymotrypsin at a 1:1 molar ratio by forming a stable complex. X-ray data were collected to 2.8 Å resolution from a single crystal of the SPCI–chymotrypsin binary complex under cryogenic conditions. The crystal belongs to space group $P2_12_12_1$, with unit-cell parameters $a = 45.28$, $b = 64.57$, $c = 169.23$ Å, and the R_{merge} is 0.122 for 11 254 unique reflections. A molecular-replacement solution was found using the preliminary crystal structure of SPCI and the structure of chymotrypsin (PDB code 4cha) independently as search models.

1. Introduction

Proteinases are crucial for a wide variety of biological processes (Neurath, 1997) that are essential to life and their activity is of great importance both *in vivo* and for therapeutic intervention (Phillips & Fletterick, 1992). Naturally occurring canonical serine proteinase inhibitors (PIs) are proteins that inactivate the functions of serine proteinases by providing a reactive site, which in turn serves as a substrate analogue for the cognate enzyme (Laskowski & Kato, 1980; Bode & Huber, 1992). Proteinase inhibitors are found in micro-organisms, plants and animals and play an important role in the regulation of metabolic pathways in which proteinases are one of the major components (Joanitti *et al.*, 2006). Natural inhibitors have been classified into at least 18 different families (Laskowski & Qasim, 2000); among the most extensively studied are the Bowman–Birk and Kunitz serine proteinase inhibitors.

Kunitz inhibitors are proteins with one or two polypeptide chains, a molecular weight of about 6–20 kDa and one reactive site. These inhibitors are cross-linked by two or three disulfide bonds that confer a compact and stable tertiary structure. They have been the subject of several studies, especially in the Graminaceae, Leguminosae and Solanaceae (Richardson, 1977), and are mainly found in the seeds of the Caesalpinoideae and Mimosoideae (Norioka *et al.*, 1988).

A soybean Kunitz trypsin inhibitor (STI) has been reported to have the potential to suppress ovarian cancer cell invasion and peritoneal disseminated metastasis *in vivo* (Kobayashi *et al.*, 2004). STI inhibits cell invasiveness through suppression of the urokinase-type plasminogen activator signalling cascade and its specific receptor observed in HRA human ovarian cancer cells. In addition, STI has an adverse effect on insect development and might serve as a transgenic resistance factor (Shukle & Wu, 2003). Bioassays with this inhibitor revealed that it caused a significant delay in the development of *Sitotroga cerealella* (one of the major storage pests of cereals) larvae when incorporated into the diet. These results indicated that a plant protease inhibitor could provide antibiotic resistance toward *S. cerealella* larvae.

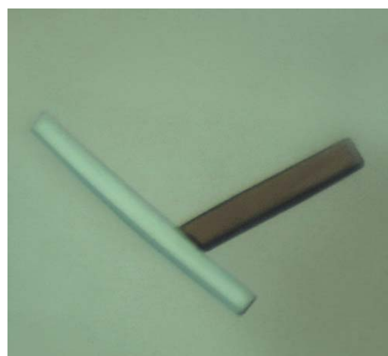

© 2008 International Union of Crystallography
All rights reserved

Schizolobium parahyba chymotrypsin inhibitor (SPCI) is a Kunitz chymotrypsin inhibitor with a single polypeptide chain of 180 amino-acid residues isolated from *S. parahyba* seeds (Teles *et al.*, 2004). This inhibitor suppresses the proteolytic activity of chymotrypsin through the formation of a stable complex with a 1:1 stoichiometry and has been characterized as a highly stable protein over a broad pH and temperature range (Teles *et al.*, 2005).

The secondary structure of SPCI is formed by β-strands and its native structure is stabilized by hydrophobic forces and electrostatic interactions (Souza *et al.*, 1995, 2000; Teles *et al.*, 1999, 2004). Disulfide-bond reduction caused conformational changes in SPCI, as evidenced by the maximum fluorescence emission shifting from 336 to 328 nm with increased intensity without alteration of the inhibitory activity. Indeed, 1 m*M* dithiothreitol (DTT) did not affect the time course of thermoinactivation of SPCI (Souza *et al.*, 1995, 2000) at 363 K after 1 h incubation and did not interfere in the secondary-structure content as evidenced by far-UV circular-dichroism spectroscopy (unpublished data). These findings suggest that disulfide bonding plays no crucial role in maintaining either the inhibitory function or the conformational stability of SPCI. The molecular arrangements of SPCI at pH 7.0, as visualized by atomic force microscopy at high resolution in nanopure water, indicated an organization in various oligomeric states, with a predominance of hexagonal forms (Leite *et al.*, 2002). In order to elucidate the three-dimensional structure of SPCI, this inhibitor was crystallized (Teles *et al.*, 2007) and its structure determination is in progress.

The three-dimensional structure of an inhibitor–proteinase complex reveals the residues and intermolecular contacts that contribute to the specificity profile and tight association. For this reason, the structural studies of inhibitor complexes with chymotrypsin are helpful not only to comprehend models of protein–protein recognition but also to understand conformational changes during enzyme–inhibitor interactions, aiming towards biotechnological applications. In this work, we present the purification of the SPCI–chymotrypsin complex, its crystallization, data collection and phasing at 2.8 Å resolution.

2. Materials and methods

2.1. Purification of SPCI and SPCI–chymotrypsin complex

SPCI was initially purified from a crude extract of triturated *S. parahyba* seeds following trichloroacetic acid (TCA) precipitation and ion-exchange chromatography (Teles *et al.*, 2004). Proteins from the crude extract were precipitated with 1.2%(*v*/*v*) TCA for 5 min in an Omnimixer homogenizer at medium speed. After centrifugation at 13 000*g* for 30 min, the supernatant was dialyzed against water at 277 K and lyophilized. The sample (100 mg) obtained from TCA precipitation was dissolved in 5–10 ml 50 m*M* acetate buffer pH 3.2. The soluble protein fraction was applied onto a SP-Sephadex C 25-120 column (2 × 15 cm) equilibrated with 50 m*M* acetate buffer pH 3.2. The inhibitor was eluted with a linear salt gradient from 0 to 1.0 *M* NaCl in the same buffer. Eluted samples were monitored at 280 nm and purity was confirmed by 13% SDS–PAGE (Laemmli, 1970).

The binary complex (SPCI–chymotrypsin) was obtained by mixing SPCI with α-chymotrypsin (bovine pancreatic α-chymotrypsin type II, thrice crystallized; Sigma-C4129, St Louis, Missouri, USA) in a 1:1 molar ratio at a concentration of 500 µ*M* in 50 m*M* Tris–HCl, 0.2 *M* KCl pH 7.5 for 30 min at room temperature. The concentrations of the proteins were determined from absorbance measurements using a Jasco V-530 spectrophotometer (Jasco, Tokyo, Japan) and using the following values: α-chymotrypsin (MW = 25 kDa), $A^{1\%}_{280,\,1\,\rm cm}$ = 20.4; SPCI (MW = 20 460 Da), $A^{1\%}_{280,\,1\,\rm cm}$ = 6.18 (Souza *et al.*, 1995). The resulting binary complex was purified from the mixture by size-exclusion chromatography using a Sephadex G-75 (3 × 100 cm) with a flow rate of 25 ml h^{-1} previously equilibrated with the same buffer as indicated above. The purified complex was dialyzed against water and lyophilized for storage at 253 K.

2.2. Crystallization and data collection and processing

The SPCI–chymotrypsin binary complex was crystallized using the sitting-drop vapour-diffusion method (McPherson, 1990) at 291 K and an automatic system for crystallization using Matrix Maker and Honeybee robots to set up 96-well crystallization plates. Initial crystallization trials were performed using different precipitant types from commercial screens: the sparse-matrix screen from the Joint Center for Structural Genomics (JCSG; Page *et al.*, 2003), the PACT Suite for a systematic analysis of the effect of pH, anions and cations (Newman *et al.*, 2005), precipitant synergy (Majeed *et al.*, 2003), Wizard Screens I and II (Hol *et al.*, 2001), SaltRx (Gilliland *et al.*,

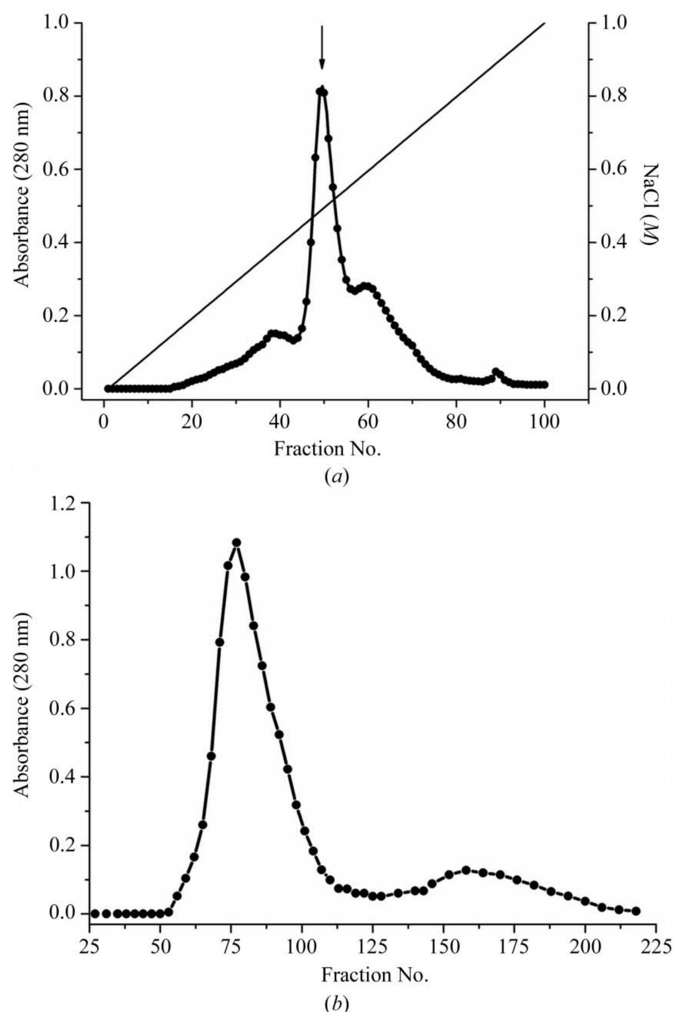

Figure 1
(*a*) Cation-exchange chromatography of SPCI on SP-Sephadex eluted with a linear gradient (0–1.0 *M*) of NaCl. The arrow indicates the eluted SPCI. (*b*) Size-exclusion chromatography of the SPCI–chymotrypsin binary complex on Sephadex G-75 with 50 m*M* Tris–HCl pH 7.6. First peak, SPCI–chymotrypsin complex; second peak, free SPCI and chymotrypsin.

1994; Kanaujia *et al.*, 2007), and Crystal Screen and Crystal Screen 2 from Hampton Research (Jancarik & Kim, 1991). The reservoirs contained 80 µl solution and the drops were prepared by adding 0.2 µl reservoir solution to 0.2 µl protein solution (lyophilized protein dissolved in Milli-Q water) at concentrations of 10 and 20 mg ml^{-1}.

After screening, optimization of the crystallization conditions was performed by varying the pH of the buffers and the precipitant concentration and using the Additive Screen 2 HR-430 kit (Hampton Research). The drops were prepared by adding 0.9 µl reservoir solution (300 ml) to 0.9 µl protein solution (14 mg ml^{-1}) and 0.2 µl additive. The best crystals were grown in drops using a solution consisting of 100 m*M* MES–NaOH pH 5.5, 20%(*w*/*v*) PEG 6000, 200 m*M* LiCl as precipitant and 200 m*M* nondetergent sulfobetaine molecular weight 201 Da (NDSB-201) as an additive. Crystals were soaked in reservoir solution containing 20%(*v*/*v*) glycerol as a cryoprotectant for less than 30 s and mounted in a loop.

Diffraction data were collected on the W01B-MX2 beamline of the Brazilian Synchrotron Light Laboratory (LNLS; Campinas, Brazil), which is equipped with a two-crystal monochromator and a MAR CCD detector with a square X-ray-sensitive surface of 225 × 225 mm combined with a MAR DTB goniostat. A wavelength of 1.459 Å was used together with oscillations of 1°. Crystals were cryocooled in a stream of nitrogen gas at 100 K in order to minimize radiation damage. A total of 360 frames were recorded. Data processing was performed with the *HKL*-2000 software package (Otwinowski & Minor, 1997).

2.3. Molecular replacement

The Matthews coefficient (Matthews, 1968) was calculated using 45 kDa as the molecular weight of the binary complex in order to indicate the number of molecules per asymmetric unit. A calculated Matthews coefficient of 2.74 Å^3 Da^{-1} is compatible with the presence of one heterodimer of the SPCI–chymotrypsin complex in the asymmetric unit with a solvent content of 55%. A molecular-replacement (MR) solution was found using the partially refined crystallographic structure of SPCI (Teles *et al.*, 2007) and the structure of chymotrypsin (Tsukada & Blow, 1985; PDB code 4cha) independently as a search models. This procedure was performed using the *MOLREP* program (Vagin & Teplyakov, 1997) from the *CCP*4 package (Collaborative Computational Project, Number 4, 1994). The first MR was carried out using the structure of chymotrypsin (Tsukada & Blow, 1985; PDB code 4cha) as the search model. The solution was used in the second MR as a fixed model and the structure of SPCI was used as the search model. In both searches, the chymotrypsin and SPCI molecules contained all the protein atoms; all other atoms, such as waters and other ligands, were removed.

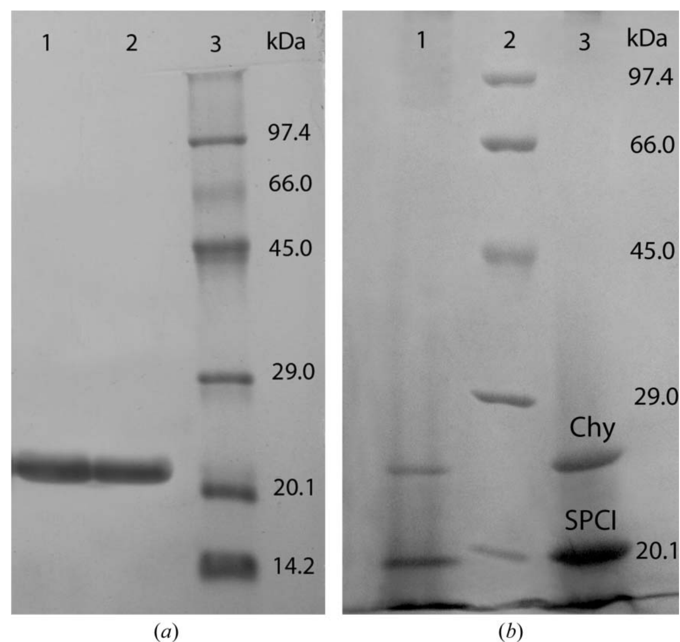

Figure 2
Coomassie-stained (13%) SDS–PAGE of SPCI and the SPCI–chymotrypsin complex. (*a*) Lanes 1 and 2, SPCI (20.46 kDa). Lane 3, molecular-weight markers from Amersham Pharmacia Biotech UK (part No. 17-0446-01): rabbit muscle phosphorylase b (97.4 kDa), bovine serum albumin (66 kDa), egg albumin (45 kDa), bovine erythrocyte carbonic anhydrase (29 kDa), soybean trypsin inhibitor (20.1 kDa) and bovine milk α-lactalbumin (14.2 kDa). (*b*) Lanes 1 and 3, SPCI (20.46 kDa) and chymotrypsin (25 kDa) from the binary complex under denaturing conditions; lane 2, molecular-weight markers.

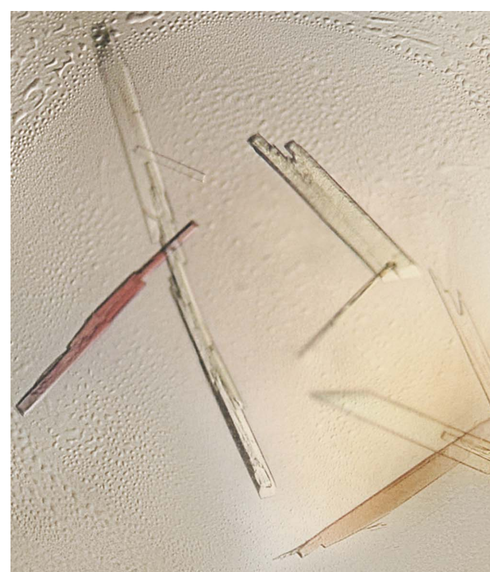

(*a*)

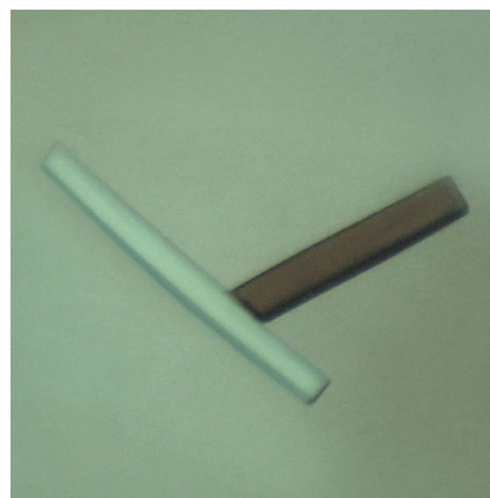

(*b*)

Figure 3
Crystals of the SPCI–chymotrypsin complex obtained by sitting-drop vapour diffusion at 291 K with an average length of 400 µm in the longest dimension. (*a*) Crystals obtained using 100 m*M* MES–NaOH pH 5.5, 20%(*w*/*v*) PEG 6000, 200 m*M* LiCl as precipitant. (*b*) Optimized crystals diffracting to 2.8 Å obtained in the same precipitant solution with the additive 200 m*M* NDSB-201 from the Additive Screen 2 HR-430 kit (Hampton Research).

Table 1
SPCI–chymotrypsin complex data-collection and processing statistics.

Values in parentheses are for the last resolution shell.

Space group	$P2_12_12_1$
Unit-cell parameters (Å)	a = 45.28, b = 64.57, c = 169.23
Mosaicity (°)	0.94
Temperature (K)	291
Wavelength (Å)	1.459
Frame oscillation (°)	1
Crystal-to-detector distance (mm)	170.00
No. of frames	360
Resolution limits (Å)	16.00–2.80 (2.90–2.80)
$\langle I/\sigma(I)\rangle$ after merging	23.4 (1.3)
Completeness (%)	88.3 (51.8)
Redundancy (%)	12.0 (6.0)
$R_{\rm merge}$†	0.12 (0.59)
No. of reflections	135446
No. of unique reflections	11254 (638)

† $\sum_{hkl}\sum_i |I_i(hkl) - \langle I(hkl)\rangle| / \sum_{hkl}\sum_i I_i(hkl)$, where $I(hkl)$ is the intensity of reflection hkl, $\sum_{hkl}$ is the sum over all reflections and $\sum_i$ is the sum over i measurements of reflection hkl.

3. Results and discussion

SPCI was purified from a crude extract by a precipitation step with 1.2%(*v*/*v*) TCA followed by ion-exchange chromatography (Fig. 1*a*) as described by Teles *et al.* (2004) and corresponds to a band of approximately 21 kDa on SDS–PAGE (Fig. 2*a*). The SPCI–chymotrypsin complex was purified by size-exclusion molecular chromatography (Fig. 1*b*). Both proteins present in the complex are shown in the SDS gel, which contains two bands of the expected molecular weights for chymotrypsin (25 kDa) and SPCI (21 kDa) (Fig. 2*b*).

The crystallization conditions for this binary complex were obtained using the vapour-diffusion method with a robotic system. After two weeks, small crystals of SPCI–chymotrypsin complex were observed in several screening conditions, but the best crystals grew in (i) 100 m*M* sodium acetate–HCl pH 5.0, 20%(*w*/*v*) PEG 6000, 10 m*M* $ZnCl_2$, (ii) 100 m*M* MES–NaOH pH 6.0, 20%(*w*/*v*) PEG 6000, 200 m*M* LiCl, (iii) 100 m*M* bis-tris–HCl pH 5.5, 17%(*w*/*v*) PEG 10 000, 100 m*M* ammonium acetate and (iv) 200 m*M* potassium formate pH 7.3, 20%(*w*/*v*) PEG 3350. Optimization of these initial conditions was performed using the same precipitants, varying the pH and PEG concentration, combined with the Additive Screen 2 HR-430 kit (Hampton Research) and the protein solution at concentration of 14 mg ml^{-1}. Improved crystals grew using 100 m*M* MES–NaOH pH 5.5, 20%(*w*/*v*) PEG 6000, 200 m*M* LiCl as precipitant (Fig. 3*a*) and 200 m*M* NDSB-201 as an additive (Fig. 3*b*). The best and largest monocrystals (Fig. 3*b*) suitable for X-ray analysis were used for data collection.

After data collection and processing, the crystals were found to belong to space group $P2_12_12_1$, with unit-cell parameters a = 45.28, b = 64.57, c = 169.23 Å. Data were collected in the resolution range 16.00–2.80 Å with an overall $R_{\rm merge}$ of 0.12, a completeness of 88.3% (11 254 unique reflections recorded) and an $\langle I/\sigma(I)\rangle$ of 23.4. Details of the data-collection and processing statistics are presented in Table 1. First using the structure of the enzyme as a search model in the molecular-replacement protocol and then fixing it and using the inhibitor molecule in a new search resulted in rotation-function and translation-function peaks that clearly corresponded to one binary complex in the asymmetric unit, as corroborated by the Matthews coefficient of 2.74 Å^3 Da^{-1}. The rotation function over σ, translation function over σ, score and R factor for the first (correct solution) and second highest peaks in the chymotrypsin search of the MR procedure are 12.0 and 4.0, 16.3 and 4.7, 0.58 and 0.32, and 0.49 and 0.62, respectively. The same data for the SPCI search yielded values of 8.0 and 4.7, 44.2 and 18.4, 0.64 and 0.48, and 0.45 and 0.54, respectively. These data clearly represent the correct solution of the binary complex.

At present, refinement is being performed and new crystallization attempts are being carried out in order to improve crystal quality and resolution.

This work was supported in part by Conselho Nacional de Desenvolvimento Científico e Tecnológico (CNPq), Coordenação de Aperfeiçoamento de Pessoal de Nível Superior (CAPES), Fundação de Amparo à Pesquisa do Estado de São Paulo (FAPESP) and Associação Brasileira de Tecnologia de Luz Síncrotron (ABTLuS).

References

Bode, W. & Huber, R. (1992). *Eur. J. Biochem.* **204**, 433–451.
Collaborative Computational Project, Number 4 (1994). *Acta Cryst.* D**50**, 760–763.
Gilliland, G. L., Tung, M., Blakeslee, D. M. & Ladner, J. E. (1994). *Acta Cryst.* D**50**, 408–413.
Hol, W. G. J., Sarfaty, S. H., Stewart, L. J. & Kim, H. (2001). US Patent 6267935.
Jancarik, J. & Kim, S.-H. (1991). *J. Appl. Cryst.* **24**, 409–411.
Joanitti, G. A, Freitas, S. M. & Silva, L. P. (2006). *Curr. Enzyme Inhib.* **2**, 199–217.
Kanaujia, S. P., Ranjani, C. V., Jeyakanthan, J., Baba, S., Chen, L., Liu, Z.-J., Wang, B.-C., Nishida, M., Ebihara, A., Shinkai, A., Kuramitsu, S., Shiro, Y., Sekar, K. & Yokoyama, S. (2007). *Acta Cryst.* F**63**, 27–29.
Kobayashi, H., Suzuki, M., Kanyama, N. & Terao, T. (2004). *Clin. Exp. Metastasis*, **21**, 159–166.
Laemmli, U. K. (1970). *Nature (London)*, **227**, 680–685.
Laskowski, M. & Kato, I. (1980). *Annu. Rev. Biochem.* **49**, 593–626.
Laskowski, M. & Qasim, M. A. (2000). *Biochim. Biophys. Acta*, **1477**, 324–337.
Leite, J. R. S. A., Silva, L. P., Taveira, C. C., Teles, R. C. L., Freitas, S. M. & Azevedo, R. B. (2002). *Protein Pept. Lett.* **9**, 179–185.
McPherson, A. (1990). *Eur. J. Biochem.* **189**, 1–23.
Majeed, S., Ofek, G., Belachew, A., Huang, C. C., Zhou, T. & Kwong, P. D. (2003). *Structure*, **11**, 1061–1070.
Matthews, B. W. (1968). *J. Mol. Biol.* **33**, 491–497.
Neurath, H. (1997). *Trends Biochem. Sci.* **14**, 268–271.
Newman, J., Egan, D., Walter, T. S., Meged, R., Berry, I., Ben Jelloul, M., Sussman, J. L., Stuart, D. I. & Perrakis, A. (2005). *Acta Cryst.* D**61**, 1426–1431.
Norioka, N., Hara, S., Ikenaka, T. & Abe, J. (1988). *Agric. Biol. Chem.* **52**, 1245–1252.
Otwinowski, Z. & Minor, W. (1997). *Methods Enzymol.* **276**, 307–326.
Page, R., Grzechnik, S. K., Canaves, J. M., Spraggon, G., Kreusch, A., Kuhn, P., Stevens, R. C. & Lesley, S. A. (2003). *Acta Cryst.* D**59**, 1028–1037.
Phillips, M. A. & Fletterick, R. J. (1992). *Curr. Opin. Struct. Biol.* **2**, 713–720.
Richardson, M. (1977). *Phytochemistry*, **16**, 159–169.
Shukle, R. H. & Wu, L. (2003). *Environ. Entomol.* **32**, 488–498.
Souza, E. M. T., Mizuta, K., Sampaio, M. U. & Sampaio, C. M. (1995). *Phytochemistry*, **39**, 521–525.
Souza, E. M. T., Teles, R. C. L., Siqueira, E. M. A. & Freitas, S. M. (2000). *J. Protein Chem.* **9**, 507–513.
Teles, R. C. L., Calderon, L. A., Medrano, F. J., Barbosa, J. A. R. G., Santoro, M. M. & Freitas, S. M. (2005). *Biophys. J.* **88**, 3509–3517.
Teles, R. C. L., Esteves, G. F., Araújo, M. A. M., Bloch, C., Barbosa, J. A. R. G. & de Freitas, S. M. (2007). *Acta Cryst.* F**63**, 929–931.
Teles, R. C. L., Freitas, S. M., Kawano, Y., Souza, E. M. T. & Áreas, E. P. G. (1999). *Spectrochim. Acta A*, **55**, 1279–1289.
Teles, R. C. L., Souza, E. M. T., Calderon, L. A. & Freitas, S. M. (2004). *Phytochemistry*, **65**, 793–799.
Tsukada, H. & Blow, D. M. (1985). *J. Mol. Biol.* **184**, 703–711.
Vagin, A. & Teplyakov, A. (1997). *J. Appl. Cryst.* **30**, 1022–1025.

Apidologie (2011) 42:252–269
© The Author(s) 2011. This article is published with open access at SpringerLink.com
DOI: 10.1007/s13592-011-0025-9

Original article

Calcium effect and pH-dependence on self-association and structural stability of the *Apis mellifera* major royal jelly protein 1

Gabriel C. N. Cruz[1], Liudy Garcia[2], Adelson J. Silva[4], João A. R. G. Barbosa[3], Carlos A. O. Ricart[1], Sonia M. Freitas[4], Marcelo V. Sousa[1]

[1]Brazilian Center for Protein Research, Department of Cell Biology, University of Brasilia (UnB), Brasilia, DF, Brazil
[2]Mass Spectrometry Group, Physics Department, CEADEN, Havana, Cuba
[3]Center for Structural Molecular Biology (CeBiME), Brazilian Synchrotron Light Laboratory (LNLS), Campinas, SP, Brazil
[4]Laboratory of Biophysics, Department of Cell Biology, University of Brasilia (UnB), Brasilia, DF, Brazil

Received 4 November 2009 – Revised 18 March 2010 – Accepted 25 March 2010

Abstract – The major royal jelly protein 1 (MRJP1) is the main glycoprotein in honey bee royal jelly. In brain tissues, MRJP1 is found in intercellular spaces and associated to cytoskeleton within cells. MRJP1 must be involved in multiple biological functions, yet there is a lack of structural information on the protein. MRJP1 was herein purified from royal jelly and characterized through electrophoresis and mass spectrometry as the same protein found in cerebral tissue. Unfolding curves obtained by circular dichroism analyses strongly suggest its high stability under different pHs. However, calcium ions made MRJP1 susceptible to temperature and pH effects. In the presence of 2 mM calcium, very high stabilities were achieved at pH 6.0 and 7.0 with ΔG^{25} over 62 kJ mol^{-1}. Overall, the present results represent a valuable effort aimed at the structural characterization of MRJP1, representing an essential step toward the determination of its roles in honey bee neural processes.

MRJP1 / *Apis mellifera* / protein stability / mass spectrometry / circular dichroism

1. INTRODUCTION

The honey bee (*Apis mellifera*) is a social insect that presents complex behaviors and is able to execute multiple tasks (Page and Peng 2001; Menzel et al. 2006). It has long been acknowledged for their crucial function in plant pollination in natural environments as well as in agricultural crops.

Royal jelly is produced in the cephalic glands of both nurse and forager worker bee subcastes. It is the main food for larvae, and is imperative for caste differentiation from larvae to queen (Winston 1987; Ohashi et al. 1997). This is a case of insect polyphenism regulated by differential nourishment (Evans and Wheeler 2001; Malecova et al. 2003). Royal jelly is fed to honey bee larvae, but is provided to the queen throughout its whole lifespan, and sustains its high reproductive ability (Ohashi et al. 1997).

A large family of major royal jelly proteins (MRJPs) is present in this secretion. MRJPs are similar to yellow proteins from *Drosophila melanogaster* and other insects as well as to putative proteins from bacteria (Albert and Klaudiny 2004; Drapeau et al. 2006). Little is

Corresponding author: S.M. Freitas, nina@unb.br
Manuscript editor: Klaus Hartfelder

known about biological functions of such a class of proteins, but some suggestions have been proposed like sex-specific reproductive maturation (Drapeau et al. 2006) and developmental processes in bee nervous system (Peixoto et al. 2009). They are linked to queen development by still unclear mechanisms (Albert and Klaudiny 2004; Consortium, 2006). In addition, they are believed to exert defensive functions against fungi and bacteria, as assigned in the Gene Ontology database. Finally, a structural motif of dopachrome-conversion enzyme is apparently present along some MRJPs sequences, as found in some yellow proteins (Futahashi et al. 2008).

The most abundant protein in royal jelly is MRJP1 (major royal jelly protein 1) (Scarselli et al. 2005) that is encoded by a single gene and composed of 413 amino acids in its processed form (Malecova et al. 2003; Drapeau et al. 2006). It appears to be posttranslationally modified at different extents and displays at least eight isoforms with similar isoelectric points (p*I*) when separated by isoelectric focusing (Hanes and Simuth 1992). This was suggested to be caused by polymorphisms with some amino acid substitutions and/or by genetic variability of honey bee individuals in the hive (Schmitzova et al. 1998).

MRJP1 is a 55–57 kDa protein as determined by gel electrophoresis, but goes down to 47 kDa after treatment with N-glycosidase F (Ohashi et al. 1997), in agreement to the theoretical mass calculated for MRJP1 without the signal peptide (19 N-terminal residues) (Schmitzova et al. 1998). Three MRJP1 hypothetical glycosylation sites have been proposed based on its primary structure (Ohashi et al. 1997). Another interesting feature of MRJPl is that it is present in monomeric and oligomeric forms in royal jelly (Simuth 2001; Tamura et al. 2009a).

Several changes at structural and proteomic levels are observed during the ontogenetic differentiation from nurse to forager worker subcastes (Fahrbach and Robinson 1995; Wolschin and Amdam 2007; Garcia et al. 2009). Recently, we showed by two-dimensional electrophoresis and proteome analysis that MRJP1 is the most abundant protein in the nurse brain, suffering downregulation toward forager brain during the differentiation process (Garcia et al. 2009). In addition, it was immunolocalized in intercellular spaces between cells in mushrooms bodies (presumed centers of learning and memory in the honey bee brain), indicating that it is a secreted protein (Garcia et al. 2009). However, MRJP1 was also detected in the cytoplasm of brain cells of the antennal lobe, optical lobe and mushroom body (Garcia et al. 2009; Peixoto et al. 2009), which is an indication of the multiple functions associated to this protein. Additionally, it was deposited on the rhabdom, a structure of the retinular cells composed of numerous tubules, suggesting its association to proteins of filamentous structures such as cytoskeleton (Garcia et al. 2009). (Kucharski et al. 1998) had previously found the mRNA for this protein in the mushroom bodies of *A. mellifera* brain, concentrated in a defined population of Kenyon cells.

Therefore, besides the nutritional role in royal jelly, MRJP1 is thought to have other possible unknown functions in the neural tissue, that possibly appeared during the evolution of sociality (Albert et al. 1999; Consortium, 2006). Ontological bioinformatics analysis suggested that MRJP1 is potentially involved in developmental processes in the *A. mellifera* nervous system (Peixoto et al. 2009). Diverse biological activities have been reported for MRJP1. It shows growth stimulation of human lymphocytes in a serumfree medium (Watanabe et al. 1998), enhancement of cell proliferation in rat hepatocytes (Kamakura et al. 2001c), antifatigue effect in mice (Kamakura et al. 2001b), stimulation of TNF-α release by mouse macrophages, and possible roles in cytokine-induced activation of genes important for immune response of honey bees and humans (Simuth et al. 2004; Majtan et al. 2006).

Despite the knowledge gathered about MRJP1, there is still a lack of structural information on such intriguing protein. In the present work, MRJP1 was isolated from royal jelly, compared to its honey bee brain counterpart by mass spectrometry, and character-

ized regarding its structural features by dynamic light scattering and circular dichroism spectroscopy.

2. MATERIALS AND METHODS

2.1. Royal jelly fractionation

About 250 mg of commercial royal jelly (Apivita, Rio Claro, Brazil) were homogenized in 1.2 mL of 50 mM Tris–HCl pH 7.5 (buffer A) containing 10 mM ethylenediaminetetraacetic acid (EDTA) and a cocktail of proteases inhibitors (cOmplete Mini, Roche, Mannheim, Germany). The extract was stirred for 2 min in vortex and centrifuged at 16,000 g for 30 min at room temperature. The soluble material (~10 µg/µL proteins) was submitted to anion-exchange chromatography using a Mono-Q® HR 10/10 column (Pharmacia, Uppsala, Sweden) coupled to a FPLC system. The column (8 mL) was equilibrated with buffer A under a 1.5 mL/min flow. Elution was performed using a 0–1 M NaCl gradient in buffer A: 0–10 min, buffer A; 10–60 min, 0–0.2 M NaCl; 60–90 min, 0.2–0.5 M NaCl; 90–95 min, 0.5–1 M NaCl; 95–100 min, 1 M NaCl. All solutions were filtered using 0.22 µm pores and degassed before use. The chromatographic run was conducted at room temperature, and accompanied by optical absorption at 280 nm. Protein quantification was performed according to Bradford (1976). Collected fractions were analyzed by SDS-PAGE, and those of interest were pooled, dialyzed against distilled water at 4°C and lyophilized.

2.2. Extraction of honey bee brains

Nurse honey bees (*A. mellifera*) were acquired from Vereda Rosa Apiaries (Brasilia, Brazil). Bees were anesthetized with chloroform, and brains were dissected and thoroughly washed in cold TBS (20 mM Tris–HCl pH 7.5, 150 mM NaCl) and then in lysis buffer (7 M urea, 2 M thiourea, 85 mM dithiothreitol (DTT), 2.5% (*v*/*v*) Triton X-100, 0.5% immobilized pH gradient (IPG) buffer pH 4–7) containing a cocktail of protease inhibitors (cOmplete Mini, Roche). Honey bee brain extracts were prepared out of ten pooled through homogenization using a Sample Grinding Kit (GE Healthcare, Uppsala, Sweden) into 200 µL of lysis buffer in ice; immediately immersed in liquid nitrogen and stored at −20°C. Before use, brain extract was centrifuged by 16,000 g, 15 min at room temperature. Protein quantification of the supernatant was performed using 2-D Quant Kit (GE Healthcare).

2.3. SDS-PAGE

Sodium dodecyl sulfate polyacrylamide gel electrophoresis (SDS-PAGE) was carried out at 30 mA constant current at 10% T polyacrylamide, 1.5 mM thick gel, connected to a cooling bath using a TE-2000 (Tecnal, Piracicaba, Brazil) apparatus. Proteins in gel were silver stained according to Blum et al. (1987). Phosphorylase b (97 kDa), bovine serum albumin (66 kDa), egg albumin (45 kDa), carbonic anydrase (30 kDa) and trypsin inhibitor (20.1 kDa) were used as molecular weight markers.

2.4. Two-dimensional electrophoresis

Two-dimensional electrophoresis (2-DE) was performed using an Ettan IPGphor 3 system (GE Healthcare) for the first dimension and a Protean II system (BioRad, Hercules, CA, USA) for the second one, both at 20°C. Proteins were separated by isoelectric focusing (IEF) in 18 cm IPG strips (GE Healthcare), previously rehydrated for 6 h in 350 µL lysis buffer containing 10% isopropanol (Garcia et al. 2009). Samples containing 50 µg brain extract protein or 10 µg purified MRJP1 were separated in 4–7 pH range under the following conditions: rehydration for 6 h, 30 V for 6 h, 500 V for 1 h, 1,000 V (gradient) for 1 h and 8,000 V (gradient) for 3 h and 8,000 V for 1 h and 40 min (28,630 total Vh). Before the second-dimension step, the IPG gel strips were subjected to reduction and alkylation. Thus, strips were soaked for 20 min in a solution containing 6 M urea, 30% (*v*/*v*) glycerol, 2% (*w*/*v*) SDS and 125 mM DTT and for additional 20 min in the same buffer containing 300 mM acrylamide instead of DTT. SDS-PAGE was performed on 10% T polyacrylamide gels, 1.0 mM thick, connected to a cooling bath using the same molecular weight markers and running conditions as described for the SDS-PAGE. Proteins were monitored using a mass

spectrometry (MS) compatible silver staining procedure (Blum et al. 1987).

2.5. In situ digestion

Bands or spots of interest were excised from gel and distained in a freshly prepared 15 mM potassium ferricyanide, 50 mM sodium thiosulfate solution for 10 min (Gharahdaghi et al. 1999). Gel pieces were rinsed two to three times in Milli-Q water (Millipore, Billerica, MA, USA) to stop the reaction; washed three times in water and acetonitrile alternately, 10 min each; and then vacuum dried using a Speed Vac system (Savant, Farmingdale, NY, USA). Samples were subjected to in situ reduction and alkylation. Reduction of disulfide bonds was performed by incubating gel pieces in 100 mM ammonium bicarbonate solution with 10 mM DTT for 1 h at 56°C. After removing this solution, cysteine residues were alkylated in 100 mM ammonium bicarbonate solution with 55 mM iodoacetamide for 45 min at room temperature in the dark. A new washing cycle water/acetonitrile was carried out before drying. Gel slices were then rehydrated in 50 mM ammonium bicarbonate, 5 mM calcium chloride solution containing sequencing grade modified trypsin (Promega, Madison, WI, USA) at 12.5 ng/μL and incubated at 37°C overnight. Peptides were extracted twice with 66% (*v/v*) acetonitrile, 0.1% (*v/v*) trifluoroacetic acid solution by sonication, desalted and concentrated using ZipTips C18 (Millipore, Bedford, MA, USA).

2.6. Protein identification

Tryptic digests eluted from the gels were mixed in a matrix solution (10 μg/μL α-cyano-4-hydroxycinnamic acid) prepared in 50% (*v/v*) acetonitrile, 0.1% (*v/v*) trifluoroacetic acid. Each sample was spotted onto the sample plate, and was allowed to dry before matrix-assisted laser desorption/ionization—time of flight (MALDI-TOF) MS analysis. The spectra were collected using an Autoflex II MALDI-TOF/TOF mass spectrometer (Bruker Daltonics, Bremen, Germany) in delayed extraction and reflector modes. External calibration was performed using a peptide standard kit (Bruker Daltonics). Known trypsin autolysis and keratin peaks (842.50 and 1475.77, respectively) were used for the internal calibration. Peptide masses (MH^+) were recorded in 750 to 3,000 Da range. The peptides mass spectra were generated using the software FlexControl v. 2.4 (Bruker Daltonics). The software FlexAnalysis v. 2.4 (Bruker Daltonics) was used to acquire and process the peak lists that were employed for database search using BioTools v. 2.0 (Bruker Daltonics) linked to Mascot (http://www.matrixscience.com/) (Perkins et al. 1999) against the NCBI protein database (National Center for Biotechnology Information, Bethesda, USA). Monoisotopic masses of tryptic peptides were used to identify the proteins by Peptide Mass Fingerprinting (PMF). Error tolerance for peptide mass was lower than 100 ppm and no restrictions were imposed on protein molecular mass or phylogenetic lineage. Further search parameters were methionine oxidation as variable modification and propionamide cysteine (acrylamide alkylation) or carbamidomethyl cysteine (iodoacetamide alkylation) as fixed modification. Missed cleavages sites were set up to 1. Hits were considered significant if the protein score exceeded the threshold score calculated by Mascot software assuming *P*-value <0.05.

Tandem mass spectra (MS/MS) were also acquired using Autoflex II MALDI-TOF/TOF mass spectrometer (Bruker Daltonics). Parental ions were selected within 2% parent mass error, and spectra accumulated from 400 laser shots. Fragmentation was then performed using a boost of 150% in detector gain and of 20% in laser power after parental spectrum selection. Further processing of the MS/MS spectra were performed using FlexAnalysis v. 2.4. All MS/MS data from each individual spot were merged into a single file using BioTools v. 2.0 before search. MS/MS datasets were searched against the protein sequence database using the following parameters: only tryptic peptides with up to one missed cleavage site were allowed; mass tolerances of 100 ppm for MS and 0.5 Da for MS/MS fragment ions; propionamide cysteine as fixed modification and oxidized methionine as variable modification.

2.7. Dynamic light scattering analysis

Dynamic light scattering (DLS) provides information about the size, distribution and homogeneity of

macromolecules in solution, and can be used to monitor protein aggregation. The light scattering measurements by DLS is used to calculate the hydrodynamic radius, which is defined as the radius of a spherical particle with the same diffusion coefficient as the macromolecule of interest. DLS assays were carried out through a laser wavelength of 800 nm, using a DynaPro–LSD model (Wyatt Technology Corporation, Santa Barbara, CA, USA) molecular-sizing instrument equipped with a Peltier system for temperature control, reaching 60°C. Solutions of MRJP1 were centrifuged at 15,000 g for 20 min at 4°C, and the supernatant filtered through a 0.22 μm filter (Millipore) and added to the cuvette. The hydrodynamic parameters were measured at different pHs, temperatures, and concentrations of protein.

The measured intensity of scattered light from each sample was normalized considering the buffer scattering contribution. Polydispersity parameter (*Pd*), averaged hydrodynamic radius (R_H), averaged hydrodynamic diameter (D_H), molecular weight, sum of squares (SOS) were determined from the intensity correlation function using the cumulants method (Frisken 2001; Hassan and Kulshreshtha 2006) and using the Dynamics V.6 software.

2.8. Circular dichroism spectroscopy

Circular Dichroism (CD) assays were carried out using Jasco J-815 spectropolarimeter (Jasco, Tokyo, Japan) equipped with a Peltier type temperature controller and thermostatized cuvette cell linked to a thermostatic bath. Far-UV spectra were recorded using 0.1 or 0.2 cm pathlength quartz cuvettes. MRJP1 (2.5 μM or 5 μM) was analyzed in different buffer conditions: 2 mM sodium citrate pH 3.0, 2 mM sodium acetate pH 4.0, 5.0 or 6.0, 2 mM Hepes pH 7.0 or 8.0, 2 mM CHES pH 9.0. Four consecutive measurements were accumulated and the mean spectra recorded. Eventual errors due to buffer or instrument effects were discarded by the subtraction of the baseline spectrum from each protein spectrum. Thermal denaturation assays were performed raising the temperature at 0.5°C/min, from 20°C to 95°C, unless specified otherwise. The observed ellipticities were converted into molar ellipticity ([θ]) based on molecular mass per residue of 113 Da. Protein structure was tracked by changes in [θ] at 218 nm, where the maximal signal intensity was verified in all conditions at 25°C.

The unfolded protein fraction (f_U), the equilibrium constant (*K*eq) and the Gibbs free energy (ΔG^{25}) were calculated using the following equations (Pace et al. 1997):

$$f_U = (y_N - y)/(y_N - y_U) \quad (1)$$

$$K_{eq} = [U]/[N] = f_U/(1 - f_U) \quad (2)$$

$$\Delta G = -RTlnK_{eq} \quad (3)$$

where y_N and y_U represent the amount of y protein present in native and unfolded state, respectively. [U] and [N] denote the protein concentration in unfolded and native state, respectively; *R*, the universal gas constant (8.314 J K^{-1} mol^{-1} or 1.987 cal K^{-1} mol^{-1}) and *T*, the temperature in Kelvin (K). The melting temperature (*Tm*) where the unfolding occurs was calculated from the Δ*G* versus temperature plot. Enthalpy (Δ*Hm*) and entropy (Δ*Sm*) parameters were calculated from van't Hoff plot, Eq. 5:

$$\Delta G = \Delta H - T\Delta S \quad (4)$$

$$RlnK_{eq} = -\Delta H(1/T) + \Delta S \quad (5)$$

Secondary structure content were estimated from the CD curves adjustments (Böhm 1997) using the CDNN deconvolution software (Version 2.1, Bioinformatik.biochemtech.uni-halle.de/cdnn) considering the database that resulted on total sum of secondary structures closest to 100%.

3. RESULTS

3.1. Purification of the MRJP1

Royal jelly crude extract was fractionated by anion-exchange chromatography (Figure 1). Two

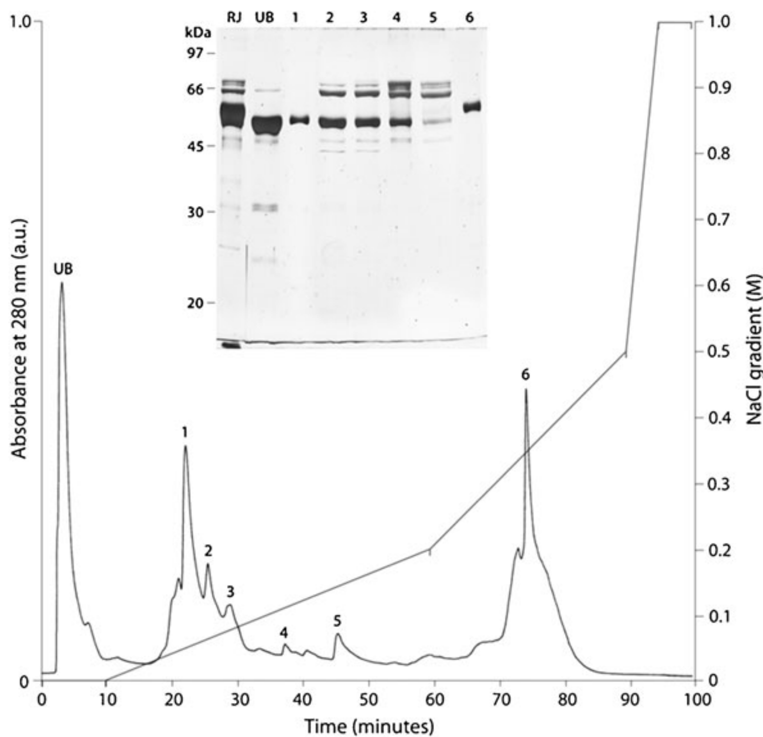

Figure 1. Separation of royal jelly proteins by anion-exchange FPLC. Soluble fraction of royal jelly was submitted to chromatography. Retained proteins were eluted by a NaCl gradient in 50 mM Tris–HCl pH 7.5 buffer. Elution was accompanied by absorbance at 280 nm. The main peaks were collected as indicated (1–6). *Inset*—SDS-PAGE of royal jelly protein fractions. Royal jelly soluble fraction (*RJ*), 5 μg, the unbound material (*UB*), 5 μg, and the eluted fractions 1–6, 2 μg, were separated in a 10% polyacrylamide gel. Molecular weight markers are represented on the left side.

main proteins were collected in the fractions represented by peaks 1 and 6, respectively. These proteins were eluted with buffer containing 40–60 mM and 300–400 mM NaCl, respectively. No visible contaminants were present in these fractions as showed in silver stained SDS-PAGE (Figure 1, inset). The main protein in fraction associated with peak 1 was identified as Major Royal Jelly Protein 2 (MRJP2), and the one associated with peak 6 as Major Royal Jelly Protein 1 (MRJP1) by PMF via MALDI-TOF MS with searches against the NCBI nonredundant protein database using Mascot software (Table I). Additional analysis of MRJP1 by 2-DE revealed nine main isoforms (Figure 2) from p*I* 4.7 to 5.2 (Table II). The protein spots were identified by PMF as MRJP1 from *A. mellifera* with high scores and sequence coverage (Table II).

3.2. Comparison between royal jelly and brain MRJP1s

Nurse honey bee brain proteome was analyzed by 2-DE (Figure 3) to check the overlapping between royal jelly MRJP1 (Figure 2) and brain MRJP1. Previous report had identified the MRJP1 in honey bee brain (Garcia et al. 2009), which was confirmed herein by PMF resulting in a high score of 148, with 19 matched peptides and 43% sequence coverage. MRJP1 isoforms from both royal jelly and brain

Table I. Mass spectrometric identification of proteins separated by anion exchange chromatography.

Peak	Identified protein	Organism/Protein ID	Score mascot	Matched peptides	Coverage (%)	Mr (kDa) (Theor./Obs.)
1	Major royal jelly protein 2	*Apis mellifera*/gi|58585108	117	9	23	51.041/51.3
6	Major royal jelly protein 1	*Apis mellifera*/gi|58585098	167	13	39	48.855/56.0

were localized on coinciding areas in their respective 2-DE gels (Figures 2 and 3).

Similarity between MRJP1s from the two sources was evaluated comparing MS spectra from royal jelly isoform 6 and a central isoform from brain (Figure 4). Almost all tryptic peptides that matched peptide masses in database searches were actually found in the spectra from both isoforms under MS analysis (Figure 4). Few differences could be detected between peptide masses generated from the MRJP1 primary sequence and peptide masses recorded by MS. The ion at *m/z* 1614.8 was more intense in the spectrum from the brain isoform, which corresponds to the ion at *m/z* 1630.8 minus a methionine oxidation, only present in the royal jelly isoform spectrum. Isotope overlaps of ions were found at *m/z* 1631.7 and 1630.8 from brain and royal jelly isoforms respectively. The ion at *m/z* 1746.7 is more abundant in the brain spectrum while its methionine oxidized counterpart at *m/z* 1762.7 is richer in the royal jelly isoform spectrum. Considering these results, above mentioned ions (*m/z* 1614.8, 1630.8,

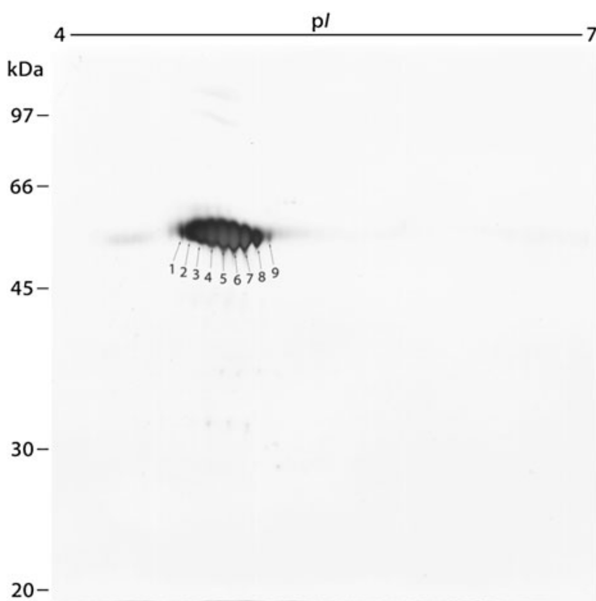

Figure 2. 2-DE of peak 6 fraction. An amount of 10 μg of protein was separated by immobilized pH gradient (4–7) in the first dimension and 10% polyacrylamide SDS-PAGE, in the second one. Proteins were silver stained. *Arrows* indicate protein spots that were identified by PMF as shown in Table II. Molecular weight markers are represented on the left side.

Table II. Mass spectrometric identification of proteins separated by two-dimensional electrophoresis.

Spot	Identified protein	Organism/Protein ID	Score mascot	Matched peptides	Coverage (%)	p*I* (Theor./ Obs.)	(Theor./ Obs.)
1	Major royal jelly Protein 1	*Apis mellifera*/gi|58585098	111	11	37	5.10/4.72	48.855/56.1
2	Major royal jelly Protein 1	*Apis mellifera*/gi|58585098	155	16	46	5.10/4.77	48.855/56.1
3	Major royal jelly Protein 1	*Apis mellifera*/gi|58585098	151	16	48	5.10/4.82	48.855/56.1
4	Major royal jelly Protein 1	*Apis mellifera*/gi|58585098	126	14	43	5.10/4.88	48.855/55.6
5	Major royal jelly Protein 1	*Apis mellifera*/gi|58585098	141	15	42	5.10/4.95	48.855/55.0
6	Major royal jelly Protein 1	*Apis mellifera*/gi|58585098	163	17	44	5.10/5.00	48.855/54.5
7	Major royal jelly Protein 1	*Apis mellifera*/gi|58585098	142	14	42	5.10/5.05	48.855/54.0
8	Major royal jelly Protein 1	*Apis mellifera*/gi|58585098	145	16	50	5.10/5.12	48.855/54.0
9	Major royal jelly Protein 1	*Apis mellifera*/gi|58585098	90	9	31	5.10/5.20	48.855/54.0

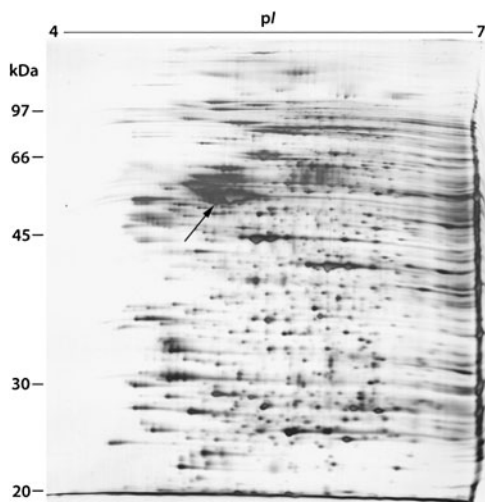

Figure 3. 2-DE of total protein extract from nurse bee brains. 50 μg of protein was separated by immobilized pH gradient (4–7) in the first dimension and 10% polyacrylamide SDS-PAGE, in the second one. Proteins were silver stained. *Arrow* indicates the MRJP1 spot that was identified by PMF and compared to the royal jelly MRJP1. Molecular weight markers are represented on the left side.

1746.7 and 1762.7) were submitted to MS/MS analysis. Their sequence and modifications (methionine oxidation) could then be confirmed by searches over the NCBI database. The ions at *m*/*z* 1746.7 and 1614.8 were identified as the MRJP1 peptides Met388 - Arg401 (MVNNDFNFDDVNFR) and Ile402 - Arg415 (IMNANVNELILNTR), respectively. Their putatively modified counter-parts at *m*/*z* 1762.7 and 1630.8 showed the same sequences above, but oxidations in methionines. A missed cleavage after Lys96 resulted in *m*/*z* 2075.1 in the brain sample. This peptide had one more lysine residue than the ion at *m*/*z* 1946.9, present in both spectra. The peak at *m*/*z* 2264.3 in brain represented the *m*/*z* 2335.1 without the alkylation at Cys329. Another missed cleavage after Lys38 generated *m*/*z* 2501.1 in the royal jelly MRJP1, which could correspond to a larger peptide constituted by the peptides at *m*/*z* 1122.5 and 1397.5.

Other superimposed MRJP1 isoforms from brain and royal jelly were also compared in terms of MS spectra of tryptic digests, similarly

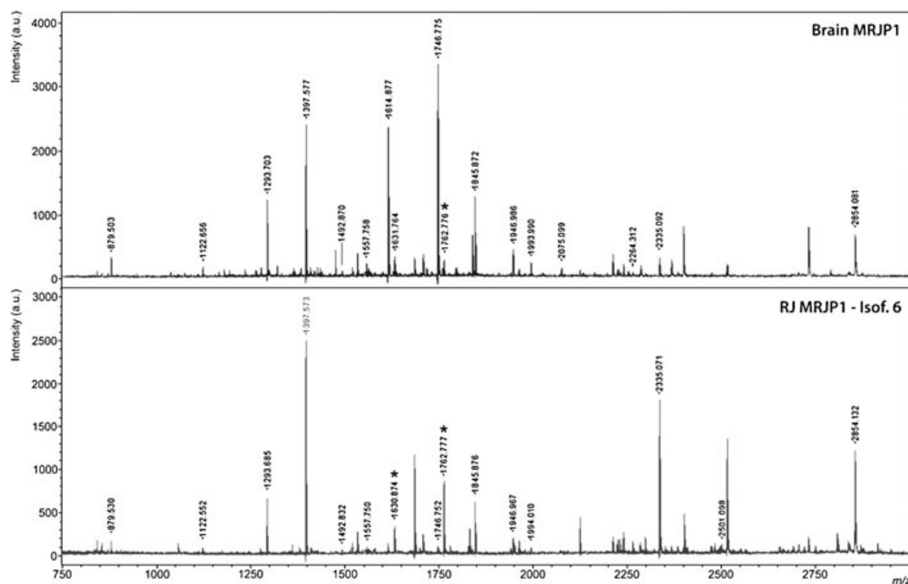

Figure 4. MALDI-TOF mass spectra of tryptic digests from spots of brain and royal jelly MRJP1s. Protein spot isoform 6 in Figure 2 and protein spot indicated by an *arrow* in Figure 3 were submitted to identification by MALDI-TOF MS analysis. Both proteins were identified as major royal jelly protein 1 from *Apis mellifera*. Only *m*/*z* values of peptides matched to database are indicated in the spectra. *Molecular ions matching to peptides containing oxidized methionine.

presenting high numbers of ion peak with identical masses and intensities (data not shown). These data suggest that the MRJP1 purified from royal jelly is the same protein as the one found in bee brain.

3.3. Conformational state and stability of MRJP1

The purified MRJP1 presented a polydisperse profile (25–30% *Pd*) as evaluated by DLS. The sample showed averaged hydrodynamic diameter (D_H) of 13.4 nm for pH 7.0, which allowed inferring a pentameric structure for MRJP1 (with ~290 kDa) at 1 μM, 3 μM (data not shown) and 10 μM (Figure 5). However, a hexameric state of MRJP1 was found at pH 8.0 and pH 9.0, with D_H=14.3 nm (~340 kDa). The main peak at pH 6.0 also evidenced the pentameric formation (Figure 5). As expected, some aggregation (about 2.5% mass) was observed for 25 μM MRJP1 at pH 7.0 (data not shown).

Physicochemical and structural characterization of MRJP1 was carried out by using thermal denaturation, evaluated by Far-UV circular dichroism spectroscopy. Thermal stability of the protein at pH 7.0 was assessed upon raising the temperature from 20 to 95°C (Figure 6). The thermostability was assumed considering a curve decline in molar ellipticity along with the increase of temperature. The secondary structure content of MRJP1 at pH 7.0 calculated from the CD spectrum at 20°C was: 9.6% α-helix, 38.3% antiparallel and parallel β-sheets and 20% β-turn. The CD spectra in temperature ranging from 20 to 95°C show a gradual, slight increase of the dichroic signal (downward), suggesting that the protein gains structure as a function of temperature (Figure 6). A little decrease was observed in terms of α-helix content (from 9.6% to 9.1%) and β-sheet (from 38.3% to 37.2%), and a discrete increase in β-turn (from 20.0% to 21.6%) and random structures (from 36.0% to 36.7%) (Figure 6, inset).

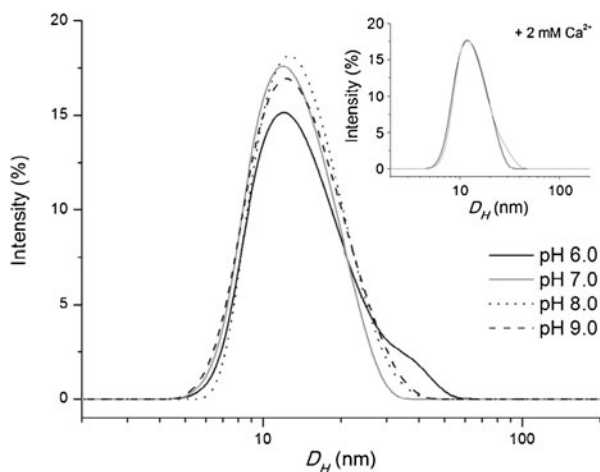

Figure 5. Analysis of the MRJP1 size distribution by DLS. 10 μM of MRJP1 was used for all conditions. Protein was diluted in 10 mM sodium acetate pH 6.0, 10 mM HEPES pH 7.0 or pH 8.0, 10 mM CHES pH 9.0, as indicated. *Inset graphic*—Light scattering profile of MRJP1 in absence—and presence—of 2 mM $CaCl_2$ in 10 mM HEPES pH 7.0.

The thermostability of MRJP1 was also observed either in presence of 200 and 400 mM sodium chloride or 0.5, 1.0 and 1.5 M guanidine, as evidenced by no significant changes on the molar ellipticity as function of the temperature (data not shown). A reduction in the dichroic signal was observed when adding 400 mM sodium chloride or 1.5 M guanidine at 20°C, but no indicative of full protein denaturation (data not shown). The denaturation was only achieved when 2 mM calcium chloride was added to the buffer at pH 4.0, pH 5.0 (data not shown), pH 6.0 (Figure 7c and d) or pH 7.0 (Figure 7d), but not at pH 3.0 (Figure 7a), pH 8.0 (Figure 7b) or pH 9.0 (not shown).

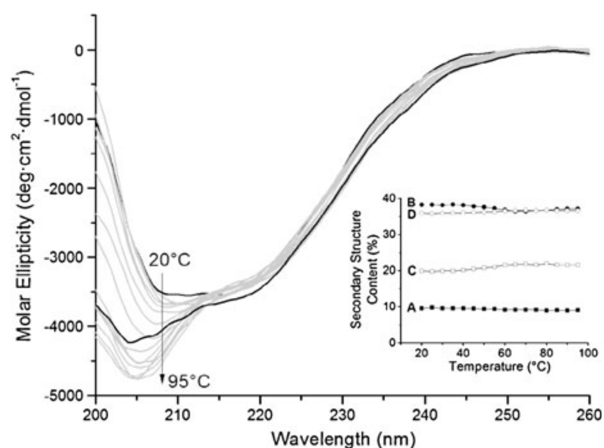

Figure 6. Far-UV CD spectra of MRJP1 as a function of temperature. Protein (5 μM) was solubilized in 2 mM HEPES pH 7.0. The *arrow* indicates the increase in molar ellipticity as a function of the increase of temperature. The secondary structure contents estimated from these spectra are presented in the inset as follows: **a** α-helix; **b** β-sheet; **c** β-turn; and **d** other content as a function of the temperature.

DLS analyses showed that MRJP1 appears as an aggregate at pH 4.0 or pH 5.0, in spite of showing typical denaturation curves in CD analyses, when in the presence of 2 mM $CaCl_2$ (data not shown). Thus, no thermodynamic parameters characterizing the structural stability of the protein could be calculated for these conditions.

Protein stability is defined by measurements of thermodynamic parameters, and the reversibility of the unfolding reaction is essential for such experiments (Pace et al. 1997). Indeed, the degree of irreversibility for a protein increases as a function of its exposition time to unfolding conditions. In the case of MRJP1, the thermal unfolding took approximately 3 h, a drastic condition that promoted the protein aggregation and turned the thermal unfolding reaction irreversible (data not shown). In spite of that, we estimated the thermodynamic parameters from the normalized CD data at pH 6.0 and 7.0. However, such thermodynamic parameters do not correspond to the real stability of MRJP1, once its thermal unfolding was an irreversible process. The melting temperature of unfolding (*Tm*) was higher at pH 6.0 (87.34°C) than at pH 7.0 (82.80°C). The Gibbs free energy (ΔG^{25}) calculated for pH 6.0 and 7.0 were 68.262 kJ mol^{-1} and 62.943 kJ mol^{-1}, respectively, which suggests a high stability for MRJP1 in these conditions. This can also be depicted by the higher value of enthalpy change (ΔHm above 387 kJ mol^{-1}) estimated for these two conditions. The entropy change (ΔSm) was low for the tested conditions, indicating the predominant contribution of enthalpy change to the ΔG^{25} of the protein. In general, the much higher value of ΔHm reflects a higher ΔG^{25} given by the Gibbs-Helmholtz relationship or likewise by Eq. 4 (see Section 2).

The CD spectra of MRJP1 in the presence of 2 mM calcium chloride were very similar for pH 4.0, pH 5.0, pH 6.0 and pH 7.0 at 25°C (data not shown). Moreover, 2 mM $CaCl_2$ did not cause significant change in the molecule as indicated by DLS profile at pH 7.0 and 25°C (Figure 5, inset), suggesting that calcium itself does not promote considerable structure alteration in MRJP1 at room temperature.

4. DISCUSSION

Major Royal Jelly Protein 1 (MRJP1) is an acidic protein and the most abundant component of royal jelly, representing 48% of total water soluble protein (Simuth et al. 2004; Scarselli et al. 2005). Due to abundance in royal jelly, the purification was performed from that material. A single purification step using anion exchange FPLC chromatography was required to purify MRJPs. Two of the main fractions presented single bands in silver staining under SDS-PAGE (Figure 1, inset) indicating the co-isolation of two polypeptides with different masses by our new single step purification procedure, MRJP1 and MRJP2 (Table I). Ordinary isolation methods of MRJPs led to protein precipitates and aggregates designated as water-insoluble proteins (Chen and Chen 1995) and previous MRJP1 purification methods were multi-step and time consuming (Kamakura et al. 2001a; Simuth 2001). An earlier attempt to purify and characterize MRJPs was carried out by low resolution chromatographic and electrophoretic methods, which led to obtaining a mixture of MRJPs (Hanes and Simuth 1992). The MRJP1 purification herein was confirmed by SDS-PAGE, 2DE and MS analyses (Figure 1, inset; 2 and 4). As MRJP1 is the principal royal jelly protein, we focused on its characterization in this work, whereas MRJP2 will be treated elsewhere after further characterization.

Hanes and Simuth (1992) had found eight isoforms from p*I* 4.5 to 5.0 for the major royal jelly protein (which was further classified as MRJP1 later) by isoelectric focusing. In this work, we could observe nine different isoforms of MRJP1 by 2-DE (Figure 2; Table II). This multiplicity of isoforms is probably due to posttranslational modifications (PTMs) in the protein, as different degrees of protein glycosylation (Ohashi et al. 1997) or maybe to the genetic variability among the bees in the hive (Schmitzova et al. 1998). Phosphorylation is

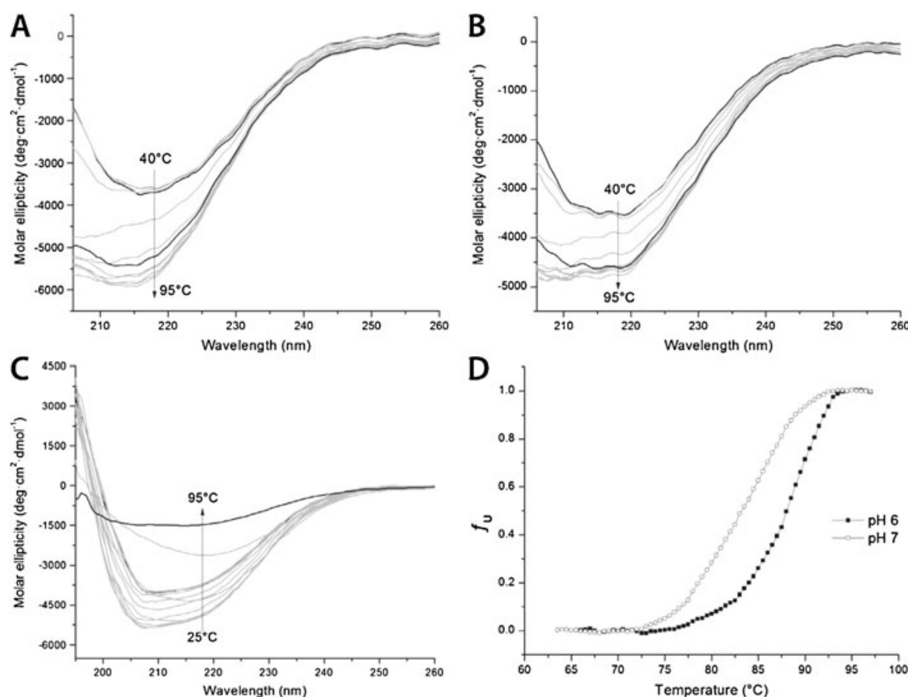

Figure 7. Fitted heat-induced unfolding curves of MRJP1. **a** CD spectra of MRJP1 in 2 mM sodium citrate pH 3.0 containing 2 mM $CaCl_2$. **b** CD spectra of MRJP1 in 2 mM HEPES pH 8.0 containing 2 mM $CaCl_2$. **c** CD spectra of MRJP1 in 2 mM sodium acetate pH 6.0 containing 2 mM $CaCl_2$. **d** Normalized data for the denaturing conditions (pH 6.0 and 7.0 with 2 mM $CaCl_2$); fraction of unfolded protein (f_U) as a function of temperature. The *arrows* indicate the decrease (*downward*) or increase (*upward*) of the molar ellipticity as the temperature increases.

disregarded as 2-DE analysis showed that MRJP1 isoforms are glycoproteins, but not phosphoproteins (Furusawa et al. 2008).

Despite the existence of a single gene coding for MRJP1 in the honey bee genome (Consortium 2006; Drapeau et al. 2006), the expressed gene products can only be assessed at the proteomic level. Alternative splicing of a gene transcript may result in distinct protein species. PTMs can also provide protein diversity. Additionally, the mRNA abundance is not always correlated to protein levels (Gygi et al. 1999; Chen et al. 2002).

In a previous work, we showed the presence of MRJP1 in the honey bee brain both by 2-DE of the brain proteome and by immunocytochemistry of brain tissue (Garcia et al. 2009). Comparing the MRJP1s purified from royal jelly and brain tissue by 2-DE (Figures 2 and 3) and MS of tryptic digests (Figure 4), a great similarity was observed considering the mass peaks of MRJP1 peptides from both sources. Two of the peptides presenting methionine oxidation, *m/z* 1630.8 and 1762.7, appeared more intense in the spectrum of royal jelly MRJP1, whereas the unmodified components (*m/z* 1614.8 and 1746.7) showed to be more intense in the brain sample. Those ions were then selected and actually confirmed by fragmentation and MS/MS sequencing as MRJP1 peptides, both oxidized and non-modified. Methionine oxidation is a spontaneous process occurring in proteins when exposed to reactive oxygen species (Vogt 1995). Once the cerebral MRJP1 is found in the brain cells (Garcia et al. 2009; Peixoto et al. 2009), it would be less

susceptible to oxidation reactions than royal jelly MRJP1. Royal jelly presents a certain antioxidative activity (Nagai et al. 2001, 2006), and its collection and storage often occurs carefully (Kamakura et al. 2001a; Furusawa et al. 2008) because of its commercial use. However, its constituent proteins are exposed for longer to the air than those enclosed in a tissue, so that they may undergo greater oxidative modifications.

Two low intense peaks (*m*/*z* 2075.1 and 2264.3) were found only in the brain MRJP1 spot and another one (*m*/*z* 2501.1) was verified only in the spectrum of the secreted protein. However, these peaks are probably derived from processes normally occurring during the experiments, like missed cleavages at lysines or alkylation of cysteines. Altogether, data from relative mobility of protein in gels (SDS-PAGE and 2-DE), protein identification by PMF and comparison of the tryptic digests by MS, lead us to propose that the MRJP1 purified from royal jelly is the same glycoprotein present in honey bee brain.

DLS demonstrated the structural self-assembling of MRJP1 in solution, in agreement with previous reports (Kimura et al. 1995, 1996, 2003; Tamura et al. 2009a, b). The predominance of pentamers (~290 kDa) was evidenced at pH 6.0 and pH 7.0 (Figure 5), which are in agreement with recent works of Tamura et al. (2009a, b). However, herein we also show that MRJP1 predominantly forms hexamers (~340 kDa) at pH 8.0 and pH 9.0 (Figure 5), indicating a pH-dependence on the MRJP1 oligomerization process.

Actually, a 350 kDa bioactive glycoprotein (later named apisin) was isolated from royal jelly (Yonekura et al. 1992; Kimura et al. 1995) as a heterocomplex composed by two distinct subunits (Kimura et al. 1996). One of them showed the N-terminal sequence Asn-Ile-Leu-Arg-Gly identical to that of MRJP1, while the other one presented the N-terminal sequence of apisimin (Lys-Thr-Ser-Ile-Ser), a peptide characterized 6 year later (Bilikova et al. 2002). A tryptic peptide from apisin showed an identical sequence to the region Gln167-Lys182 of MRJP1 (Kimura et al. 2003). Recently, it was revealed that MRJP1 forms an hetero-oligomeric complex with apisimin, which was suggested to serve as a subunit-joining protein within the MRJP1 oligomer (Tamura et al. 2009a).

About 2.5% of MRJP1 appeared as aggregate at concentrations as high as 25 μM in pH 7.0 (data not shown). It is well known that high concentrations of protein may lead to self-association of the native state. To date, there is little available information about the physico-chemical or structural characterization of MRJP1. In this work we analyzed some structural features of this protein, important for the nourishment of honey bee larvae and probably possessing an unknown function into the neural tissue of the insect. CD analyses showed the secondary structure content of MRJP1 predominantly formed by β-sheets (38.3% parallel and antiparallel). Protein stability can be indirectly evaluated by the Gibbs energy change estimated from the transition curves of native to the unfolded state (Pace 1990; Pace et al. 1997; Teles et al. 2005). The thermal denaturation curves analyzed from Far-UV CD measurements strongly indicated the MRJP1 as a thermally stable protein (Figure 6). The conformational changes could be verified by analyzing its secondary structure content throughout the temperature range of 20 to 95°C (Figure 6, inset), even so this was not considered a denaturation process. However, in order to estimate the structural stability of the MRJP1, we searched for conditions in which the denaturation process could occur. Changing the ionic strength of the solution with sodium chloride or disturbing the protein environment with a low concentration of guanidine hydrochloride, significant structural changes were not observed as indicated by low variations on the Far-UV CD spectra (data not shown). In a recent work, we had identified MRJP1 as a calmodulin-binding protein (CaMBP) (Calabria et al. 2008). Calmodulin interacts with target proteins under regulation of calcium (Rhoads and Friedberg 1997). Considering this feature we analyzed the effect of the calcium ion on

MRJP1 structural stability. The MRJP1 denaturation process was followed after the addition of 2 mM $CaCl_2$ to the protein solution at pH 4.0, pH 5.0 (data not shown), pH 6.0 (Figure 7c and d) and pH 7.0 (Figure 7d). The thermodynamic parameters obtained at pH 6.0 and pH 7.0 indicate a remarkable stability of MRJP1 in which *Tm* occurs at temperatures above 82.8°C, in agreement with most mesophilic and thermophilic globular proteins (Kumar et al. 2000, 2001), human lysozyme, parvalbumin, RNase T1, thioredoxin and whale myoglobin (Robertson and Murphy 1997).

The high stability of MRJP1 was also verified by the enthalpy change (>387 kJ mol^{-1}) and the Gibbs free energy (>62 kJ mol^{-1}), indicating that MRJP1 is well packed by many non-covalent interactions. The ΔG^{25} is very high and quite dependent on the ΔHm values. The value attributed to the entropy is associated with the increase of conformational freedom in the polypeptide chain and with the hydration of groups that become exposed on unfolded state.

DLS analyses also revealed the tendency of MRJP1 to aggregate at pH 4.0 and pH 5.0 (close to its p*I* values between 4.7 and 5.2), in spite of a transition curve obtained from an unfolding process in presence of calcium as seen in CD experiments. However, unfolding assays devoided of aggregation should be developed in order to gather further concluding data about the high stability of MRJP1 in pHs close to p*I* values.

Analyses of CD spectra of MRJP1 reveal a pH-dependence of its thermal denaturation with the maximum stability (~68 kJ mol^{-1}) coinciding with pH 6.0. CD spectra of MRJP1 at pH 4.0–7.0 revealed a typical two-state transition from native to unfolded states (see Figure 7c and d for pH 6.0 and 7.0). However, the thermal unfolding of MRJP1 was an irreversible process, as indicated by CD rescanning under protein sample cooling (40°C) after its complete thermal unfolding (95°C) (data not shown). Thermodynamic measurements require the unfolding reaction to reach the equilibrium and to be reversible (Pace et al. 1997). Hence, present CD data collection was performed taking into account a slow increase in temperature (0.5°C/min), allowing the equilibrium to be achieved. On the other hand, it is known that protein solubility drastically decreases at high temperatures, resulting in aggregation due to hydrophobic amino acid residues exposure. The longer a protein is submitted to high temperature conditions, greater its aggregation is, preventing the refolding process. As considered by Pace et al. (1997), reversibility of thermal unfolding barely occurs due to the above mentioned effect. Therefore, thermodynamic parameter estimated herein could not correspond the real values of MRJP1 stability.

The electrostatic interactions, the chemical basis and the mechanistic origin that would explain the pH-dependence on MRJP1 self-association and stability could be elucidated from the three-dimensional structure of the protein, which has not been solved so far.

No pattern of protein denaturation could be verified on the CD spectra at pH 3.0 (Figure 7a), pH 8.0 (Figure 7b) or pH 9.0 (not shown) conditions, even in the presence of calcium ions. Calcium form ionic interactions with the side chains of aspartate and glutamate residues (Marsden et al. 1990; Handford et al. 1991), which can modify interactions in the protein, and consequently, its conformational stability. These residues are largely protonated at pH 3.0 and the protein interactions with calcium would be hampered, keeping the protein conformation closest to the native state. In alkaline conditions, as well as pH 3.0, it was verified a gain in structure by MRJP1 when raising the temperature (Figure 7a and b). This fact was also observed for other pH conditions before the occurrence of denaturation process. Possibly the protein unfolding at extreme pHs would take place at higher temperatures not assessed by the present techniques.

In conclusion, the purification of both MRJP1 and MRJP2 was concomitantly achieved through a simple, fast and single step method. Purified MRJP1 was obtained in oligomeric states, and showed to be a thermally stable protein. Upon heating, calcium ions

probably caused conformational changes on MRJP1 that make it susceptible to temperature and pH effects. The present work represents an effort on the structural characterization of MRJP1. The MRJP1 gene transcription (Kucharski et al. 1998) and expression in the honey bee brain (Garcia et al. 2009; Peixoto et al. 2009) reinforce the hypothesis of a protein possessing novel functions besides the nutritional role. The physicochemical and structural data of MRJP1 will certainly lead to better comprehension of its functions in honey bee neural processes in the future.

ACKNOWLEDGEMENTS

The authors thank the collaboration of Dr. Fabio A. Schaberle (LNLS) for the help on conducting DLS and CD experiments, Manoel Silva for the supply of honey bees and Nuno M. Domingues for technical assistance in FPLC.

This work was supported by grants from Research and Projects Financing (FINEP, Brazil) to the Brazilian Center for Protein Research, University of Brasilia, and from the Brazilian Council for Scientific and Technological Development (CNPq) to M.V.S. [477258/2007-7], C.A.O.R. [474609/2008-1] and S. M.F. [305022/2009-1]. A grant from the Brazilian Association of Synchrotron Light Technology (ABT-LuS) supports LNLS facilities. Fellowship to G.C.N. C was awarded by Coordination for the Improvement of Higher Level Personnel (CAPES) and to L.G.H. by The Academy of Sciences for the Developing World (TWAS).

Effet du calcium et dépendance au pH sur l'autoassociation et la stabilité structurelle de la protéine majeure 1 de la gelée royale d'*Apis mellifera*.

MRJP1 / *Apis mellifera* / stabilité de la protéine / spectrométrie de masse / dichroïsme circulaire

Zusammenfassung – Bedeutung des Kalzium Effekts und der pH-Abhängigkeit für die Selbstassoziation und Strukturstabilität des *Apis mellifera* Gelée royale Proteins 1 (major royal jelly protein 1). Die Hauptproteine in Gelée royale (Major royal jelly proteins, MRJPs) der Honigbiene sind eine Nahrungsquelle für Larven und von Bedeutung für deren Differenzierung in Königinnen. MRJPs weisen Sequenzähnlichkeit mit den Yellow Proteinen von *Drosophila melanogaster* und anderen Insekten, sowie mit bakteriellen Proteinen auf. Über die biologische Funktion von MRJPs ist wenig bekannt, einige Untersuchungen deuten aber auf eine Rolle in der geschlechtsspezifischen reproduktiven Reifung und in Entwicklungsprozessen des Nervensystems hin. MRJP1 ist das Hauptprotein in Gelée royale. Es ist ein 55–57 kDa Glykoprotein, das im Drüsensekt in monomerer oder oligomerer Form vertreten sein kann. Im Gehirn kommt MRJP1 in Interzellularräumen und in Verbindung mit dem Zytoskelett vor und ist dort während der Entwicklung und während des

Übergangs von der Stockbiene zur Sammlerin differentiell exprimiert. MRJP1 könnte demzufolge in verschiedenen biologischen Vorgängen eine Rolle spielen, wenngleich seine Bedeutung im Nervengewebe noch unklar ist und nur wenige Strukturinformationen über dieses Protein vorliegen. MRJP1 wurde aus Gelée royale mittels einer neuen, schnellen Einschrittmethode chromatographisch aufgereinigt (Abb. 1, Table I). Neun verschiedene MRJP1 Isoformen konnten mittels zweidimensionaler Elektrophorese aufgetrennt werden (Abb. 2, Table II). Durch die Kopplung einer zweidimensionalen Elektrophorese mit Massenspektrometrieanalyse konnten wir proteomisch zeigen, dass MRJP1 des Nervengewebes mit dem entsprechenden Protein aus Gelée royale identisch ist (Abb. 3 und 4). Mittels Dynamischer Lichtverteilung (Dynamic Light Scattering, DLS) wurden die oligomeren Formen von MRJP1 ermittelt. Eine pentamere Form war bei pH-Werten von 6,0 und 7,0 zu finden, während eine hexamere bei pH-Werten von 8,0 und 9,0 auftrat (Abb. 5). Anhand von Zirkulärdichroismus(CD)-Spektren konnten wir zeigen, dass MRJP1 ein sehr stabiles Protein ist (Abb. 6). Eine β-Faltenstruktur war mit 38,3% die überwiegende Proteinstruktur in MRJP1 (Einsatz in Abb. 6). Entfaltungskurven, die mittels CD-Spektrenanalyse bei unterschiedlichen Temperaturen aufgenommen wurden, deuten ebenfalls auf hohe Stabilität bei unterschiedlichen pH-Werten hin. Die Zugabe von Kalziumionen führte jedoch zu Konformationsänderungen, die MRJP1 für Temperatur- und pH-Effekte anfällig mach-ten (Abb. 7). In der Gegenwart von 2 mM Kalzium lag die maximale Stabilität bei pH 6,0, mit einem *Tm*–Wert über 87°C, ΔHm über 394 kJ mol^{-1} und ΔG^{25} über 68 kJ mol^{-1}. Hohe *Tm*–Werte von über 82°C, ΔH_m über 387 kJ mol−1 und ΔG^{25} über 62 kJ mol−1 wurden auch bei pH 7,0 gefunden. Der Nach-weis der Expression des

MRJP1-Gens im Gehirn der Honigbiene deutet darauf hin, das dieses Protein eine Rolle spielen könnte, die über die der Nah-rungsfunktion hinausgeht. Die Ergebnisse dieser Studie stellen einen Ansatz zur Struktur-Funktions- Charakterisierung von MRJP1 dar, und derartige physikochemische Daten können zu einem besseren Verständnis der Funktionen dieses Proteins bei-tragen.

MRJP1 / *Apis mellifera* / Proteinstabilität / Massenspektrometrie / Zirkulärdichroismus

Open Access This article is distributed under the terms of the Creative Commons Attribution Noncommercial License which permits any noncommercial use, distribution, and reproduction in any medium, provided the original author(s) and source are credited.

REFERENCES

Albert, S., Klaudiny, J. (2004) The MRJP/YELLOW protein family of *Apis mellifera*: identification of new members in the EST library. J. Insect Physiol. **50**, 51–59

Albert, S., Bhattacharya, D., Klaudiny, J., Schmitzova, J., Simuth, J (1999) The family of major royal jelly proteins and its evolution. J. Mol. Evol. **49**, 290–297

Bilikova, K., Hanes, J., Nordhoff, E., Saenger, W., Klaudiny, J., Simuth, J. (2002) Apisimin, a new serine-valine-rich peptide from honeybee (*Apis mellifera* L.) royal jelly: purification and molecular characterization. FEBS Lett. **528**, 125–129

Blum, H., Beier, H., Gross, H.J. (1987) Improved silver staining of plant proteins. RNA and DNA in polyacrylamide gels. Electrophoresis **8**, 93–99

Böhm, G. (1997) CDNN—CD Spectra Deconvolution, Halle

Bradford, M.M. (1976) A rapid and sensitive method for the quantitation of microgram quantities of protein utilizing the principle of protein-dye binding. Anal. Biochem. **72**, 248–254

Calabria, L.K., Garcia, L., Teixeira, R.R., Sousa, M.V., Espindola, F.S. (2008) Identification of calmodulin-binding proteins in brain of worker honeybees. Comp. Biochem. Physiol. B. Biochem. Mol. Biol. **151**, 41–45

Chen, C., Chen, S.-Y. (1995) Changes in protein components and storage stability of Royal Jelly under various conditions. Food Chem. **54**, 195–200

Chen, G., Gharib, T.G., Huang, C.C., Taylor, J.M., Misek, D.E., Kardia, S.L., Giordano, T.J., Iannettoni, M.D., Orringer, M.B., Hanash, S.M., Beer, D.G. (2002) Discordant protein and mRNA expression in lung adenocarcinomas. Mol. Cell Proteomics **1**, 304–313

Consortium, T.H.G.S. (2006) Insights into social insects from the genome of the honeybee *Apis mellifera*. Nature **443**, 931–949

Drapeau, M.D., Albert, S., Kucharski, R., Prusko, C., Maleszka, R. (2006) Evolution of the Yellow/Major Royal Jelly Protein family and the emergence of social behavior in honey bees. Genome Res. **16**, 1385–1394

Evans, J.D., Wheeler, D.E. (2001) Gene expression and the evolution of insect polyphenisms. Bioessays **23**, 62–68

Fahrbach, S.E., Robinson, G.E. (1995) Behavioral development in the honey bee: toward the study of learning under natural conditions. Learn. Mem. **2**, 199–224

Frisken, B.J. (2001) Revisiting the method of cumulants for the analysis of dynamic light-scattering data. Appl. Opt. **40**, 4087–4091

Furusawa, T., Rakwal, R., Nam, H.W., Shibato, J., Agrawal, G.K., Kim, Y.S., Ogawa, Y., Yoshida, Y., Kouzuma, Y., Masuo, Y., Yonekura, M. (2008) Comprehensive royal jelly (RJ) proteomics using one- and two-dimensional proteomics platforms reveals novel RJ proteins and potential phospho/glycoproteins. J. Proteome Res. **7**, 3194–3229

Futahashi, R., Sato, J., Meng, Y., Okamoto, S., Daimon, T., Yamamoto, K., Suetsugu, Y., Narukawa, J., Takahashi, H., Banno, Y., Katsuma, S., Shimada, T., Mita, K., Fujiwara, H. (2008) *Yellow* and *ebony* are the responsible genes for the larval color mutants of the silkworm *Bombyx mori*. Genetics **180**, 1995–2005

Garcia, L., Garcia, C.H.S., Calabria, L.K., Cruz, G.C.N., Puentes, A.S., Bao, S.N., Fontes, W., Ricart, C.A., Espindola, F.S., Sousa, M.V. (2009) Proteomic analysis of honey bee brain upon ontogenetic and behavioral development. J. Proteome Res. **8**, 1464–1473

Gharahdaghi, F., Weinberg, C.R., Meagher, D.A., Imai, B. S., Mische, S.M. (1999) Mass spectrometric identification of proteins from silver-stained polyacrylamide gel: a method for the removal of silver ions to enhance sensitivity. Electrophoresis **20**, 601–605

Gygi, S.P., Rochon, Y., Franza, B.R., Aebersold, R. (1999) Correlation between protein and mRNA abundance in yeast. Mol. Cell. Biol. **19**, 1720–1730

Handford, P.A., Mayhew, M., Baron, M., Winship, P.R., Campbell, I.D., Brownlee, G.G. (1991) Key residues involved in calcium-binding motifs in EGF-like domains. Nature **351**, 164–167

Hanes, J., Simuth, J. (1992) Identification and partial characterization of the major royal jelly protein of the honey bee (*Apis mellifera* L.). J. Apic. Res. **31**, 22–26

Hassan, P.A., Kulshreshtha, S.K. (2006) Modification to the cumulant analysis of polydispersity in quasielastic light scattering data. J. Colloid Interface Sci. **300**, 744–748

Kamakura, M., Fukuda, T., Fukushima, M., Yonekura, M. (2001a) Storage-dependent degradation of 57-kDa protein in royal jelly: a possible marker for

freshness. Biosci. Biotechnol. Biochem. **65**, 277–284

Kamakura, M., Mitani, N., Fukuda, T., Fukushima, M. (2001b) Antifatigue effect of fresh royal jelly in mice. J. Nutr. Sci. Vitaminol. **47**, 394–401

Kamakura, M., Suenobu, N., Fukushima, M. (2001c) Fifty-seven-kDa protein in royal jelly enhances proliferation of primary cultured rat hepatocytes and increases albumin production in the absence of serum. Biochem. Biophys. Res. Commun. **282**, 865–874

Kimura, Y., Washino, N., Yonekura, M. (1995) N-linked sugar chains of 350-kDa royal jelly glycoprotein. Biosci. Biotechnol. Biochem. **59**, 507–509

Kimura, Y., Kajiyama, S., Kanaeda, J., Izukawa, T., Yonekura M. (1996) N-linked sugar chain of 55-kDa royal jelly glycoprotein. Biosci. Biotechnol. Biochem. **60**, 2099–2102

Kimura, M., Kimura, Y., Tsumura, K., Okihara, K., Sugimoto, H., Yamada, H., Yonekura, M. (2003) 350-kDa royal jelly glycoprotein (apisin), which stimulates proliferation of human monocytes, bears the beta1-3galactosylated N-glycan: analysis of the N-glycosylation site. Biosci. Biotechnol. Biochem. **67**, 2055–2058

Kucharski, R., Maleszka, R., Hayward, D.C., Ball, E.E. (1998) A royal jelly protein is expressed in a subset of Kenyon cells in the mushroom bodies of the honey bee brain. Naturwissenschaften **85**, 343–346

Kumar, S., Tsai, C.J., Nussinov, R. (2000) Factors enhancing protein thermostability. Protein Eng. **13**, 179–191

Kumar, S., Tsai, C.J., Nussinov, R. (2001) Thermodynamic differences among homologous thermophilic and mesophilic proteins. Biochemistry (Mosc) **40**, 14152–14165

Majtan, J., Kovacova, E., Bilikova, K., Simuth, J. (2006) The immunostimulatory effect of the recombinant apalbumin 1—major honeybee royal jelly protein—on TNFα release. Int. Immunopharmacol **6**, 269–278

Malecova, B., Ramser, J., O'Brien, J.K., Janitz, M., Judova, J., Lehrach, H., Simuth, J. (2003) Honeybee (*Apis mellifera* L.) *mrjp* gene family: computational analysis of putative promoters and genomic structure of *mrjp1*, the gene coding for the most abundant protein of larval food. Gene **303**, 165–175

Marsden, B.J., Shaw, G.S., Sykes, B.D. (1990) Calcium binding proteins. Elucidating the contributions to calcium affinity from an analysis of species variants and peptide fragments. Biochem. Cell Biol. **68**, 587–601

Menzel, R., Leboulle, G., Eisenhardt, D. (2006) Small brains, bright minds. Cell **124**, 237–239

Nagai, T., Sakai, M., Inoue, R., Inoue, H., Suzuki, N. (2001) Antioxidative activities of some commercially honeys, royal jelly, and propolis. Food Chem. **75**, 237–240

Nagai, T., Inoue, R., Suzuki, N., Nagashima, T. (2006) Antioxidant properties of enzymatic hydrolysates from royal jelly. J. Med. Food **9**, 363–367

Ohashi, K., Natori, S., Kubo, T. (1997) Change in the mode of gene expression of the hypopharyngeal gland cells with an age-dependent role change of the worker honeybee *Apis mellifera* L. Eur. J. Biochem. **249**, 797–802

Pace, C.N. (1990) Conformational stability of globular proteins. Trends Biochem. Sci. **15**, 14–17

Pace, C.N., Shirley, B.A., Thomson, J.A. (1997) Measuring the conformational stability of a protein. In: Hames BD (ed) Protein structure: a practical approach. Oxford University Press, New York, pp. 299–321

Page, R.E.J., Peng, C.Y. (2001) Aging and development in social insects with emphasis on the honey bee, *Apis mellifera* L. Exp. Gerontol. **36**, 695–711

Peixoto, L.G., Calabria, L.K., Garcia, L., Capparelli, F.E., Goulart, L.R., de Sousa, M.V., Espindola, F.S. (2009) Identification of major royal jelly proteins in the brain of the honeybee *Apis mellifera*. J. Insect Physiol. **55**, 671–677

Perkins, D.N., Pappin, D.J., Creasy, D.M., Cottrell, J.S. (1999) Probability-based protein identification by searching sequence databases using mass spectrometry data. Electrophoresis **20**, 3551–3567

Rhoads, A.R., Friedberg, F. (1997) Sequence motifs for calmodulin recognition. FASEB J. **11**, 331–340

Robertson, A.D., Murphy, K.P. (1997) Protein Structure and the Energetics of Protein Stability. Chem. Rev. **97**, 1251–1268

Scarselli, R., Donadio, E., Giuffrida, M.G., Fortunato, D., Conti, A., Balestreri, E., Felicioli, R., Pinzauti, M., Sabatini, A.G., Felicioli, A. (2005) Towards royal jelly proteome. Proteomics **5**, 769–776

Schmitzova, J., Klaudiny, J., Albert, S., Schroder, W., Schreckengost, W., Hanes, J., Judova, J., Simuth, J. (1998) A family of major royal jelly proteins of the honeybee *Apis mellifera* L. Cell Mol. Life Sci. **54**, 1020–1030

Simuth, J. (2001) Some properties of the main protein of honeybee (*Apis mellifera*) royal jelly. Apidologie **32**, 69–80

Simuth, J., Bilikova, K., Kovacova, E., Kuzmova, Z., Schroder, W. (2004) Immunochemical approach to detection of adulteration in honey: physiologically active royal jelly protein stimulating TNF-α release is a regular component of honey. J. Agric. Food Chem. **52**, 2154–2158

Tamura, S., Amano, S., Kono, T., Kondoh, J., Yamaguchi, K., Kobayashi, S., Ayabe, T., Moriyama, T. (2009a) Molecular characteristics and physiological functions of major royal jelly protein 1 oligomer. Proteomics **9**, 5534–5543

Tamura, S., Kono, T., Harada, C., Yamaguchi, K., Moriyama, T. (2009b) Estimation and characterisation of major royal jelly proteins obtained from the honeybee *Apis merifera*. Food Chem. **114**, 1491–1497

Teles, R.C., Calderon, L.A., Medrano, F.J., Barbosa, J.A., Guimaraes, B.G., Santoro, M.M., de Freitas, S.M. (2005) pH dependence thermal stability of a chymo-

trypsin inhibitor from *Schizolobium parahyba* seeds. Biophys. J. **88**, 3509–3517

Vogt, W. (1995) Oxidation of methionyl residues in proteins: tools, targets, and reversal. Free Radic. Biol. Med. **18**, 93–105

Watanabe, K., Shinmoto, H., Kobori, M., Tsushida, T., Shinohara, K., Kanaeda, J., Yonekura, M. (1998) Stimulation of cell growth in the U-937 human myeloid cell line by honey royal jelly protein. Cytotechnology **26**, 23–27

Winston, M.L. (1987) The biology of the honey bee. Harvard University Press, London

Wolschin, F., Amdam, G.V. (2007) Plasticity and robustness of protein patterns during reversible development in the honey bee (*Apis mellifera*). Anal. Bioanal. Chem. **389**, 1095–1100

Yonekura, M., Watanabe, K., Saito, S., Tsutsumi, M., Shinohara, K., Kimura, Y., Takagi, S. (1992) The 65th Congress of the Japanese Biochemical Society, Fukuoka, Japan, Abstracts, Seikagaku, **64**, p. 816 (in japanese)

8. Referências

ARANTES, V.; SADDLER, J. Access to cellulose limits the efficiency of enzymatic hydrolysis: the role of amorphogenesis. Biotechnology For Biofuels, v. 3, FEB 23 2010 2010. ISSN 1754-6834.

ARNOLD, I. et al. Yeast mitochondrial F1F0-ATP synthase exists as a dimer: identification of three dimer-specific subunits. EMBO J, v. 17, n. 24, p. 7170-8, Dec 1998.

ARO, N.; PAKULA, T.; PENTTILÄ, M. Transcriptional regulation of plant cell wall degradation by filamentous fungi. FEMS Microbiol Rev, v. 29, n. 4, p. 719-39, Sep 2005. ISSN 0168-6445.

BAILEY, J. M.; FISHMAN, P. H.; PENTCHEV, P. G. Mutarotase in higher plants: distribution and properties. Science, v. 152, n. 726, p. 1270-2, May 1966. ISSN 0036-8075.

BAYKOV, A. A.; EVTUSHENKO, O. A.; AVAEVA, S. M. A malachite green procedure for orthophosphate determination and its use in alkaline phosphatase-based enzyme immunoassay. Anal Biochem, v. 171, n. 2, p. 266-70, Jun 1988. ISSN 0003-2697.

BEG, Q. K. et al. Microbial xylanases and their industrial applications: a review. Appl Microbiol Biotechnol, v. 56, n. 3-4, p. 326-38, Aug 2001. ISSN 0175-7598.

BENTLEY, R.; BHATE, D. S. Mutarotase from Penicillium notatum. I. Purification, assay, and general properties of the enzyme. J Biol Chem, v. 235, p. 1219-24, May 1960. ISSN 0021-9258.

BERNE, B. J.; PECORA, R. Dynamic Light Scattering: with applications to Chemistry, Biology and Physics. New York: Wiley, c1976: John Wiley & Sons, 2000. 376 ISBN 0-486-41155-9 (pbk.).

BHAT, M. Cellulases and related enzymes in biotechnology. Biotechnol Adv, v. 18, n. 5, p. 355-83, Aug 2000. ISSN 0734-9750.

BISCHOFF, K. M. et al. Purification and characterization of a family 5 endoglucanase from a moderately thermophilic strain of Bacillus licheniformis. Biotechnol Lett, v. 28, n. 21, p. 1761-5, Nov 2006. ISSN 0141-5492.

BLUM, H.; BEIER, H.; GROSS, H. J. Improved silver staining of plant proteins, RNA and DNA in polyacrylamide gels ELECTROPHORESIS Volume 8, Issue 2. Electrophoresis, v. 8, n. 2, p. 93-99, 01 1987. ISSN 1522-2683.

BOLAM, D. N. et al. Pseudomonas cellulose-binding domains mediate their effects by increasing enzyme substrate proximity. Biochem J, v. 331 (Pt 3), p. 775-81, May 1998. ISSN 0264-6021.

BORGSTAHL, G. E. O. How to Use Dynamic Light Scattering to Improve the Likelihood of Growing Macromolecular Crystals. Methods Mol Biol., v. 363, p. 109-129, 2007.

BOUFFARD, G. G.; RUDD, K. E.; ADHYA, S. L. Dependence of lactose metabolism upon mutarotase encoded in the gal operon in Escherichia coli. J Mol Biol, v. 244, n. 3, p. 269-78, Dec 1994. ISSN 0022-2836.

DAY, R. et al. Binding site for chitin oligosaccharides in the soybean plasma membrane. Plant Physiol, v. 126, n. 3, p. 1162-73, Jul 2001. ISSN 0032-0889.

DAY, R. B. et al. Differential expression of two soybean apyrases, one of which is an early nodulin. Mol Plant Microbe Interact, v. 13, n. 10, p. 1053-70, Oct 2000. ISSN 0894-0282.

DE CASTRO, A. et al. Trichoderma harzianum IOC-4038: A Promising Strain for the Production of a Cellulolytic Complex with Significant beta-Glucosidase Activity from Sugarcane Bagasse Cellulignin. Appl Biochem Biotechnol, May 2010. ISSN 1559-0291.

DROUILLARD, S. et al. Serratia marcescens chitobiase is a retaining glycosidase utilizing substrate acetamido group participation. Biochem J, v. 328 (Pt 3), p. 945-9, Dec 1997. ISSN 0264-6021.

FANUTTI, C. et al. The conserved noncatalytic 40-residue sequence in cellulases and hemicellulases from anaerobic fungi functions as a protein docking domain. J Biol Chem, v. 270, n. 49, p. 29314-22, Dec 1995. ISSN 0021-9258.

FEKETE, E. et al. Lack of aldose 1-epimerase in Hypocrea jecorina (anamorph Trichoderma reesei): a key to cellulase gene expression on lactose. Proc Natl Acad Sci U S A, v. 105, n. 20, p. 7141-6, May 2008. ISSN 1091-6490.

FERNÁNDEZ-ACERO, F. J. et al. 2-DE proteomic approach to the Botrytis cinerea secretome induced with different carbon sources and plant-based elicitors. Proteomics, v. 10, n. 12, p. 2270-80, Jun 2010. ISSN 1615-9861.

FONTES, C. M.; GILBERT, H. J. Cellulosomes: highly efficient nanomachines designed to deconstruct plant cell wall complex carbohydrates. Annu Rev Biochem, v. 79, p. 655-81, 2010. ISSN 1545-4509.

FRANCO, O. et al. Effects of soybean Kunitz trypsin inhibitor on the cotton boll weevil (Anthonomus grandis). Phytochemistry, v. 65, n. 1, p. 81-9, Jan 2004. ISSN 0031-9422.

FRANK, A.; PEVZNER, P. PepNovo: de novo peptide sequencing via probabilistic network modeling. Anal Chem, v. 77, n. 4, p. 964-73, Feb 2005. ISSN 0003-2700.

GAMAUF, C. et al. Characterization of the bga1-encoded glycoside hydrolase family 35 beta-galactosidase of Hypocrea jecorina with galacto-beta-D-galactanase activity. FEBS J, v. 274, n. 7, p. 1691-700, Apr 2007. ISSN 1742-464X.

GARY, E. A. K., C. Mycoparasitism and lytic enzymes: <o:smarttagtype name="City" namespaceuri="urn:schemas-microsoft-com:office:smarttags"><st1:city w:st="on">Taylor and Francis Ltd., London, United Kingdom. 2: 153–171 p. 1998.

GASTEBOIS, A. et al. Characterization of a new beta(1-3)-glucan branching activity of Aspergillus fumigatus. J Biol Chem, v. 285, n. 4, p. 2386-96, Jan 2010. ISSN 1083-351X.

GEIGER, A. et al. Exocytosis and protein secretion in Trypanosoma. BMC Microbiol, v. 10, p. 20, 2010. ISSN 1471-2180.

GIARDINA, T. et al. Both binding sites of the starch-binding domain of Aspergillus niger glucoamylase are essential for inducing a conformational change in amylose. J Mol Biol, v. 313, n. 5, p. 1149-59, Nov 2001. ISSN 0022-2836.

GONZALEZ-VOGEL, A. et al. Proteomic analysis in non-denaturing condition of the secretome reveals the presence of multienzyme complexes in Penicillium purpurogenum. Appl Microbiol Biotechnol, v. 89, n. 1, p. 145-55, Jan 2011. ISSN 1432-0614.

GRONDONA, I. et al. Physiological and biochemical characterization of Trichoderma harzianum, a biological control agent against soilborne fungal plant pathogens. Appl Environ Microbiol, v. 63, n. 8, p. 3189-98, Aug 1997. ISSN 0099-2240.

GRÜN, C. H. et al. Mechanism of action of the endo-(1-->3)-alpha-glucanase MutAp from the mycoparasitic fungus Trichoderma harzianum. FEBS Lett, v. 580, n. 16, p. 3780-6, Jul 2006. ISSN 0014-5793.

HARTL, L. et al. Characterization of the GPI-anchored endo β-1,3-glucanase Eng2 of Aspergillus fumigatus. Fungal Genet Biol, v. 48, n. 2, p. 185-91, Feb 2011. ISSN 1096-0937.

HEUBERGER, E. H. et al. Oligomeric state of membrane transport proteins analyzed with blue native electrophoresis and analytical ultracentrifugation. J Mol Biol, v. 317, n. 4, p. 591-600, Apr 2002. ISSN 0022-2836.

HOLDEN, H. M.; RAYMENT, I.; THODEN, J. B. Structure and function of enzymes of the Leloir pathway for galactose metabolism. J Biol Chem, v. 278, n. 45, p. 43885-8, Nov 2003. ISSN 0021-9258.

JUN, H.; KIESELBACH, T.; JÖNSSON, L. J. Enzyme production by filamentous fungi: analysis of the secretome of Trichoderma reesei grown on unconventional carbon source. **Microb Cell Fact**, v. 10, p. 68, 2011. ISSN 1475-2859.

JUNQUEIRA, M. et al. Protein identification pipeline for the homology-driven proteomics. **J Proteomics**, v. 71, n. 3, p. 346-56, Aug 2008. ISSN 1874-3919.

______. Separating the wheat from the chaff: unbiased filtering of background tandem mass spectra improves protein identification. **J Proteome Res**, v. 7, n. 8, p. 3382-95, Aug 2008. ISSN 1535-3893.

JØRGENSEN, T. et al. Transcriptomic comparison of Aspergillus niger growing on two different sugars reveals coordinated regulation of the secretory pathway. **BMC Genomics**, v. 10, p. 44, 2009. ISSN 1471-2164.

KARAFFA, L. et al. D-Galactose induces cellulase gene expression in Hypocrea jecorina at low growth rates. **Microbiology**, v. 152, n. Pt 5, p. 1507-14, May 2006. ISSN 1350-0872.

KESTON, A. S. Occurrence of mutarotase in animals: its proposed relationship to transport and reabsorption of sugars and insulin. **Science**, v. 120, n. 3113, p. 355-6, Aug 1954. ISSN 0036-8075.

KONNO, N. et al. Characterization of β-N-acetylhexosaminidase (LeHex20A), a member of glycoside hydrolase family 20, from Lentinula edodes shiitake mushroom). **AMB Express**, v. 2, n. 1, p. 29, 2012. ISSN 2191-0855.

KOSUGI, A. et al. Cell-surface-anchoring role of N-terminal surface layer homology domains of Clostridium cellulovorans EngE. **J Bacteriol**, v. 184, n. 4, p. 884-8, Feb 2002. ISSN 0021-9193.

KRAUSE, F. Detection and analysis of protein-protein interactions in organellar and prokaryotic proteomes by native gel electrophoresis: (Membrane) protein complexes and supercomplexes. **Electrophoresis**, v. 27, n. 13, p. 2759-81, Jul 2006. ISSN 0173-0835.

KRAUSE, F. et al. Active oligomeric ATP synthases in mammalian mitochondria. **Biochem Biophys Res Commun**, v. 329, n. 2, p. 583-90, Apr 2005. ISSN 0006-291X.

KUMAR, R.; SINGH, S.; SINGH, O. V. Bioconversion of lignocellulosic biomass: biochemical and molecular perspectives. **J Ind Microbiol Biotechnol**, v. 35, n. 5, p. 377-91, May 2008. ISSN 1367-5435.

LI, X. et al. The molecular chaperone calnexin associates with the vacuolar H(+)-ATPase from oat seedlings. **Plant Cell**, v. 10, n. 1, p. 119-30, Jan 1998. ISSN 1040-4651.

LING, M. et al. Binding of two transcriptional factors, Xyr1 and ACEI, in the promoter region of cellulase cbh1 gene. **Biotechnol Lett**, v. 31, n. 2, p. 227-31, Feb 2009. ISSN 1573-6776.

LIU, K. et al. Two-dimensional blue native/SDS-PAGE analysis reveals heat shock protein chaperone machinery involved in hepatitis B virus production in HepG2.2.15 cells. **Mol Cell Proteomics**, v. 8, n. 3, p. 495-505, Mar 2009. ISSN 1535-9484.

LU, X. et al. The intra- and extracellular proteome of Aspergillus niger growing on defined medium with xylose or maltose as carbon substrate. **Microb Cell Fact**, v. 9, p. 23, 2010. ISSN 1475-2859.

M.G. TABKA, M. G. H.-G., I. MONOD, F. ASTHER, M. SIGOILLOT, J.C. Enzymatic saccharification of wheat straw for bioethanol production by a combined cellulase xylanase and feruloyl esterase treatment. **Enzyme and Microbial Technology**. 39: 897–902 p. 2006.

MAHAJAN, S.; MASTER, E. R. Proteomic characterization of lignocellulose-degrading enzymes secreted by Phanerochaete carnosa grown on spruce and microcrystalline cellulose. **Appl Microbiol Biotechnol**, v. 86, n. 6, p. 1903-14, May 2010. ISSN 1432-0614.

MARTINEZ, D. et al. Genome sequencing and analysis of the biomass-degrading fungus Trichoderma reesei (syn. Hypocrea jecorina). Nat Biotechnol, v. 26, n. 5, p. 553-60, May 2008. ISSN 1546-1696.

MATSUI, H.; BAN-TOKUDA, T. Studies on carboxymethyl cellulase and xylanase activities of anaerobic fungal isolate CR4 from the bovine rumen. Curr Microbiol, v. 57, n. 6, p. 615-9, Dec 2008. ISSN 1432-0991.

MAYER, A.; STAPLES, R. Laccase: new functions for an old enzyme. Phytochemistry, v. 60, n. 6, p. 551-65, Jul 2002. ISSN 0031-9422.

MIRAS, I. et al. Mapping by site-directed mutagenesis of the region responsible for cohesin-dockerin interaction on the surface of the seventh cohesin domain of Clostridium thermocellum CipA. Biochemistry, v. 41, n. 7, p. 2115-9, Feb 2002. ISSN 0006-2960.

MISHRA, P. et al. Statistical optimization of medium components for production of extracellular chitinase by Basidiobolus ranarum: a novel biocontrol agent against plant pathogenic fungi. J Basic Microbiol, Feb 2012. ISSN 1521-4028.

MONTEIRO, V. N. et al. New insights in Trichoderma harzianum antagonism of fungal plant pathogens by secreted protein analysis. Curr Microbiol, v. 61, n. 4, p. 298-305, Oct 2010. ISSN 1432-0991.

MOUYNA, I. et al. Deletion of GEL2 encoding for a beta(1-3)glucanosyltransferase affects morphogenesis and virulence in Aspergillus fumigatus. Mol Microbiol, v. 56, n. 6, p. 1675-88, Jun 2005. ISSN 0950-382X.

______. Molecular characterization of a cell wall-associated beta(1-3)endoglucanase of Aspergillus fumigatus. Med Mycol, v. 40, n. 5, p. 455-64, Oct 2002. ISSN 1369-3786.

MURASHIMA, K.; KOSUGI, A.; DOI, R. H. Synergistic effects of cellulosomal xylanase and cellulases from Clostridium cellulovorans on plant cell wall degradation. J Bacteriol, v. 185, n. 5, p. 1518-24, Mar 2003. ISSN 0021-9193.

NAGY, T. et al. Characterization of a double dockerin from the cellulosome of the anaerobic fungus Piromyces equi. J Mol Biol, v. 373, n. 3, p. 612-22, Oct 2007. ISSN 0022-2836.

NEFF, D.; DENCHER, N. A. Purification of multisubunit membrane protein complexes: isolation of chloroplast FoF1-ATP synthase, CFo and CF1 by blue native electrophoresis. Biochem Biophys Res Commun, v. 259, n. 3, p. 569-75, Jun 1999. ISSN 0006-291X.

NIDETZKY, B. et al. Cellulose hydrolysis by the cellulases from Trichoderma reesei: a new model for synergistic interaction. Biochem J, v. 298 Pt 3, p. 705-10, Mar 1994. ISSN 0264-6021.

OHTSUKI, T. et al. Production of large multienzyme complex by aerobic thermophilic fungus Chaetomium sp. nov. MS-017 grown on palm oil mill fibre. Lett Appl Microbiol, v. 40, n. 2, p. 111-6, 2005. ISSN 0266-8254.

PERCIVAL ZHANG, Y. H.; HIMMEL, M. E.; MIELENZ, J. R. Outlook for cellulase improvement: screening and selection strategies. Biotechnol Adv, v. 24, n. 5, p. 452-81, 2006 Sep-Oct 2006. ISSN 0734-9750.

POHLSCHRÖDER, M.; LESCHINE, S. B.; CANALE-PAROLA, E. Multicomplex cellulase-xylanase system of Clostridium papyrosolvens C7. J Bacteriol, v. 176, n. 1, p. 70-6, Jan 1994. ISSN 0021-9193.

POLIZELI, M. et al. Xylanases from fungi: properties and industrial applications. Appl Microbiol Biotechnol, v. 67, n. 5, p. 577-91, Jun 2005. ISSN 0175-7598.

PORTNOY, T. et al. Differential regulation of the cellulase transcription factors XYR1, ACE2, and ACE1 in Trichoderma reesei strains producing high and low levels of cellulase. Eukaryot Cell, v. 10, n. 2, p. 262-71, Feb 2011. ISSN 1535-9786.

REIFSCHNEIDER, N. et al. Defining the mitochondrial proteomes from five rat organs in a physiologically significant context using 2D blue-native/SDS-PAGE. J Proteome Res, v. 5, n. 5, p. 1117-32, May 2006. ISSN 1535-3893.

REISINGER, V.; EICHACKER, L. Solubilization of membrane protein complexes for blue native PAGE. J Proteomics, v. 71, n. 3, p. 277-83, Aug 2008. ISSN 1874-3919.

ROSELI GARCIA MEDEIROS, F. G. D. S. J., SÔNIA NAIR BÁO, ROGÉRIO HANADA; FILHO, A. E. X. F. Application of Xylanases from Amazon Forest Fungal Species in Bleaching of Eucalyptus Kraft Pulps. 50: 231-238 p. 2007.

RUBIO, M. B. et al. Cloning and characterization of the Thcut1 gene encoding a cutinase of Trichoderma harzianum T34. Curr Genet, v. 54, n. 6, p. 301-12, Dec 2008. ISSN 1432-0983.

SALOHEIMO, M. et al. Swollenin, a Trichoderma reesei protein with sequence similarity to the plant expansins, exhibits disruption activity on cellulosic materials. Eur J Biochem, v. 269, n. 17, p. 4202-11, Sep 2002. ISSN 0014-2956.

SCHAEFFER, F. et al. Duplicated dockerin subdomains of Clostridium thermocellum endoglucanase CelD bind to a cohesin domain of the scaffolding protein CipA with distinct thermodynamic parameters and a negative cooperativity. Biochemistry, v. 41, n. 7, p. 2106-14, Feb 2002. ISSN 0006-2960.

SCHÄGGER, H. Tricine-SDS-PAGE. Nat Protoc, v. 1, n. 1, p. 16-22, 2006. ISSN 1750-2799.

SCHÄGGER, H.; CRAMER, W.; VON JAGOW, G. Analysis of molecular masses and oligomeric states of protein complexes by blue native electrophoresis and isolation of membrane protein complexes by two-dimensional native electrophoresis. Anal Biochem, v. 217, n. 2, p. 220-30, Mar 1994. ISSN 0003-2697.

SCHÄGGER, H.; CRAMER, W. A.; VON JAGOW, G. Analysis of molecular masses and oligomeric states of protein complexes by blue native electrophoresis and isolation of membrane protein complexes by two-dimensional native electrophoresis. Anal Biochem, v. 217, n. 2, p. 220-30, Mar 1994. ISSN 0003-2697.

SCHÄGGER, H.; VON JAGOW, G. Blue native electrophoresis for isolation of membrane protein complexes in enzymatically active form. Anal Biochem, v. 199, n. 2, p. 223-31, Dec 1991. ISSN 0003-2697.

SEIBOTH, B. et al. The galactokinase of Hypocrea jecorina is essential for cellulase induction by lactose but dispensable for growth on d-galactose. Mol Microbiol, v. 51, n. 4, p. 1015-25, Feb 2004. ISSN 0950-382X.

______. Role of the bga1-encoded extracellular {beta}-galactosidase of Hypocrea jecorina in cellulase induction by lactose. Appl Environ Microbiol, v. 71, n. 2, p. 851-7, Feb 2005. ISSN 0099-2240.

SEIBOTH, B.; HOFMANN, G.; KUBICEK, C. Lactose metabolism and cellulase production in Hypocrea jecorina: the gal7 gene, encoding galactose-1-phosphate uridylyltransferase, is essential for growth on galactose but not for cellulase induction. Mol Genet Genomics, v. 267, n. 1, p. 124-32, Mar 2002. ISSN 1617-4615.

SEIBOTH, B.; METZ, B. Fungal arabinan and L-arabinose metabolism. Appl Microbiol Biotechnol, v. 89, n. 6, p. 1665-73, Mar 2011. ISSN 1432-0614.

SELIG, M. J. et al. Synergistic enhancement of cellobiohydrolase performance on pretreated corn stover by addition of xylanase and esterase activities. Bioresour Technol, v. 99, n. 11, p. 4997-5005, Jul 2008. ISSN 0960-8524.

SELVARAJ, V. R., A. THANGAVELU, V. Production, properties and industrial applications of microbial xylanase 2000.

SHEVCHENKO, A.; VALCU, C. M.; JUNQUEIRA, M. Tools for exploring the proteomosphere. J Proteomics, v. 72, n. 2, p. 137-44, Mar 2009. ISSN 1874-3919.

SHOHAM, Y.; LAMED, R.; BAYER, E. A. The cellulosome concept as an efficient microbial strategy for the degradation of insoluble polysaccharides. Trends Microbiol, v. 7, n. 7, p. 275-81, Jul 1999. ISSN 0966-842X.

SILVA, A. J. et al. BN-PAGE analysis of Trichoderma harzianum secretome reveals cellulases and hemicellulases working as multienzymatic complexes. Proteomics, Jun 2012a. ISSN 1615-9861.

SOUTHALL, S. M. et al. The starch-binding domain from glucoamylase disrupts the structure of starch. FEBS Lett, v. 447, n. 1, p. 58-60, Mar 1999. ISSN 0014-5793.

SRIVASTAVA, K. et al. Multi-crystallin complexes exist in the water-soluble high molecular weight protein fractions of aging normal and cataractous human lenses. Exp Eye Res, v. 87, n. 4, p. 356-66, Oct 2008. ISSN 1096-0007.

STERNBERG, D.; MANDELS, G. R. Induction of cellulolytic enzymes in Trichoderma reesei by sophorose. J Bacteriol, v. 139, n. 3, p. 761-9, Sep 1979. ISSN 0021-9193.

STRICKER, A. et al. Xyr1 (xylanase regulator 1) regulates both the hydrolytic enzyme system and D-xylose metabolism in Hypocrea jecorina. Eukaryot Cell, v. 5, n. 12, p. 2128-37, Dec 2006. ISSN 1535-9778.

STRICKER, A.; MACH, R.; DE GRAAFF, L. Regulation of transcription of cellulases- and hemicellulases-encoding genes in Aspergillus niger and Hypocrea jecorina (Trichoderma reesei). Appl Microbiol Biotechnol, v. 78, n. 2, p. 211-20, Feb 2008. ISSN 0175-7598.

STRICKER, A.; STEIGER, M.; MACH, R. Xyr1 receives the lactose induction signal and regulates lactose metabolism in Hypocrea jecorina. FEBS Lett, v. 581, n. 21, p. 3915-20, Aug 2007. ISSN 0014-5793.

SUNNA, A.; ANTRANIKIAN, G. Xylanolytic enzymes from fungi and bacteria. Crit Rev Biotechnol, v. 17, n. 1, p. 39-67, 1997. ISSN 0738-8551.

SUNNA, A.; PULS, J.; ANTRANIKIAN, G. Characterization of the xylanolytic enzyme system of the extreme thermophilic anaerobic bacteria Thermotoga maritima, T. neapolitana, and T. thermarum. Comparative Biochemistry and Physiology Part A: Physiology, v. 118, n. 3, p. 453-461, 1997. ISSN 0300-9629.

SUÁREZ, M. B. et al. Proteomic analysis of secreted proteins from Trichoderma harzianum. Identification of a fungal cell wall-induced aspartic protease. Fungal Genet Biol, v. 42, n. 11, p. 924-34, Nov 2005. ISSN 1087-1845.

TABKA, M. G.; SIGOILLOT, I. H.-G. F. M. M. A. J. C. Enzymatic saccharification of wheat straw for bioethanol production by a combined cellulase xylanase and feruloyl esterase treatment. 39: 897-902 p. 2006.

______. Synergistic associations between *Clostridium cellulovorans* enzymes XynA, ManA and EngE against sugarcane bagasse. Enzyme and Microbial Technology. 42: 492-498 p. 2008.

TUNG, J. Y. et al. Crystal structures of the starch-binding domain from Rhizopus oryzae glucoamylase reveal a polysaccharide-binding path. Biochem J, v. 416, n. 1, p. 27-36, Nov 2008. ISSN 1470-8728.

ULHOA, C. J.; PEBERDY, J. F. Regulation of chitinase synthesis in Trichoderma harzianum. J Gen Microbiol, v. 137, n. 9, p. 2163-9, Sep 1991. ISSN 0022-1287.

VITERBO, A. et al. Significance of lytic enzymes from Trichoderma spp. in the biocontrol of fungal plant pathogens. Antonie Van Leeuwenhoek, v. 81, n. 1-4, p. 549-56, Aug 2002. ISSN 0003-6072.

VON JAGOW, G. et al. b.c1 complex from beef heart: hydrodynamic properties of the complex prepared by a refined hydroxyapatite chromatography in trition X-100. *Biochim Biophys Acta*, v. 462, n. 3, p. 549-58, Dec 1977. ISSN 0006-3002.

WALLENFELS, K.; HUCHO, F.; HERRMANN, K. [Enzymatically catalyzed mutarotation of aldoses. Studies on aldose-1-epimerase from E. coli]. *Biochem Z*, v. 343, n. 3, p. 307-25, Dec 1965. ISSN 0366-0753.

WANG, Z. J. et al. Sample preparation for two-dimensional blue native/SDS polyacrylamide gel electrophoresis in the identification of Streptomyces coelicolor cytoplasmic protein complexes. *J Biochem Biophys Methods*, v. 70, n. 4, p. 565-72, Jun 2007. ISSN 0165-022X.

WIATER, A. et al. Identification and characterization of the Trichoderma harzianum gene encoding alpha-1,3-glucanase involved in streptococcal mutan degradation. *Pol J Microbiol*, v. 60, n. 4, p. 293-301, 2011. ISSN 1733-1331.

WITTIG, I.; BRAUN, H.; SCHÄGGER, H. Blue native PAGE. *Nat Protoc*, v. 1, n. 1, p. 418-28, 2006. ISSN 1750-2799.

WITTIG, I.; SCHÄGGER, H. Features and applications of blue-native and clear-native electrophoresis. *Proteomics*, v. 8, n. 19, p. 3974-90, Oct 2008. ISSN 1615-9861.

______. Native electrophoretic techniques to identify protein-protein interactions. *Proteomics*, v. 9, n. 23, p. 5214-23, Dec 2009. ISSN 1615-9861.

YANG, H. H. et al. Induced proteome of Trichoderma harzianum by Botrytis cinerea. *Mycol Res*, v. 113, n. Pt 9, p. 924-32, Sep 2009. ISSN 1469-8102.